CLIMATE CHANGE AND CLEAN ENERGY INITIATIVE

Assessment of the Risk of Amazon Dieback

Main Report

February 4, 2010

Environmentally and Socially Sustainable Development Department
Latin America and Caribbean Region
The World Bank

Acronyms

ANSG	Atlantic North-South Gradient
AOGCM	Atmospheric Ocean General Circulation Models
CDD	Consecutive Dry Days
CDF	Cumulative Distribution Function
CGCM	Coupled General Circulation Model
CSIRO	Australia's Commonwealth Scientific and Industrial Research Organisation
CMIP3	Coupled Model Intercomparison Project 3
CPTEC	Centro de Previsão de Tempo e Estudos Climáticos
CRU	Climatic Research Unit–University of East Anglia
DGVM	Dynamic Global Vegetation Model
DJF	December January February (Wet Season)
ENSO	El Niño Southern Oscillation
FC	Forest Cover
FCP	Forest Conservation Plan
FPC	Foliar Projective Cover
GCM	General Circulation Model
GHG	Greenhouse Gases
GPCP	Global Precipitation Climatology Project
GRDC	Global River Discharge Center
IBIS	Integrated Biosphere Simulator Model
INPE	Brazilian Institute for Space Research
IPCC	Intergovernmental Panel on Climate Change
ITCZ	Intertropical Convergence Zone
JJA	June July August (Dry Season)
JMA	Japan Meteorological Agency
LPJmL	Lund-Potsdam-Jena managed Land Dynamic Global Vegetation and Water Balance Model
MAM	March April May (Wet Season)
MRI	Meteorological Research Institute
NPP	Net Primary Production
ORCHIDEE	Organizing Carbon and Hydrology In Dynamic Ecosystems
PDF	Probability Density Function
PEWG	Pacific East-West Gradient
PFT	Plant Functional Type
PgC	Petagram Carbon
RX5D	Maximum 5-day precipitation total
SACZ	South Atlantic Convergence Zone
SON	September October November (Dry Season)
SRES	Special Report on Emission Scenarios
SST	Sea Surface Temperature
TDO	Task Development Objective

Contents

The task was carried out by a team in the World Bank, led by W. Vergara with the assistance of S. Scholz, A. Deeb, N. Toba, A. Zarzar and A. Valencia, and was undertaken with the collaboration of several institutions with considerable experience and skills relevant to the proposed analysis. These include the Meteorological Research Institute of Japan (team led by A. Kitoh), Exeter University of England (team led by P. Cox and T. Jupp), the Potsdam Institute of Germany (team led by W. Lucht and A. Ramming), CPET/INPE Brazil (team led by C. Nobre and G. Sampaio) and Earth3000 of Germany (team led by M. Koch-weser), all coordinated by the task team in the World Bank. The results of the analysis were reviewed by a blue-ribbon panel of internationally renowned scientists and practitioners; the list of panel members is attached as an annex to the main report.

I. Introduction

The Amazon basin is a key component of the global carbon cycle. The old-growth rainforests in the basin represent a storage of ~ 120 petagrams of carbon (Pg C, equal to 120 billion metric tons of carbon) in their biomass. Annually, these tropical forests process approximately 18 Pg C through respiration and photosynthesis. This is more than twice the rate of global anthropogenic fossil fuel emissions (Dirzo and Raven 2003). The basin is also the largest global repository of biodiversity and produces about 20% of the world's flow of fresh water into the oceans. Despite the large CO_2 efflux from recent deforestation, the Amazon rainforest ecosystem is still considered to be a net carbon sink of 0.8–1.1 Pg C per year because growth on average exceeds mortality (Phillips et al. 2008).

However, current climate trends and human-induced deforestation may be transforming forest structure and behavior (Phillips et al. 2009). Increasing temperatures may accelerate respiration rates and thus carbon emissions from soils (Malhi and Grace 2000). High probabilities for modification in rainfall patterns (Malhi et al. 2008) and prolonged drought stress may lead to reductions in biomass density. Resulting changes in evapotranspiration and therefore convective precipitation could further accelerate drought conditions and destabilize the tropical ecosystem as a whole, causing a reduction in its biomass carrying capacity or dieback. In turn, changes in the structure of the Amazon and its associated water cycle would have implications for the many endemic species it contains and result in changes at a continental scale. Clearly, with much at stake, if climate-induced damage alters the state of the Amazon ecosystem, there is a need to better understand its risk, process and dynamics.

1. OBJECTIVE

The objective of this study is to assist in understanding the risk, process and dynamics of potential Amazon dieback and its implications. The task is organized in five activities that address key aspects of the analysis (see Figure I.1): a) a modeling of future climate (end of century) over the basin, using a high-resolution model; b) an assessment of the impact of climate on rainfall over the region; c) an assessment of biomass response to rainfall anomalies and associated changes; d) an assessment of linkages between deforestation and potential for dieback; and e) on the basis of these assessments, a qualification of potential economic consequences is described.

2. SCOPE

Amazon dieback is defined as the process by which the Amazon basin loses biomass density as a consequence of climate impacts. Although there is no consensus definition on how to characterize forest dieback, for purposes of this analysis reductions in biomass carbon resulting from climate impacts, which would exceed 25% of the standing stock of carbon, are considered to be an indication of dieback.

The analysis considers that climate-induced biomass response in the basin will result not only from changes in rainfall but also from other factors that are linked to climate changes, such as: a)

increased probabilities for prolonged drought stress which may lead to increased physiological stress for trees, increased tree mortality, and thus carbon emissions; b) increasing atmospheric CO_2 concentrations, which may alter the drought response of forests; c) increasing temperatures which may accelerate heterotrophic respiration rates and thus carbon emissions; and d) resulting changes in evapo-transpiration and therefore convective precipitation could further accelerate drought conditions and destabilize the tropical ecosystem as a whole.

The structure of the analysis is presented in Figure I.1. Results from the modeling of future climate in the Amazon basin, based on the high-resolution atmospheric general circulation model of the Meteorological Research Institute of the Japan Meteorological Agency, and using the Earth Simulator, are reported in Section II (**Modeling future climate in the Amazon using the Earth Simulator)**. It summarizes estimates of future climate extremes (using indexes for extreme wet and extreme dry periods), rainfall, soil dryness, runoffs and stream flows, under different greenhouse gas emission trajectories or SRES scenarios (see explanation of SRES scenarios below). The outputs of the model are used to estimate biomass response in Sections IV and V. Section III (**Assessment of future rainfall over the Amazon basin)** examines the difficulties of predicting future rainfall over the region and reviews the outputs from 24 Global Circulation Models (GCM) used by the IPCC from a perspective of the ability to simulate current rainfall, akin to an "Amazon Prediction" index. Section III also presents probability density functions of future rainfall based on this index and on the ability to reproduce sea surface temperature dipoles, for use in assessing biomass response.

Section IV (**Analysis of Amazon forest response to climate change)** presents the results of the application of the Lund-Potsdam-Jena managed Land Dynamic Global Vegetation and Water Balance Model (LPJmL) to the outputs and the implications of rainfall changes. It results in estimates of future vegetation carbon in the region in the form of probability density functions. Finally, Section V (**Interplay of climate impacts and deforestation in the Amazon)** presents the potential combined effects of climate change and deforestation in the Amazon, using the results of the Earth Simulator, the outputs of the Center for Weather Forecasting and Climate Studies Global Circulation Models (*Centro de Previsão de Tempo e Estudios Climáticos,* CPTEC GCM) and the CPTEC vegetation model. Section VI (**Review of impacts**) summarizes the type of impacts that would be expected from the anticipated changes.

3. GEOGRAPHICAL DOMAIN

Because the Amazon basin covers a wide region subject to different stresses and conditions, all assessments have focused on five geographical domains (windows) defined to capture different momentums in land use. Eastern Amazonia is a region continuous to Northeastern Brazil, where somewhat drier conditions are already the norm and growing anthropogenic impacts can be observed. Northwestern Amazonia is a region with little if any current direct anthropogenic impact and relatively intact ground cover. Southern Amazonia is a region subjected to strong land use change drivers. Northeastern Brazil is a region subjected to dry conditions. Southern Brazil[1] would suffer the consequences of any change in climate in Amazonia (see Figure I.2).

[1] The exact geographical coordinates are provided in Figure I.2.

4. DATA SOURCES

Observations: The Climate Research Unit (CRU) dataset

Observed data for air temperature (°C), precipitation (mm), cloud cover (%) and the number of wet days at a 0.5° resolution (latitude/longitude grid) were available for monthly time-steps throughout the 1901–2003 period from the Climate Research Unit, University of East Anglia (CRU, New et al. 2000). These data are assumed to represent the "true" state of the climate (from the CRU TS 3.0 archive: http://www.cru.uea.ac.uk/cru/data/hrg-interim/). Three additional climatology archives were used for comparison purposes: the CMAP, GPCP and TRMM 3A25[2] datasets.

Greenhouse Gas Emission Trajectories (SRES scenarios)

The projected global greenhouse gas emission trajectories (SRES scenarios) adopted by the Intergovernmental Panel on Climate Change (IPCC) and used in its fourth assessment report (FAR), cover a wide range of driving forces of future emissions, including demographic, technological and economic developments. The Amazon dieback study is based on the scenario of moderate but consistent improvements in energy efficiency and deployment of renewable energy (called A1B), which estimates an end-of-century temperature anomaly (increase) of 2.8 degrees Celsius. This has been used until recently as the mid-range scenario for climate work under the IPCC. However, this scenario may be an underestimate, as the current trajectory already far surpasses the estimates used to define it. For the analysis of the interplay between deforestation and climate change, the Amazon Dieback report uses two more scenarios, one where fossil fuels remain predominant (A2) and one with a greater penetration of renewable and more significant gains in energy efficiency (B1), with respective net increases in temperature of 3.4 to 1.8 degrees Celsius respectively, that provide a wider set of estimates than A1B.

IPPC AR 4 Coupled General Circulation Models

Climate outputs were available from the Coupled General Circulation Models (CGCMs) that participated in the Coupled Model Intercomparison Project 3 (CMIP3; coupled atmosphere-ocean models) carried out for the IPCC's Fourth Assessment Report (IPCC 2007). These data comprise the output from 24 climate models (available at https://esg.llnl.gov:8443/).

High-resolution GCM data

In addition, super-high-resolution (20 km) and high-resolution (60 km) temperature, precipitation and cloud cover simulations from the Meteorological Research Institute (MRI) and Japan Meteorological Agency (JMA) AGCM using the Earth Simulator were available for three periods: The 1979–2003 period represents the present climate conditions (P conditions). Scenario output for future conditions under the SRES-A1B emission scenario is available for the 2015–2039 period (near future, N conditions) and the 2075–2099 period (far future, F conditions).

[2] These are the CPC Merged Analysis of Precipitation for 29 years (1979–2007) on a 2.5° lat/lon grid (CMAP: Xie and Arkin 1997), the GPCP One-Degree Daily Precipitation Data Set for 10 years (1998–2007) on a 1.0° lat/lon grid (GPCP: Huffman et al. 2001), the Tropical Rainfall Measuring Mission (TRMM) PR3A25 V6 dataset for 9 years (1998–2006) on a 0.5° lat/lon grid (TRMM 3A25: Iguchi et al. 2000)

Table I.1. Projected global average surface warming and sea level rise at the end of the 21st century according to different SRES scenarios (IPCC 2007).

Case	Temperature change (°C at 2090-2099 relative to 1980-1999) [a, d]		Sea level rise (m at 2090-2099 relative to 1980-1999)
	Best estimate	*Likely* range	Model-based range excluding future rapid dynamical changes in ice flow
Constant year 2000 concentrations[b]	0.6	0.3 – 0.9	Not available
B1 scenario	1.8	1.1 – 2.9	0.18 – 0.38
A1T scenario	2.4	1.4 – 3.8	0.20 – 0.45
B2 scenario	2.4	1.4 – 3.8	0.20 – 0.43
A1B scenario	2.8	1.7 – 4.4	0.21 – 0.48
A2 scenario	3.4	2.0 – 5.4	0.23 – 0.51
A1FI scenario	4.0	2.4 – 6.4	0.26 – 0.59

Notes:

a) Temperatures are assessed best estimates and *likely* uncertainty ranges from a hierarchy of models of varying complexity as well as observational constraints.

b) Year 2000 constant composition is derived from Atmosphere-Ocean General Circulation Models (AOGCMs) only.

c) All scenarios above are six SRES marker scenarios. Approximate CO_2-eq concentrations corresponding to the computed radiative forcing due to anthropogenic GHGs and aerosols in 2100 (see p. 823 of the Working Group I TAR) for the SRES B1, AIT, B2, A1B, A2 and A1FI illustrative marker scenarios are about 600, 700, 800, 850, 1250 and 1550ppm, respectively.

d) Temperature changes are expressed as the difference from the period 1980-1999. To express the change relative to the period 1850-1899 add 0.5°C.

Sea surface temperature (SST)

Four different SSTs are used for future climate simulations by the 60-km mesh model. One experiment uses the CMIP3 model ensemble SST and sea-ice distributions as in the 20-km mesh model experiment. Second, third and fourth experiments use the SST anomalies of Australia's Commonwealth Scientific and Industrial Research Organisation (CSIRO)-Mk3.0, MRI-CGCM2.3.2 and MIROC3.2 (hires) models.

Vegetation models

Two vegetation models were used to assess biomass response to various forcings. These are the LPJmL and the CPTEC-PVM. The LPJmL is a dynamic uncoupled model. The advantage of using LPJmL for biomass response to climate is that it is a process-based model that explicitly simulates the accumulation and loss of carbon, and vegetation dynamics. The CPTEC-CPVM is a static coupled model that simulates biome distribution (one biome per grid-cell) based on bioclimatic limits. The advantage of being coupled to a climate model is that feedbacks of vegetation change to the climate can be investigated. While LPJmL simulates biomass response, CPVM focuses on simulation of anticipated biome-equilibrium states. These two instruments complement each other. A summary of the inputs, processes and outputs from each subtask is described in Table I.2.

Figure I.1. Study approach

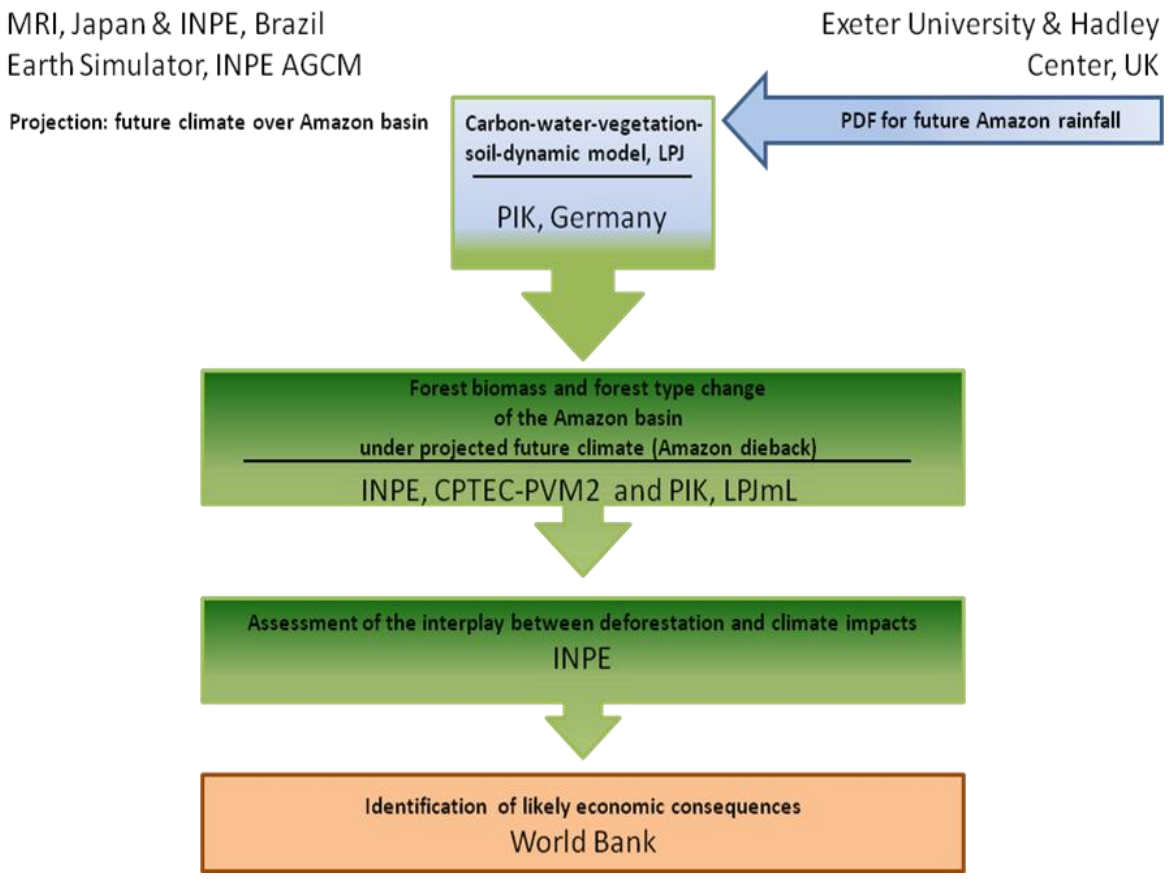

Table I.2. Summary of inputs, processes and outputs for each task

Task	Inputs	Emission trajectory	Process	Outputs
High-resolution simulation of future climate in the Amazon basin	MRI-GCM data (Earth Simulator)	A1B	High-resolution simulation to end of century though Earth Simulator	Future climate over the basin; projection of extreme events
Assessment of future rainfall over the Amazon basin	CMIP-3 data (ensemble of 24 General Circulation Models)	A1B	Use of an Amazon climate prediction index to qualify CMIP-3 outputs	Projected rainfall (weighted by model's ability to predict current climate) in the form of Probability Density Functions (PDF) of future rainfall
Forest biomass estimate	PDF results for future rainfall	A1B	LPJmL (dynamic uncoupled vegetation model)	Biomass response (weighted by rainfall prediction index); PDF for future biomass
Interplay of climate and deforestation	CMIP-3	A2-B1	CPTEC-CPVM (static coupled vegetation model)	Biome shifts in the Amazon basin

Figure I.2. Geographical Domains. Eastern Amazonia (EA; 2.5°N-5°S; 45°W-55°W);Northwestern Amazonia (NA; 5°N-5°S; 60°W-72.5° W); Southern Amazonia (SAz; 10°S-17.5°S; 50°W-65°W;Northeastern Brazil (NEB; 2.5°S-15°S; 35°W-45° W; Southern Brazil (SB; 22.5°S-35°S; 45°W-60°W)

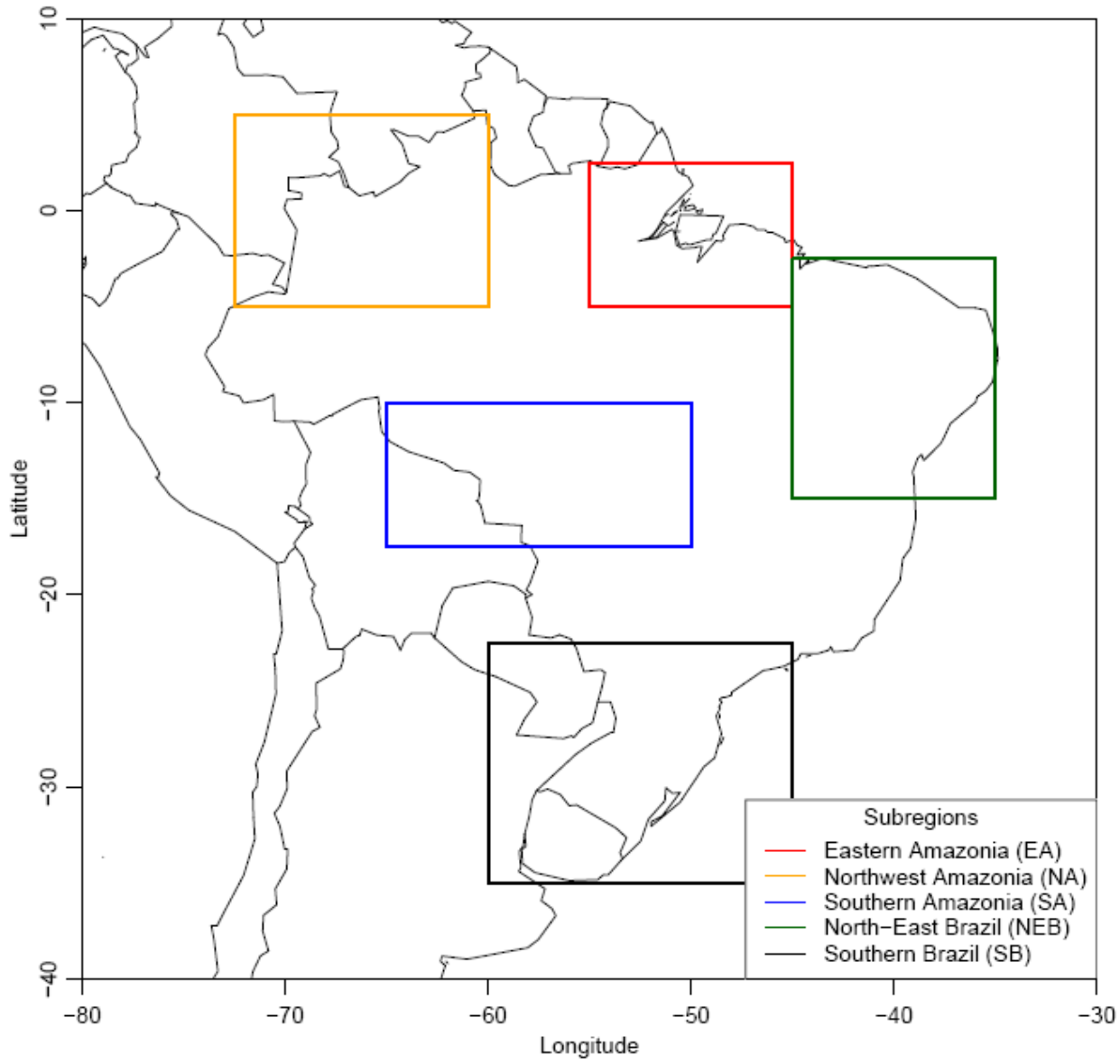

II. Modeling future climate in the Amazon using the Earth Simulator

1. THE MRI/JMA AGCM AND THE EARTH SIMULATOR

As indicated in Section I, the Fourth Assessment Report of the Intergovernmental Panel on Climate Change (AR4) uses a dataset of 24 global coupled atmosphere-ocean general circulation models (AOGCM, or GCM for short) to project future climate under various scenarios. The use of numerous models is intended to reduce errors and uncertainty. However, most of these models have a very coarse resolution (100–400km) and this has an undesirable impact on results, particularly as it relates to extreme weather events. This is because global warming would result not only in changes in mean climate conditions but also in increases in the amplitude and frequency of extreme events that would not be captured in a meaningful way with coarse resolutions. Moreover, changes in extremes are more important for assessing adaptation strategies to climate changes. Therefore, a high spatial resolution model is required to study extreme weather events and to project their intensity and frequency for adaptation studies and measures.

The Meteorological Research Institute of the Japan Meteorological Agency (MRI/JMA) atmospheric GCM is a super-high resolution atmospheric general circulation model with a horizontal grid size of about 20 km (Mizuta et al. 2006), offering an unequaled high-resolution capability. The use of the supercomputer called the Earth Simulator made this super-high-resolution model's long-term simulation possible. The atmospheric GCM is a global hydrostatic atmospheric general circulation model developed by the MRI/JMA. This model is an operational short-term numerical weather prediction model of JMA and part of the next-generation climate models for long-term climate simulation at MRI. The data generated by the Earth Simulator was made available under the five-year Memorandum of Understanding between MRI and the World Bank.

Although the global 20-km model is unique in terms of its horizontal resolution for global change studies with an integration period up to 25 years, available computing power is still insufficient to enable ensemble simulation experiments and this limits its application to a single member experiment. To address this limitation, parallel experiments with lower resolution versions of the same model (60-km, 120-km and 180-km mesh) were performed. In particular, ensemble simulations with the 60-km resolution have been performed and compared with the 20-km version for this study.

The MRI-GCM was used to project climate in the Amazon basin to mid-century (2035–2049) and to the end of the 21st century (2075–2099) and compared these projections to the present (1979–2003) under scenario A1B,[3] which projects a temperature increase of between 1.3 and 3.5 degrees Celsius by the end of the century. The analysis was done primarily to assess rainfall,

[3] Today's emissions trajectory is already well above the A1B scenario. Therefore, this scenario may no longer represent a plausible future.

runoffs and extreme events, and to estimate the anticipated impact on stream flows induced by climate change. Results on rainfall, moisture and evaporation are also reported and later compared with other model outputs in subsequent sections of the report. The simulations were performed at a grid size of about 20 km and routinely compared with 60-km mesh ensemble runs to ascertain robustness. A detailed description of the model and its performance in the 10-year present-day simulation with sea surface temperature (SST) can be found in Mizuta et al. (2006).

2. COMPARISON OF OBSERVED AND SIMULATED DATA, FOR PRESENT TIME, OVER THE AMAZON BASIN

Seasonal mean precipitation reproduced in the simulation is evaluated against available observed data. Figure II.1 shows the geographical distribution of December–February (DJF) averaged for a 25-year period (1979–2003) of mean precipitation for 180-km, 120-km, 60-km and 20-km resolutions. Observations show large seasonal mean precipitation in the austral summer over the Amazon basin. The Intertropical Convergence Zone (ITCZ) over the tropical Atlantic, and the South Atlantic Convergence Zone (SACZ) to the southeast of the Brazilian Plateau, are also well reproduced. The precipitation maximum over the Amazon tends to locate northwest of observed data.

Figure II.1. Geographical distributions of December–February (DJF) mean rainfall (mm d^{-1}) over the Amazon basin. Plots (a-d) correspond to data-sets of actual observations; Plot (e) is 180-km model, (f) 120-km model, (g) 60-km model and (h) 20-km MRI-GCM model.

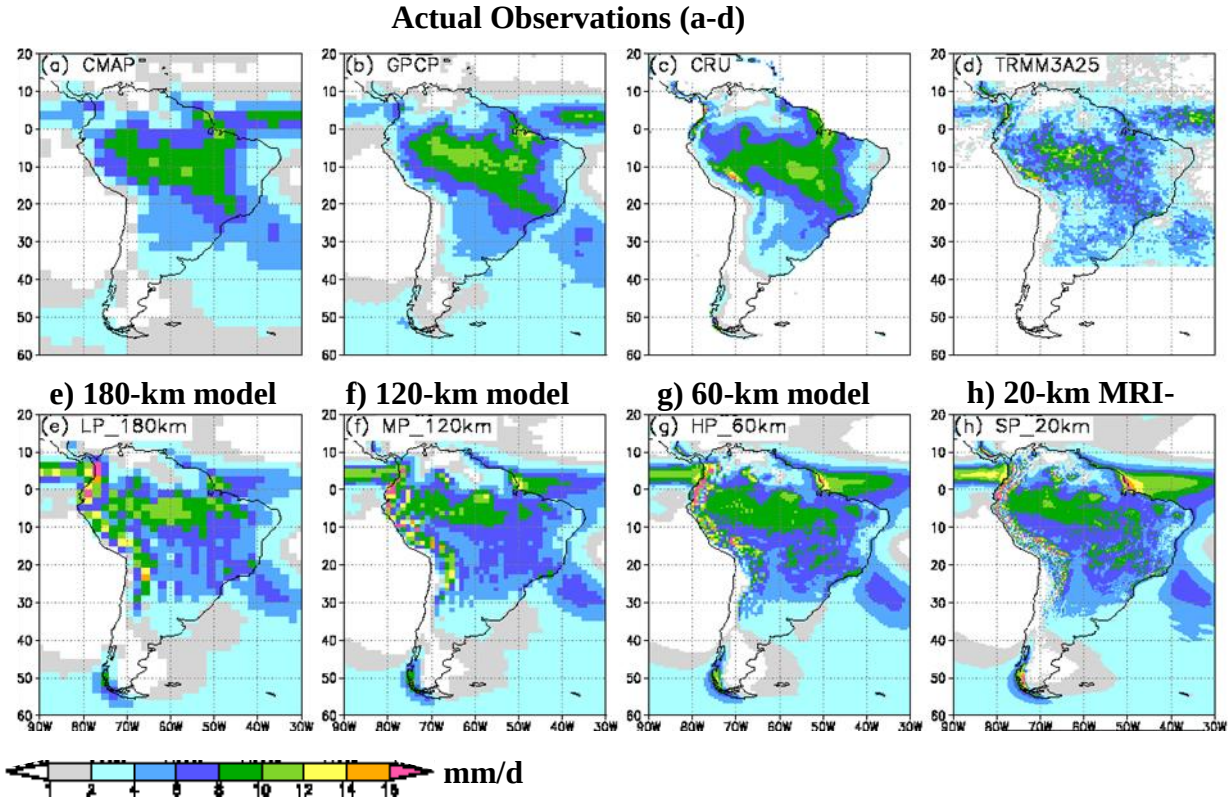

Figure II.2. Geographical distributions of June-August (JJA) mean rainfall (mm d^{-1}) over the Amazon basin. Plots (a-d) correspond to data-sets of actual observations; (e) 180-km model, (f) 120-km model, (g) 60-km model and (h) 20-km MRI-GCM model.

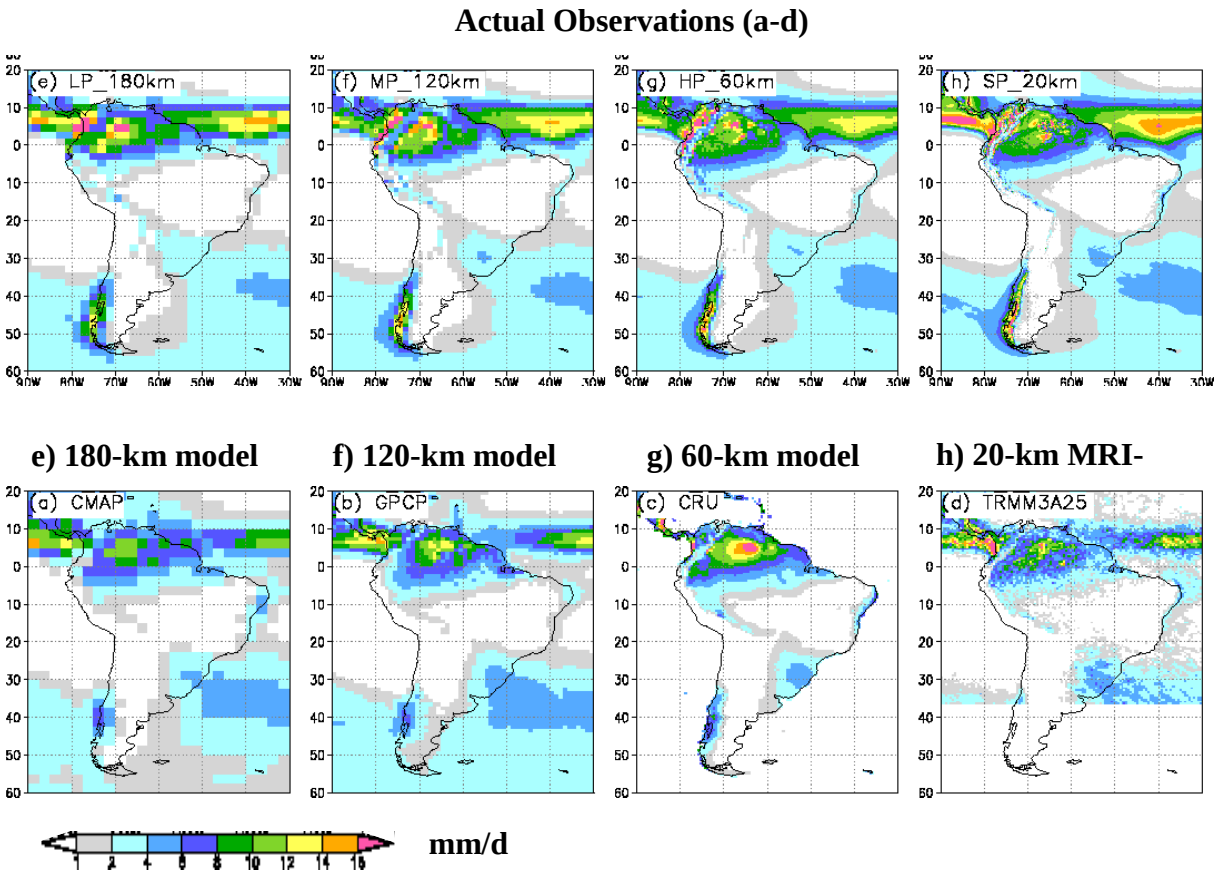

There are no distinct differences in large-scale patterns of precipitation with different horizontal resolutions. Figure II.2 shows the June–August (JJA) mean precipitation climatology of the four observed SST datasets and the model at different scales. During this season, a major rain area moves northward and large precipitation is found over northern South America while it is very dry over Northeastern Brazil and Southern Amazonia. Southern Brazil is covered with a rainy area extending from the South Atlantic. The Earth Simulator reproduces these rainfall distributions quite well.

3. PROJECTION OF FUTURE CLIMATE OVER THE AMAZON BASIN

3.1 Rainfall

Projected changes at the end of the 21st century (2075–2099) were compared to the present (1979–2003). An overall pattern of precipitation change simulated by the 20-km and 60-km

models is similar to that of ensemble means of CMIP3 models reported in IPCC (2007) with a large increase in the tropics, an increase in the mid- and high latitudes and a decrease in the subtropics. Four different boundary conditions (sea surface temperature change experiments) were undertaken. Figure II.3 shows the annual mean precipitation change between the present and the future at a 60-km resolution for four different SSTs, that is, CMIP3 ensemble SST, CSIRO SST, MIROCH SST, and MRI SST. The general pattern of precipitation changes is similar and thus robust among different SSTs used, with a large increase in precipitation over the ITCZ and the Northwestern Amazon and reductions in the Northeast and in the South.

Figure II.3. Annual mean precipitation changes (mm d^{-1}) between the present and the end of the 21st century for 60-km resolution for different sea surface temperatures [(a) CMIP3 ensemble SST, (b) CSIRO SST, (c) MIROCH SST, and (d) MRI SST]. Areas statistically significant at 95% level are colored. Contour interval is 1 mm d^{-1}.

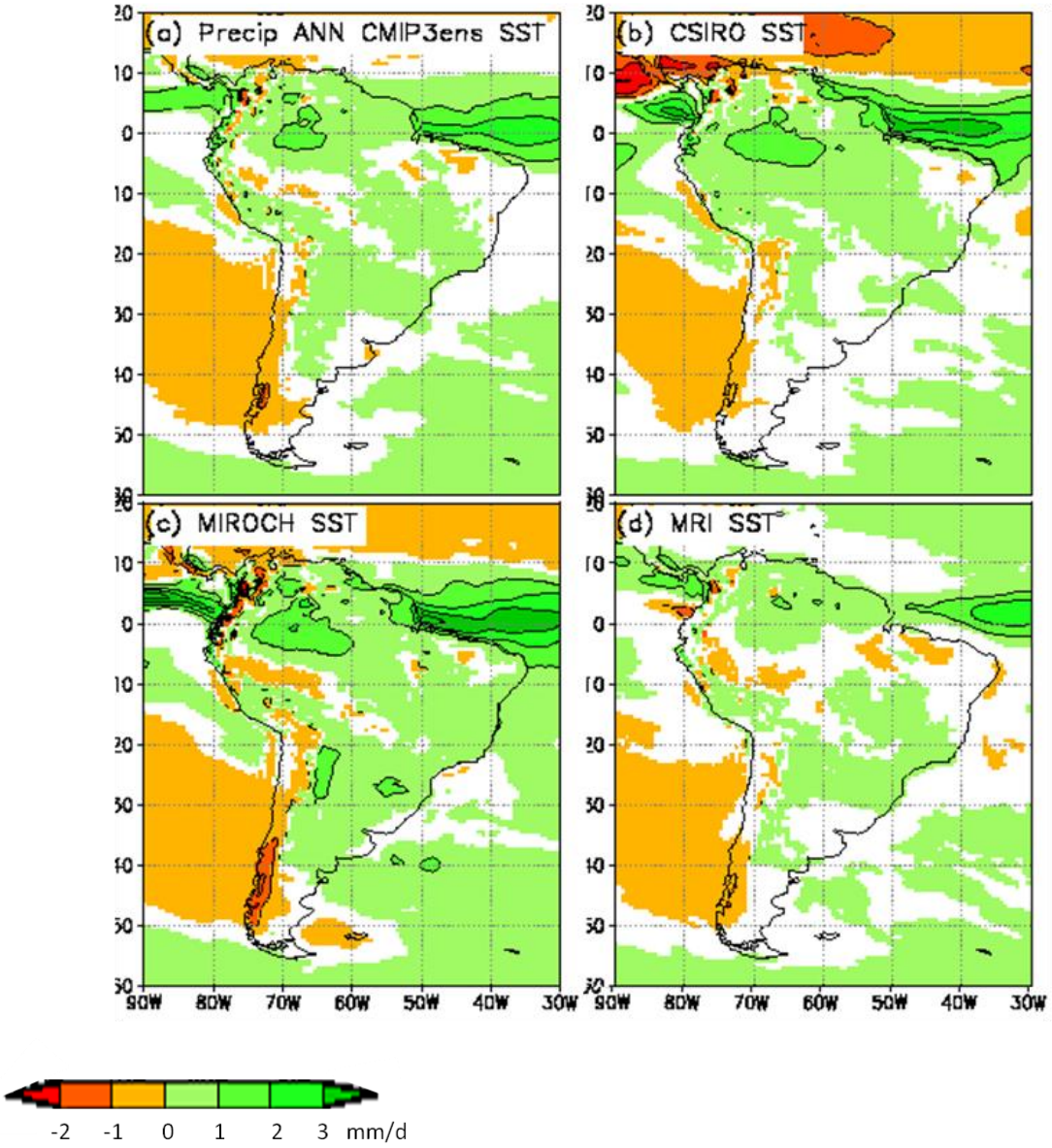

3.2 Evaporation, soil moisture and surface runoff

Due to the temperature increase, seasonal mean changes in evaporation, soil wetness at the uppermost layer, and surface runoff between the present and the future are anticipated. Evaporation increases are projected throughout the year over almost all of South America. An exception is Northeastern Brazil where evaporation is projected to decrease in the dry season (June, July, August and September, October, November). This is associated with drier soil over that region (Figure IV). Drier soil is not restricted to Northeastern Brazil but is projected to occur over most of the continent, particularly in the dry season. Even in the wet season (DJF), the Amazon is expected to be much drier at the uppermost layer of the soil.

Figure II.4. Seasonal changes in soil moisture in topsoil (in %) between the present and the end of the 21st century for 60-km and 20-km resolution. For 60-km, areas statistically significant at 95% level are colored, and areas where all four different SST experiments show consistent changes in sign are hatched. For 20-km model, areas statistically significant at 90% level are colored. Contour interval is 1 mm d^{-1}.

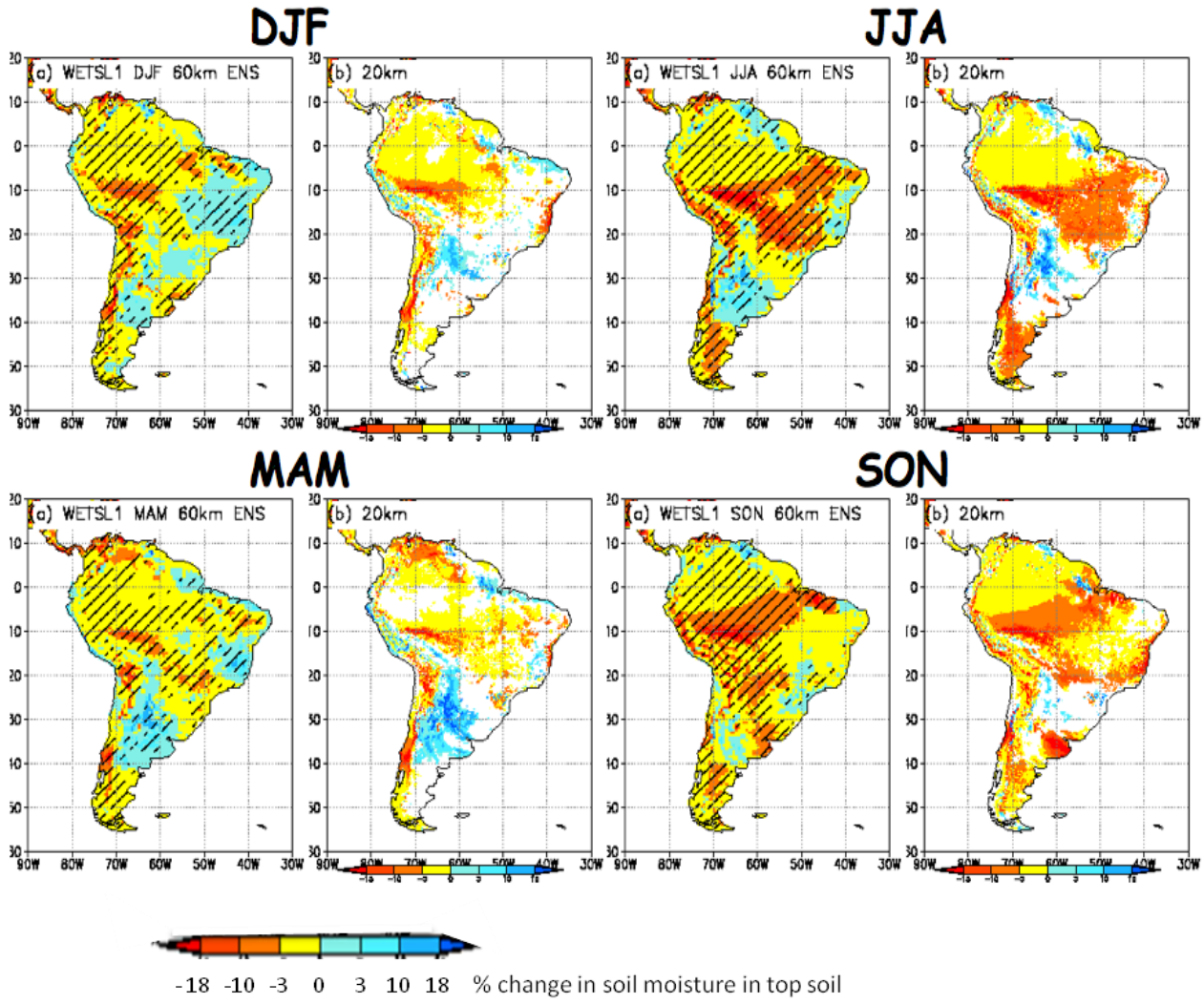

Significant changes in runoff are predicted for some regions. In September, October, November, and December, January, February, runoff in the Western Amazon will decrease while it increases in Eastern and Southern Brazil. In March to May, Northwestern Amazonia experiences more runoff. Further analyses should be conducted to better ascertain regional hydrological changes.

3.3 Extreme events

Global warming will result not only in changes in mean conditions but also in increases in the amplitude and frequency of extreme precipitation events. Changes in extremes are more important for the visualization of adaptation measures. Two extreme indexes for precipitation are used to illustrate changes in precipitation extremes over the Amazon, one for heavy precipitation and one for dryness. Figure II.5 shows the changes in the maximum 5-day precipitation total in mm (RX5D) for the 60-km and 20-km resolution. Throughout the basin, RX5D is projected to increase in the future. The largest RX5D increases (rainfall intensification) are found over the Northwestern Amazon and Southern Brazil. At a higher resolution (20-km), the model projects even larger increases in RX5D by the end of the century.

Figure II.5. Changes in maximum 5-day precipitation total (mm) between the present and the end of the 21st century for (a) 60-km and (b) 20-km, respectively. For 60-km model, areas where all four different SST experiments show consistent changes in sign are hatched. Zero lines are contoured.

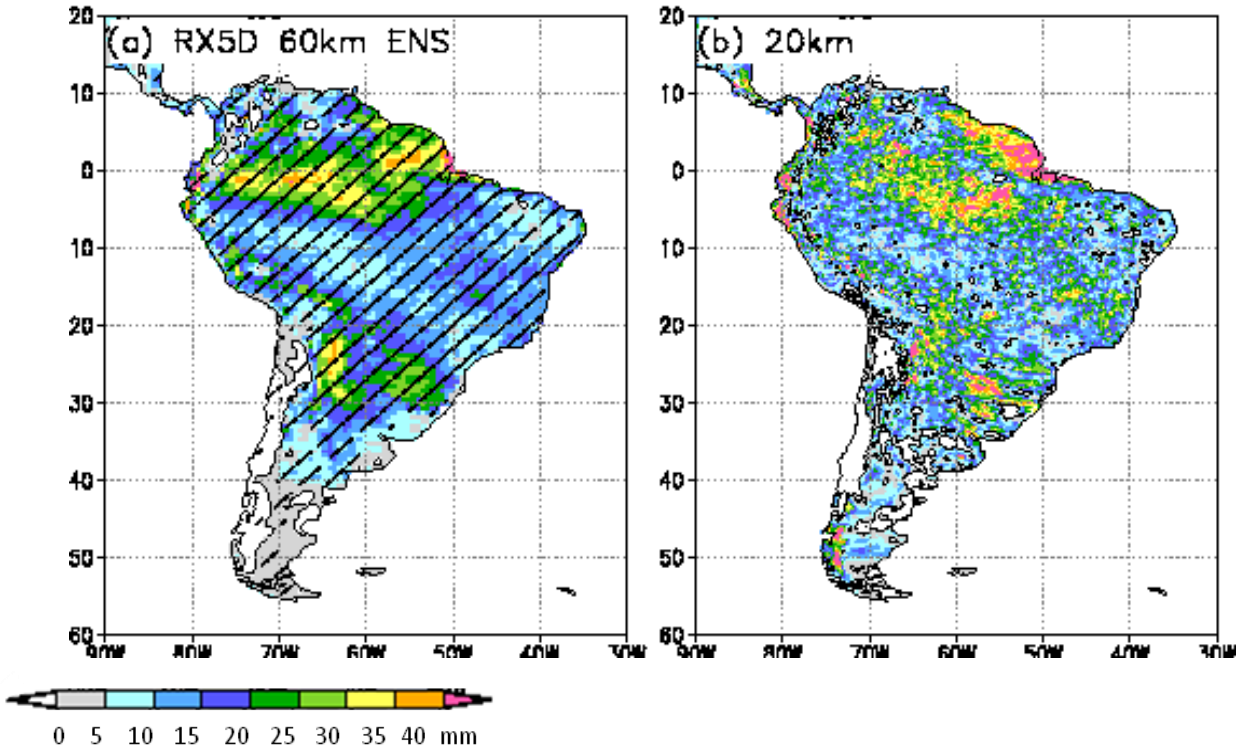

Likewise, Figure II.6 shows the changes in maximum number of consecutive dry days (CDD). A "dry day" is defined as a day with precipitation of less than 1 mm d^{-1}. Large CDD change is projected over the entire basin.

Figure II.6. The same as in Figure 5 except for consecutive dry days (day)

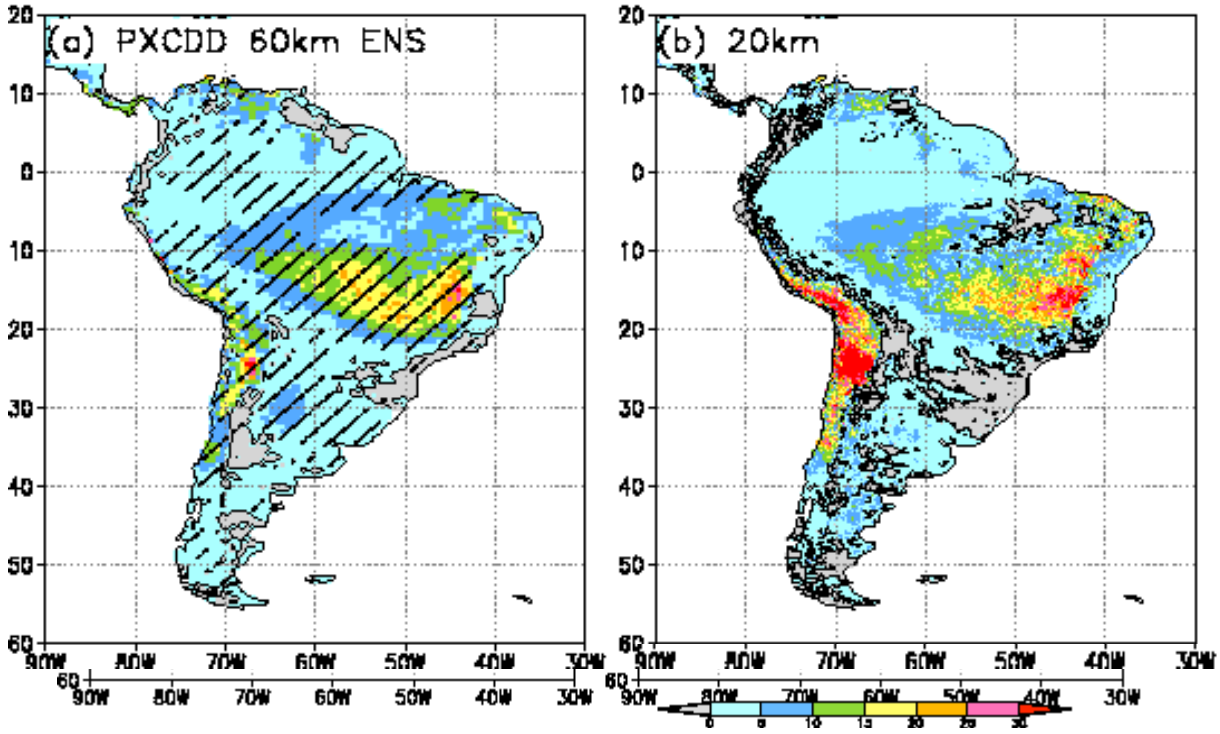

In the present-day simulation, some intermittent rain occurs in the dry season, which is approximately from June to August over the Amazon. This intermittent rain in the dry season is confirmed by ground-station data. In the future climate simulation, this rainfall during the dry season vanishes (Figure II.7), and thus stronger CDD signals are induced. Kamiguchi et al. (2006) analyzed future increases in CDD over the Amazon using a former experiment dataset with the 20-km mesh model. They found that in the present-day simulation, when rain takes place in the dry season, equatorial easterly low-level wind from the ITCZ hits the Andes and deviates to the south, bringing scattered clouds to the middle of the Amazon. In the future climate, a weak Walker circulation[4] associated with the El Niño-like SST changes and a weak Atlantic anticyclone contribute to the weakening of the equatorial easterly wind and the suppression of rainfall over Amazon.

The analysis of future increases in CDD over the Amazon is probably one of the most important findings of the application of the Earth Simulator to the future climate in the basin and could

[4] The Walker circulation is an ocean-based system of air circulation that influences weather on the Earth. The Walker circulation is the result of a difference in surface pressure and temperature over the western and eastern tropical Pacific Ocean (UCAR 2008. Online at: http://www.windows.ucar.edu/tour/link=/earth/Atmosphere/walker_circulation.html).

have significant implications for the forests' resilience (increased vulnerability) to drought periods.

Figure II.7. Ten-year run of daily rain during the dry season at Armiquedes (present [blue] vs. future [red]). Present includes current decade; future, a decade at the end of the century. The graphs indicate that intermittent dry-season rainfall in the Amazon basin is projected to disappear.

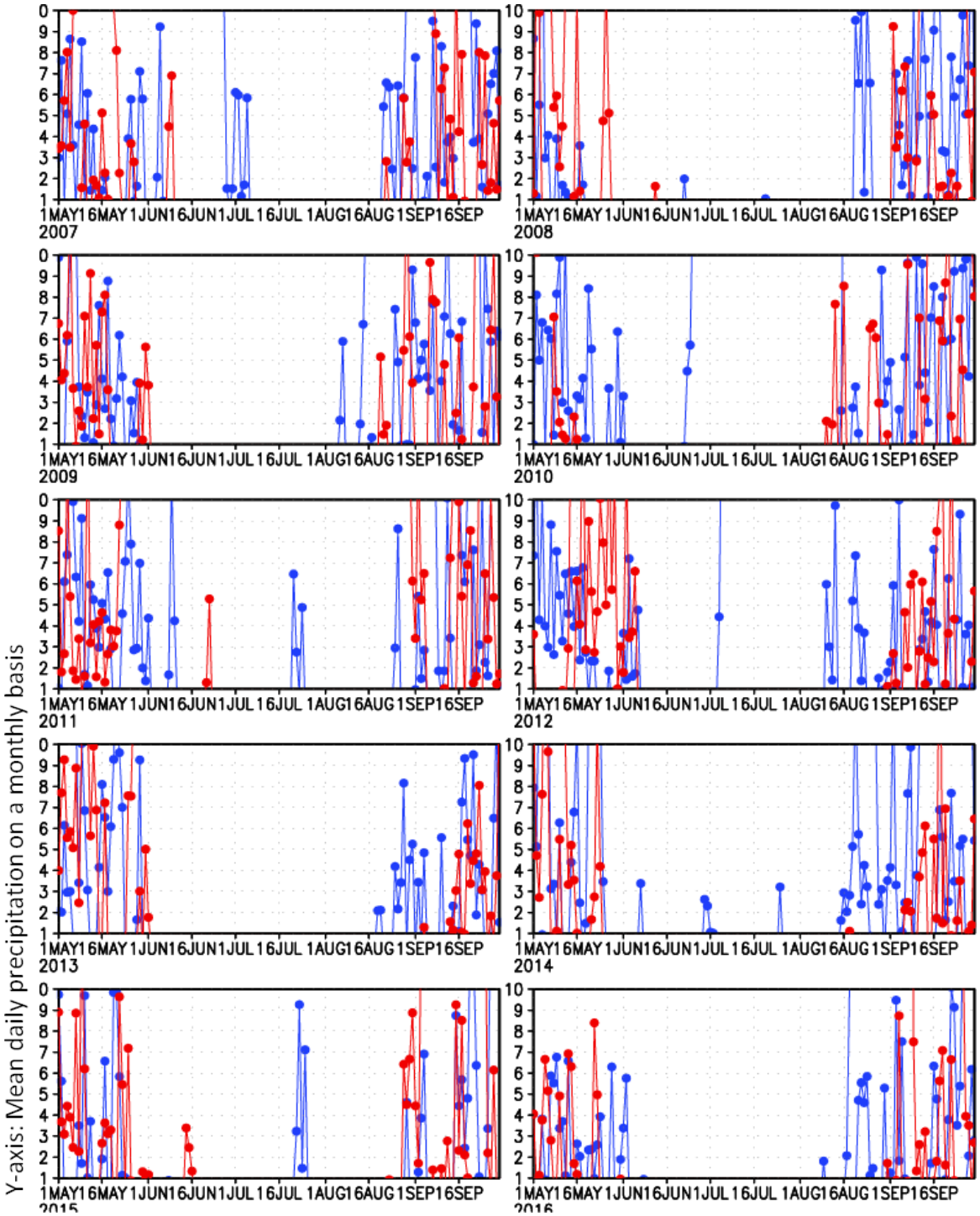

3.4 Impact on river stream flow

Using the runoff data derived from rainfall projections of the Earth Simulator, the stream flow of large rivers was calculated. The analysis used a "GRive T" river model.[5] In the present-day simulation, large rivers such as the Amazon and Parana are well represented by this model. The seasonal changes in the Amazon basin's discharges have been analyzed. The study selected the Obidos observation site situated between Northwestern Amazonia and Eastern Amazonia. The model simulates well the present seasonal cycle of stream flow. The end-of-century projection shows that the annual range of stream flow becomes larger (higher peaks and lower nodes), implying more floods in the wet season and more pronounced droughts in the dry season. This is consistent with the findings for RX5D and CDD.

Finally, the analysis included the impacts on seasonal flows of selected rivers in the Amazon. Figure II.8 (left) shows the seasonal change in the discharges of the Rio Madeira by the 20-km mesh model at the nearest grid point to the observation site at Porto Velho (64.5°W, 9.3°S). The dashed line is for the present and the solid line is for the end of the 21st century. Long-term mean values (indicating the range of interannual standard deviations by shadings) of river discharge at observation points (Porto Velho) by the Global River Discharge Center (GRDC) are shown together. This point is situated at the exit of the river from Southern Amazonia. The 20-km mesh model reasonably reproduces the present seasonal cycle of stream flow at this point with maximum flow in March and minimum flow during August–October. The model simulation does not include any anthropogenic effects in river flows (diversions, reservoirs). It is projected that in the future, compared to today, stream flow will increase at the peak flow season (February–April) while it decreases during the late dry season.

Figure II.8 (right) shows the seasonal change in the discharges of the Amazon River by the 20-km mesh model at the nearest grid point to the observation site at Obidos (55.8°W, 2.5°S). This point is situated between Northwestern Amazonia and Eastern Amazonia. Again, the model well reproduces the present seasonal cycle of stream flow at this point, but with some underestimation during low flow season.

It is projected that future stream flows in the Amazon basin will increase in the high-flow season and decrease in the low-flow season. It is also projected that the peak month of the high-flow season may be delayed and the high-flow season may become longer. It is noted that the annual range of stream flow becomes larger, implying more floods in the wet season and droughts in the dry season. For example, as a result of the intensification of the precipitation cycle and the increase in evaporation, the Amazon River projects higher amplitude in flows from 200,000 to nearly 230,000 m^3/s for the peak flow and from 80,000 to 60,000 for the lower flows.

[5] GRiveT: Global Discharge model using Total Runoff Integrating Pathways (TRIP), the 0.5 x 0.5 version with global data for discharge channels; Nohara et al. (2006). The river runoff assessed in the land surface model is horizontally interpolated as external input data into the TRIP grid so that the flow volume is saved.

Figure II.8. Monthly stream flow ($m^3 s^{-1}$) for (left) Rio Madeira and (right) Rio Amazonas. Blue shadings denote the observed measurements by GRDC with interannual standard deviations. Observed data are at Porto Velho (64.5°W, 9.3°S) and at Obidos (55.8°W, 2.5°S). The heavy dashed line and the heavy red solid line denote the simulated stream flow for the present (1979–2003) and in the future (2075–2099), respectively.

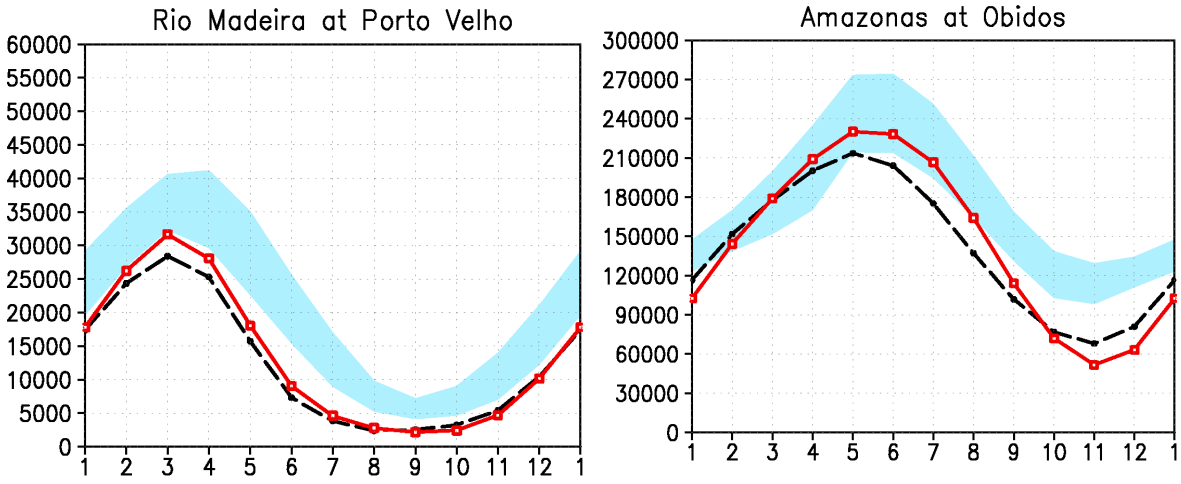

III. Assessment of future rainfall over the Amazon basin

The modeling at very high resolution by the Earth Simulator, although remarkable in its level of detail and unique in its ability to discern extreme events, represents the outcome of only one model applied to one scenario. It does confirm the expected intensification of the water cycle and, through the use of the 60 km ensembles, provides a level of robustness to its results. However, there remains a need to reduce uncertainties on modeling results over Amazonia, in particular as it concerns the projections related to rainfall, where there is considerable variance in modeling results.

Some GCMs predict increasing rainfall over the basin, while others predict drying (Li et al. 2006). In at least one major model the rainfall reduction is so severe as to undermine the status of the rainforest—leading to "dieback" (Cox et al. 2000; Cox et al. 2004; Cox et al. 2008). This section describes the development of *Probability Density Functions (PDFs)* [6] for future Amazonian rainfall, based on the projections produced by the 24 GCMs in use by the IPCC (and included in the CMIP3 archive) as a possible mechanism to reduce uncertainties in projected rainfalls in the region.

Table III.1. GCMs in the CMIP3 archive

Model Identifier	Model Name	Model Identifier	Model Name
a	bccr_bcm2.0	m	ingv_echam4
b	ccma_cgcm3_1	n	inmcm_3_0
c	ccma_cgcm3_1_t63	o	ipsl_cm4
D	cnrm_cm3	p	miroc3_2_hires
E	csiro_mk3.0	q	miroc3_2_medres
F	csiro_mk3.5	r	miub_echo_g
G	gfdl_cm2.0	s	mpi_echam5
H	gfdl_cm2.1	t	mri_cgcm2_3_2A
I	giss_aom	u	ncar_ccsm3_0
J	giss_model_e_h	v	ncar_pcm1
K	giss_model_e_r	w	ukmo_hadcm3
L	iap_fgoals1_0_g	x	ukmo_hadgem1

These GCMs produce very different predictions of rainfall in the selected geographical domains and also very different simulations of current climate in these regions (see Figure III.1). Most GCMs tend to overestimate rainfall in Northeastern Brazil but underestimate rainfall in the other four regions. The trends in 21st century rainfall vary from about +1 mm/day/century (e.g., Model "o" in the EA and NEB regions) to a drying of -2mm/day/century (e.g., Model "w" in the EA).

[6] Probability Density Functions (PDFs) define the probability that a particular variable (in this case Amazonian rainfall) falls within a given range. They can therefore be used to estimate the probability that the rainfall is less than some critical value that could lead to forest dieback.

Figure III.1. Simulation of mean annual rainfall in the 20th century (x-axis) and rainfall trend in the 21st century (y-axis) in the five study regions of Amazonia. The vertical dotted line is the observed rainfall in the 20th century. The CMIP3 GCMs are labeled as in the table above.

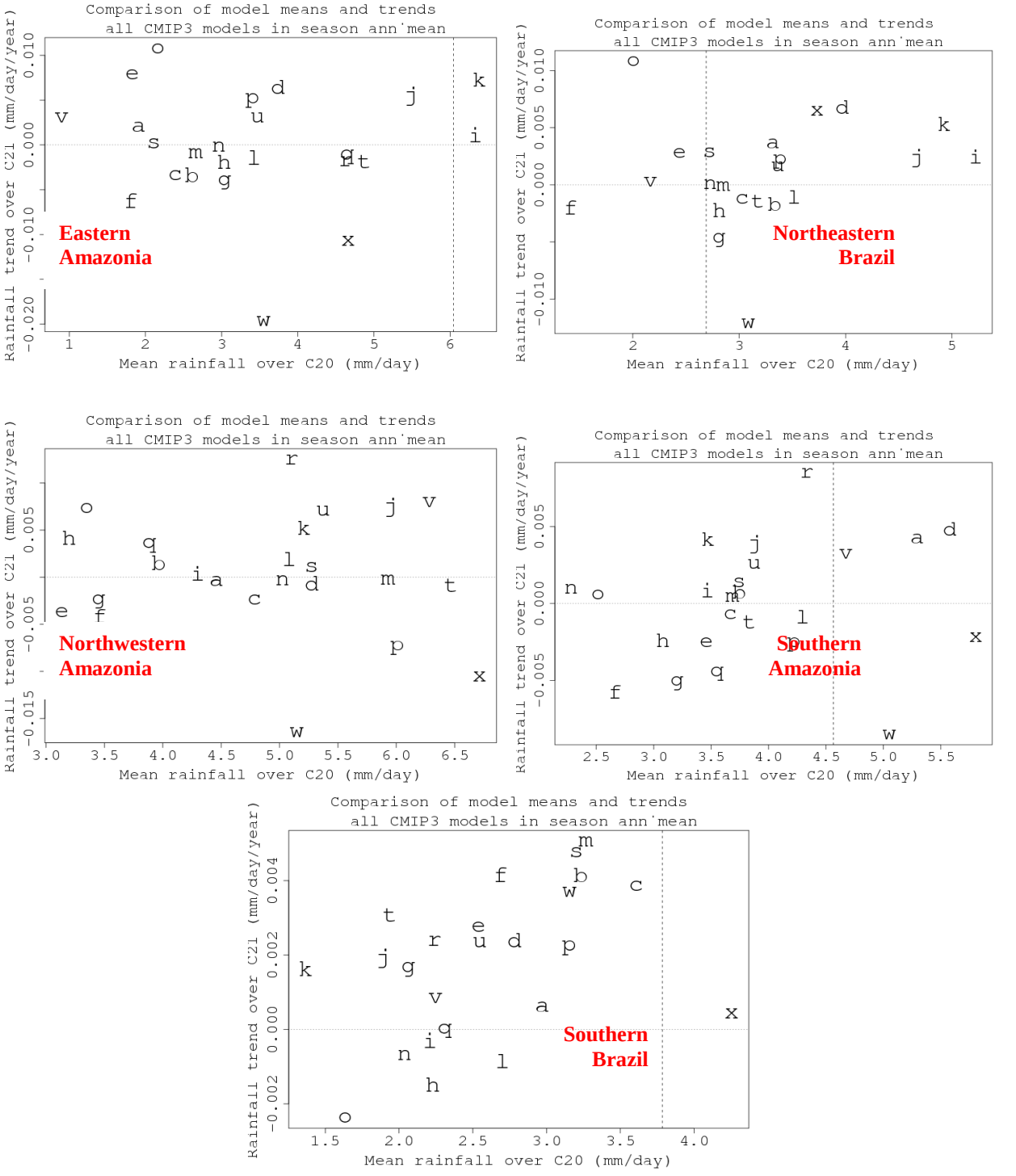

1. METHOD FOR ESTIMATING PROBABILITY DENSITY FUNCTIONS (PDFS)

One way to address uncertainty in future rainfall is to weight the various model projections based on the ability of each model to produce key aspects of the observed climate. In this way more robust predictions may be found by emphasizing the results from more realistic models and de-emphasizing the results produced by less realistic models.

The approach followed is to construct a probabilistic prediction based on a *weighted* sum of the predictions of individual GCMs, using a Bayesian approach.[7] The weight assigned to each GCM will be referred to as *the probability of the model* and will generate a probability density function (PDF) over the set of models.[8]

This procedure can be used to estimate PDFs for future rainfall in each of the five regions, using simulations produced by the 24 GCMs available in the archive of the *Coupled Model Intercomparison Archive Project (CMIP3)*. Two approaches are used to weight the respective model outputs, the first based purely on the rainfall simulated by each GCM (see below), and the second using the observed correlation between Amazonian rainfall and sea surface temperature anomalies in the Atlantic and Pacific Oceans (see below).

1.1 Models weighted according to rainfall projections

There is a need to capture errors in the simulation of the mean climate and its variability, so that the models are penalized for both the bias in the mean rainfall simulation and the Kolmogorov-Smirnov statistic[9] of the bias-corrected rainfall. Using these metrics and the Bayesian approach described in the footnote, relative model weightings for each season ("DJF," "MAM," "JJA," "SON") are derived, as well as for the entire calendar year ("ann_mean"), for each geographical domain. The annual mean weights, which have subsequently been used to weight the projections of the LPJ dynamic global vegetation model (see Section IV), are shown in Figure III.2.

The approach utilized results in the selection of some models ahead of others, with just a minority of models being favored in each region. The number of models with more than the mean weighting is between six and nine depending on the region, with most of the other models

[7] Bayes's theorem allows the model probabilities to be modified each time one considers the ability of the models to simulate some relevant aspect of current climate (such as rainfall in each season). This updating of the PDF is achieved by comparing time series of past observations with time series of model simulations for each variable.

[8] This updating of the PDF is achieved by comparing time series of past observations with time series of model simulations for each variable. In this study models are weighted based on their ability to simulate both the mean state and the variability (i.e., the statistical distribution) of current climate. In other words, the aim is to down-weight those models which simulate a climate whose mean value is far from the observed mean, or a climate whose statistical distribution is a poor fit to the observed distribution, even when any bias in the mean value has been corrected. The procedure can be summarized as follows:

(i) assign equal probability to all models—a *uniform prior* PDF; choose a climatic variable of interest;
(ii) update the model PDF based on the fit between model simulations and observations for this variable;
(iii) treat the current model PDF as a new prior, and repeat steps (i) and (iii) as required;
(iv) obtain a final posterior PDF for the models.

[9] The Kolmogorov-Smirnov statistic can be easily calculated using standard statistical software packages; it is used to measure distributional adequacy in a sample.

receiving very low weights. However, the most trusted models vary significantly between the regions, and no single model has above-average weighting for all five regions. In any one region, it is also unusual for a given model to simulate rainfall accurately in all four seasons.

However, the procedure distinguishes strongly among the models. Figure III.3 shows example PDFs and Cumulative Distribution Functions (CDFs) for Southern Amazonia, in each case for the 2001–2031 (black) and 2068–2098 (red) periods. The figure also shows the difference between the prior distributions (dotted lines), which were derived by assuming all models to be equally likely, and the posterior distributions (continuous lines), which were derived using the outlined procedure. In most cases weighting the models by their relative abilities to produce the current rainfall leads to sharper PDFs. In some cases the weighting also shifts the most likely future rainfall significantly.

The regions and seasons where significant changes in the rainfall PDF are predicted to occur during the 21st century include: Northwestern Amazonia, which is predicted to become wetter in the DJF and MAM periods; and Southern Amazonia, which has an increased probability of 2005-like drought conditions in the SON pre-wet season (see bottom-left panel of Figure III.3).

The probability of annual rainfall being less than 3 mm/day was also calculated for each of the five regions. The results are summarized in Table III.1.

Table III.1. Probability of annual rainfall being less than 3mm/day for each of the five study regions of Amazonia.

Region	**Probability 2001–2030**	**Probability 2068–2098**
EA	**0%**	**0.7%**
NEB	**80%**	**76%**
NWA	**0%**	**0%**
SAz	**0%**	**0.1%**
SB	**1.1%**	**6.8%**

Figure III.2. Relative CMIP3 model weightings based on simulation of annual rainfall (mean and variability) for the five land regions of Amazonia: Eastern Amazonia (EA)–top left, Northeastern Brazil (NEB)–top right, Northwestern Amazonia (NWA)–middle left, Southern Amazonia (SAz)–middle right, and Southern Brazil (SB)–bottom. The CMIP3 GCMs are labeled as in Table I.1.

Figure III.3. Changes in modeled rainfall distributions for Southern Amazonia. Cumulative Distribution Functions (CDFs) are shown on the left and Probability Density Functions (PDFs) are on the right. Black lines represent the 2001–2030 period and red lines show 2068–2098. The dotted lines are based on a uniform prior in which all model projections are considered equally likely, and the continuous lines are from the Bayesian weighting procedure based on the rainfall simulations of each model. Note the increased probability of extreme wet conditions in DJF, and extreme (2005-like) dry conditions in SON.

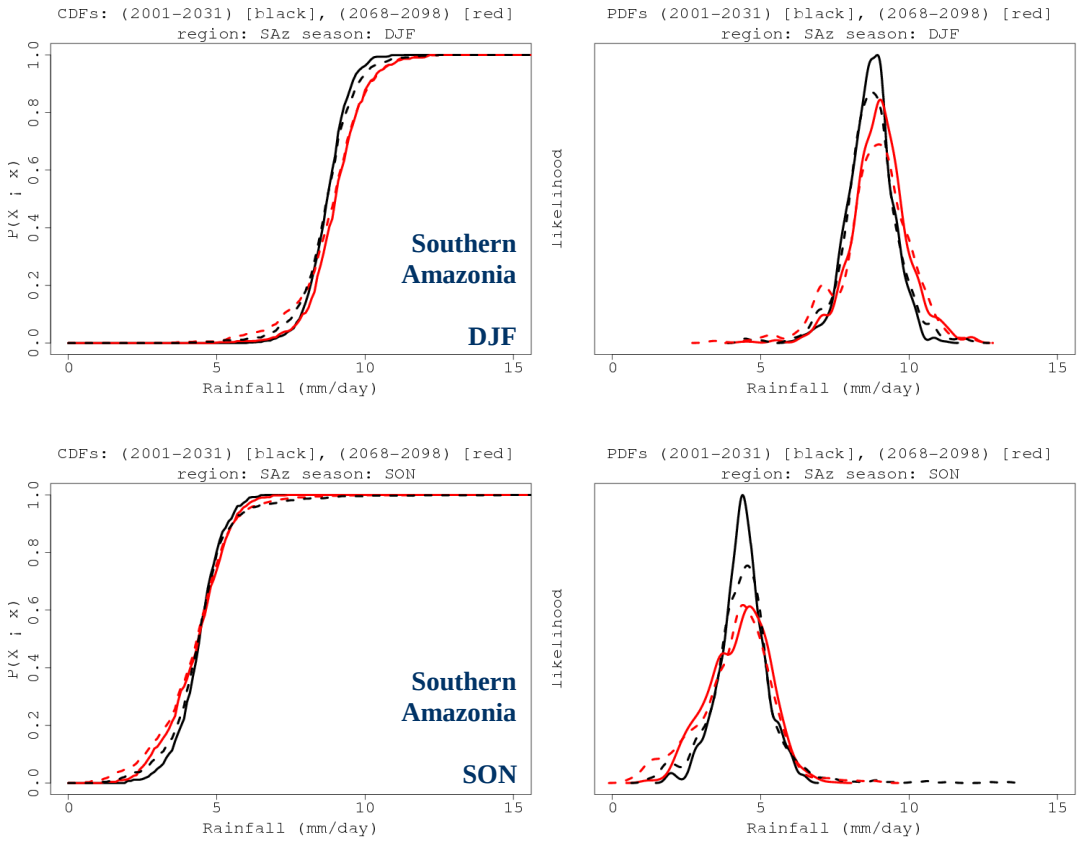

1.2 Models weighted according to SST indexes

Rainfall in Amazonia is also known to be sensitive to seasonal, interannual and decadal variations in sea surface temperatures (Marengo 2004). For example:

a) Warming of the tropical East Pacific during El Niño events suppresses wet-season rainfall through modification of the (East-West) Walker Circulation and through the Northern Hemisphere extra-tropics (Nobre and Shukla 1996). El Niño-like climate change (Meehl and Washington 1996) has similarly been shown to influence annual mean rainfall over South America in GCM climate change projections (Cox et al. 2004; Li et al. 2006);

b) Warming of the tropical North Atlantic relative to the South leads to a northwestward shift in the Intertropical Convergence Zone (ITCZ) and compensating atmospheric descent over Amazonia (Liebmann and Marengo 2001; Fu et al. 2001; Cox et al. 2008). For Northeastern Brazil the relationship between the North-South Atlantic SST

gradient and rainfall is sufficiently strong to form the basis for a seasonal forecasting system (Folland et al. 2001). Variations in SSTs in the tropical Atlantic and Pacific contribute in different ways to rainfall variability in the regions of Amazonia (Cox and Jupp 2008).

Multiple linear regressions of rainfall are reported in the various land regions of South America against indexes of the Pacific East-West SST gradient (PEWG) and the Atlantic North-South SST gradient (ANSG), based on observational data (New et al. 2000; Rayner et al. 2003).[10] Rainfall is correlated in the five selected regions against the *ANSG*, which is the SST difference between the tropical North Atlantic [75°W–30°W, 15°N–35°N] and the tropical South Atlantic [40°W–15°E, 25°S–5°S]; and the *PEWG* which is the SST difference between the tropical East Pacific [150°W–90°W, 5°S–5°N] and the tropical West Pacific [120°E–180°E, 5°S–5°N]. Linear correlations were carried out for each season (December to February=DJF; March to May=MAM; June to August=JJA; September to November=SON) and also for the annual mean.

The computed correlation coefficients and their uncertainties (given as a standard deviation) were calculated and are available upon request from the authors. From these, some significant impacts of *ANSG* and *PEWG* on rainfall in the designated regions were inferred. For example:

- An anomalously positive ANSG (i.e., 2005-like conditions in which the North Atlantic warms relative to the South) leads to reduced rainfall year-round in Northeastern Brazil, and from July to November in Eastern Amazonia.

- An anomalously positive PEWG (i.e., El Niño-like conditions in which the East Pacific warms relative to the West) leads to reduced rainfall in the East (Northeastern Brazil and Eastern Amazonia) but to increased rainfall in the South (especially in Southern Brazil).

2. GCM SIMULATION OF CURRENT AND FUTURE SST INDEXES

Given the observed correlation between the ANSG and PEWG indexes and Amazonian rainfall, the simulation of these indexes by the models is likely to have relevance to the simulation of rainfall in the future. The left panel of Figure III.4 shows the annual mean ANSG and PEWG values as simulated by each of the CMIP3 GCMs, and compares them to the values estimated from observations (red asterisk). Few models simulate both of these indexes well, with most models producing a negative bias in ANSG (South Atlantic too cold relative to North), and a positive bias in the PEWG (East Pacific too warm relative to the West).

The right panel of Figure III.4 shows the 21st century trends in PEWG and ANSG from each model. Most models seem to produce a warming of the East Pacific relative to the West (El Niño-like pattern), but there is no agreement about the sign of the trend in the ANSG, with some models presuming strong warming of the North Atlantic relative to the South (e.g., Model "w") and others producing the opposite (e.g., Model "o").

[10] The land regions are shown schematically in Figure I.1 and are labeled as *Eastern Amazonia (EA), Northeastern Brazil (NEB), Northwestern Amazonia (NWA), Southern Amazonia (SAz) and Southern Brazil (SB).*

The observed data indicate that more positive ANSG is associated with drying in all regions aside from Southern Brazil. This observed difference between the different GCMs is very likely to impact the simulated trends in rainfall.

Figure III.4. Left: Modeled annual mean value of ANSG and PEWG during the 20th century. Observed values shown by red asterisk.
Right: predicted linear trends in ANSG and PEWG over the 21st century.
Models are as labeled in Table III.1.

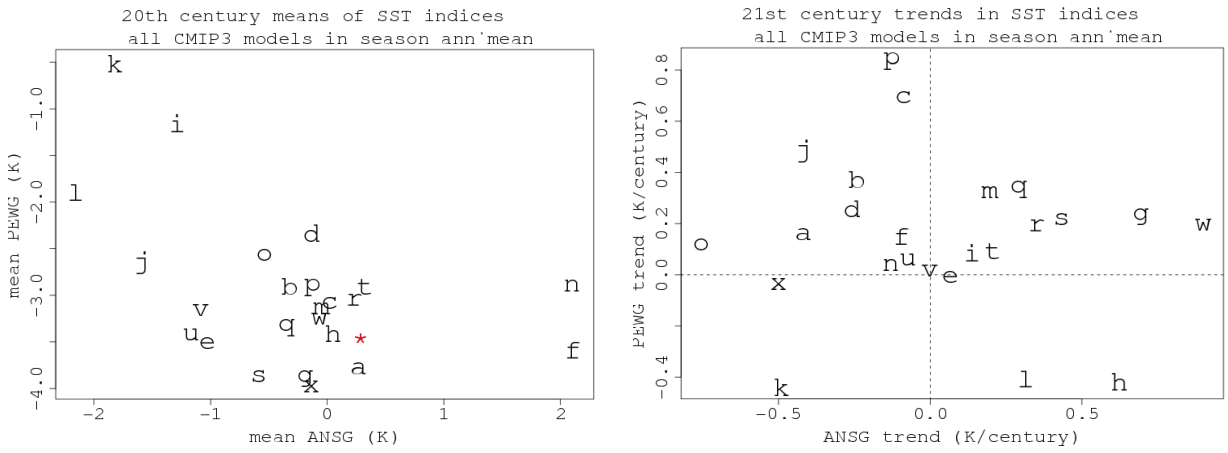

3. PDFS FOR FUTURE SST INDEXES

In this section weighting factors for each model are estimated based on simulation of the annual mean ANSG and PEWG in the 20th century.[11] Figure III.5 shows the weighting factors derived through comparison to ANSG data alone (left panel) and PEWG data alone (right panel). Six of the 24 models achieve above-average weighting on the ANSG (with model "w" being the highest weighted), and nine achieve above-average weighting for PEWG but only one significantly so (model "o").

[11] Models are penalized for any bias in the long-term mean as well as for errors in the simulation of variability (through the Kolmogorov-Smirnov statistic).

Figure III.5. Weighting of the CMIP3 models based on their relative abilities to simulate mean and variability of the key SST indexes, left: ANSG, right: PEWG.

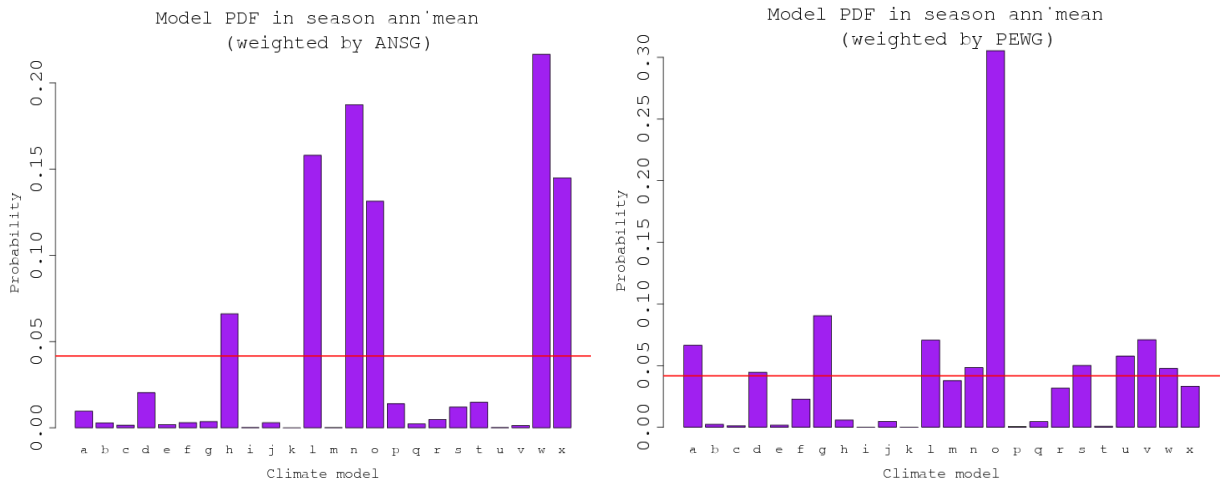

Based on these weightings, estimates can be made of CDFs and PDFs for the ANSG and PEWG; these are shown in Figures III.6 and III.7. The weighting produces a climate change signal with a suggestion that the most likely ANSG values will become more negative through the 21st century, which would make four of the five study areas wetter (see Table III.I). However, it also increases the probability of positive (2005-like) anomalies in the ANSG.

Figure III.6. Changes in modeled CDFs and PDFs for the ANSG index. Black lines represent the 2001–2030 period and red lines show 2068–2098. The dotted lines are based on a uniform prior in which all model projections are considered equally likely, and the continuous lines are from the Bayesian weighting procedure based on the ANSG simulations of each model.

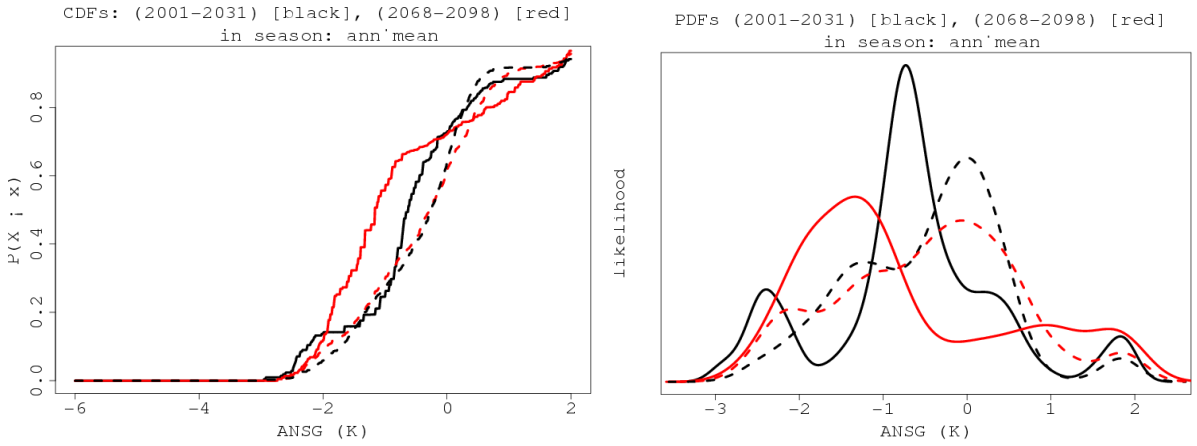

There is a suggestion of slight increases in PEWG through the 21st century, which are consistent with the El Niño-like raw model trends shown in Figure III.4.

Figure III.7. Changes in modeled CDFs and PDFs for the PEWG index. Black lines represent the 2001–2030 period and red lines show 2068–2098. The dotted lines are based on a uniform prior in which all model projections are considered equally likely, and the continuous lines are from the Bayesian weighting procedure based on the PEWG simulations of each model.

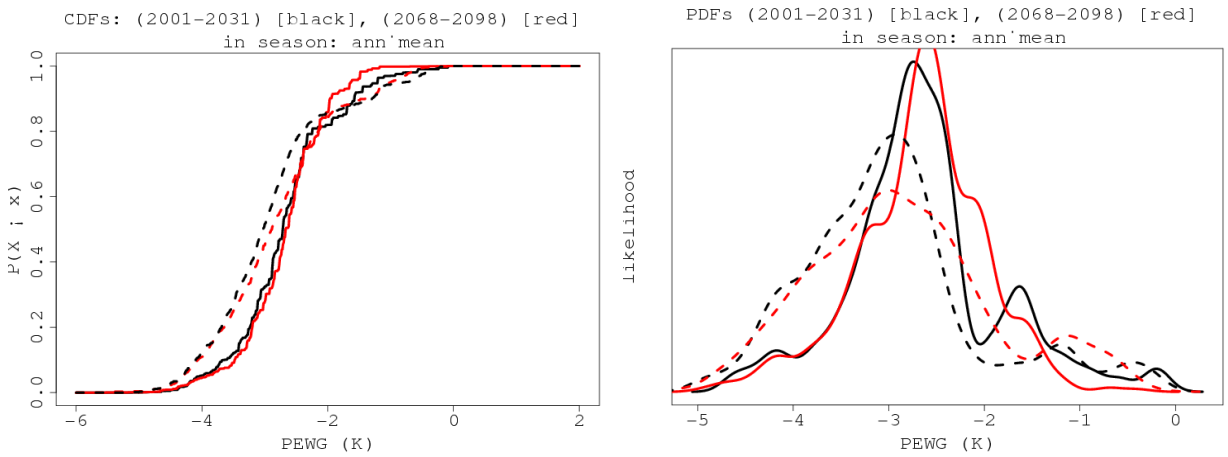

In summary, the PDF-based method calculated using the two procedures described in this section, although useful in detecting significant potential changes in rainfall in some regions, for some seasons, is not enough to support a blanket statement on whether the existing set of models predict a wet Amazon or a dry Amazon as a result of climate change. Some of the highest-ranked models indicate a tendency toward a wetter Amazon, particularly in the Northwest, but simultaneously point to an increased possibility of 2005-like events in Southern Amazonia. As for other regions, it is still difficult to discern a trend.

The analysis also indicates a significant increase in the probability of drought conditions in Southern Brazil (up from 1.1% in 2001–2030 to 6.7% in 2068–2098) or a shift from one 2005-like drought per century to one every seventeen years. Still, the overall uncertainties in future Amazonian rainfall remain significant.

IV. Analysis of Amazon forest response to climate change

1. INTRODUCTION

The analysis in section III does not lead to a blanket statement regarding an increase or reduction in rainfall over the entire Amazon basin. However, it does indicate a tendency toward a wetter Amazon, in particular in the Northwest, but simultaneously indicates an increased possibility of dry events in Southern Amazonia and even more in Southern Brazil. Remarkably, these are the same trends identified through the use of the high-resolution Earth Simulation of the Amazon basin.

Beyond rainfall, however, there are other climate-induced impacts that need to be considered for their potential effect on both the structure and behavior of the forest. As described in Section I, these include the following:

a) High probabilities for prolonged drought stress may lead to increasing physiological stress for trees, increased tree mortality, and thus carbon emissions.
b) Increasing atmospheric CO_2 concentrations may alter the drought response of forests.
c) Increasing temperatures may accelerate heterotrophic respiration rates and thus carbon emissions.
d) Resulting changes in evapotranspiration and therefore convective precipitation could further accelerate drought conditions and destabilize the tropical ecosystem as a whole.

Strong impacts of drought on tropical forest biomass and structure are corroborated by field measurements and experiments. The observed responses of rainforests to drought events such as the 1997–1998 ENSO event range from high tree mortality of ~26% in a forest with seasonal rainfall (East Kalimantan; Van Nieuwstadt and Sheil 2005) to no mortality response in seasonally dry forests (Panama; Condit et al. 2004) and several intermediate responses (Williamson et al. 2000). During the Amazon drought in 2005, Phillips et al. (2009) measured strongly increased tree mortality and rather small declines in growth in the surviving trees. Mainly fast-growing light-wooded trees were affected by carbon starvation. Similar results have been found in the 1983 drought event in Panama, where mortality of different tree species increased (Condit et al. 1995). Large trees are especially sensitive to reduction in soil water below a critical threshold and react with increased mortality (Nepstad et al. 2007). Thus, in a drought event, trees may be killed selectively and thus species composition as well as canopy structure may be altered (Nepstad et al. 2007; Phillips et al. 2009).

Rainfall is one of the most important drivers of forest growth and survival, but the signal provided by different models has a large variance. The GCM model weightings described in Section III provide information about the potential of the 24 climate models to reproduce the mean and the distribution of annual rainfall under current conditions. With the derived ranking of

the climate models, there is the possibility to estimate the response of biomass and thus the risk of a potential forest dieback according to the climate models' probability.

In this section, the risk, mechanisms and consequences of a possible dieback of undisturbed rainforests in Amazonia are assessed, using a state-of-the-art process-based vegetation model (LPJmL). The objectives were to estimate (a) the range of possible impacts of climate change on Amazonian forest ecosystems, and (b) the probability of a forest dieback, based on weighted probability density functions for the 24 climate models as estimated in Section III.

2. THE LPJML VEGETATION MODEL

Ecosystem-level responses to changing environmental conditions (temperature, water availability, ambient CO_2) are the net outcome of multiple processes, such as photosynthesis, auto- and heterotrophic respiration, growth, competition and mortality. The dynamics of ecosystem structure and vegetation composition are therefore highly nonlinear and depend strongly on geographical location and climate conditions. Observations of these processes and their net ecosystem impact exist from a range of sites throughout the tropical forest belt, and remote sensing data provide further regional-to-global integrative data. However, regionalizing these ecosystem responses for the main climatic and edaphic gradients, and extrapolating them under climate change and increasing CO_2 concentrations, require comprehensive numerical simulation models that include the main physiological, biogeochemical and stand-level processes, as well as vegetation dynamics due to competition and disturbance.[12]

For the present study, the Lund-Potsdam-Jena Dynamic Global Vegetation Model for managed Land (LPJmL) has been applied to the Amazon Region.[13] Since the goal of this task is the identification of forest responses to changing climate, all forests are assumed to be unaffected by land use change or deforestation. The LPJmL model is therefore used in its potentially natural vegetation mode. In the following section, the coupled climate-vegetation model CPTEC-PVM2.0 is then used to estimate the climate feedbacks from biome shifts and deforestation.

In LPJmL, vegetation processes are simulated for small areal units, the size of which is determined by available data. Typically, these units are cells in grids with mesh sizes of 0.5 degrees longitude and latitude.[14] The functional units of the model are plant functional types (PFTs) which can be conceived as plant species grouped by specific attributes controlling their physiology and dynamics. The projected PFTs in the Amazon basin are "tropical broadleaf evergreen," "tropical broadleaf raingreen" and "C_4 grass."

[12] For this purpose, dynamic global vegetation models have been developed (Prentice et al. 2007). Several such models exist, based on different conceptualizations, such as TRIFFID (Cox 2001), IBIS (Foley et al. 1996), LPJmL (Sitch et al. 2003; Bondeau et al. 2007) and ORCHIDEE (Essery et al. 2001; Krinner et al. 2005; Hughes et al. 2006). All these models are simplified enough to be generic for application to all major upland ecosystems of the planet, but they can also be used regionally for specific purposes.

[13] LPJmL has been evaluated using observations in a large number of studies and against many types of observations, on the global (Gerten et al. 2004) and regional scales for boreal forests (Lucht et al. 2002), and tropical ecosystems (Cowling and Shin 2006).

[14] In any grid cell, the simulation is driven by the input of monthly climatology, annual ambient CO_2 and static soil properties.

The vegetation in each grid cell is represented as a mixture of the three PFTs. Each of the PFTs covers a certain proportion of the modeled area, which is denoted as its "foliar projective cover" (FPC). Plant physiological and biogeochemical processes are simulated in a mechanistic way. Photosynthesis, water balance and maintenance respiration for each PFT are calculated on a daily time step. The assimilated carbon (NPP) is allocated to the different carbon compartments of the plant, such as leaves, wood and roots, according to specified allometric constraints.

During this work, a new fire module (SPITFIRE, Thonicke et al. in review) has been incorporated into LPJmL; it simulates detailed climatic fire danger, ignition, spread, effects and emissions of wildfires in natural vegetation caused by lightning (Thonicke et al. in review).

3. SIMULATION OF VEGETATION STATE IN THE AMAZON BASIN

To visualize the current state of the ecosystem and the level of forest degradation in the Amazon basin, three indicator variables directly derived from state variables of LPJmL are used:

a) Forest cover (FC), which was calculated from foliar projective cover (FPC) of the woody PFTs and ranges between 0 and 100%;
b) Biomass density (BD), which is the accumulated aboveground vegetation carbon in kg C m^{-2}; and,
c) a vegetation classification scheme that describes forest types by their proportion of forest cover and biomass density of the natural stand within the grid cell (Figure IV.1). In a simplified way,

- "tropical" (FC > 80, BD > 12) and "mixed" (FC > 80, BD < 12, BD > 6) forests are seen as "pristine" forest types, while
- "open forests" (FC > 80, BD < 6),
- "woodland" (FC <80, FC > 40, BD > 6),
- "shrubland" (FC < 80, FC > 40, BD < 6), and
- "savanna" (FC < 40, BD < 6) are either occurring naturally or can also be "secondary" degraded types, i.e., caused by climate or land use change. The threshold values for FC and BD were estimated following Alencar et al. (2006).

Figure IV.1. Vegetation classification for the Amazon basin based on biomass density (BD) and forest cover (FC) as simulated by LPJmL.

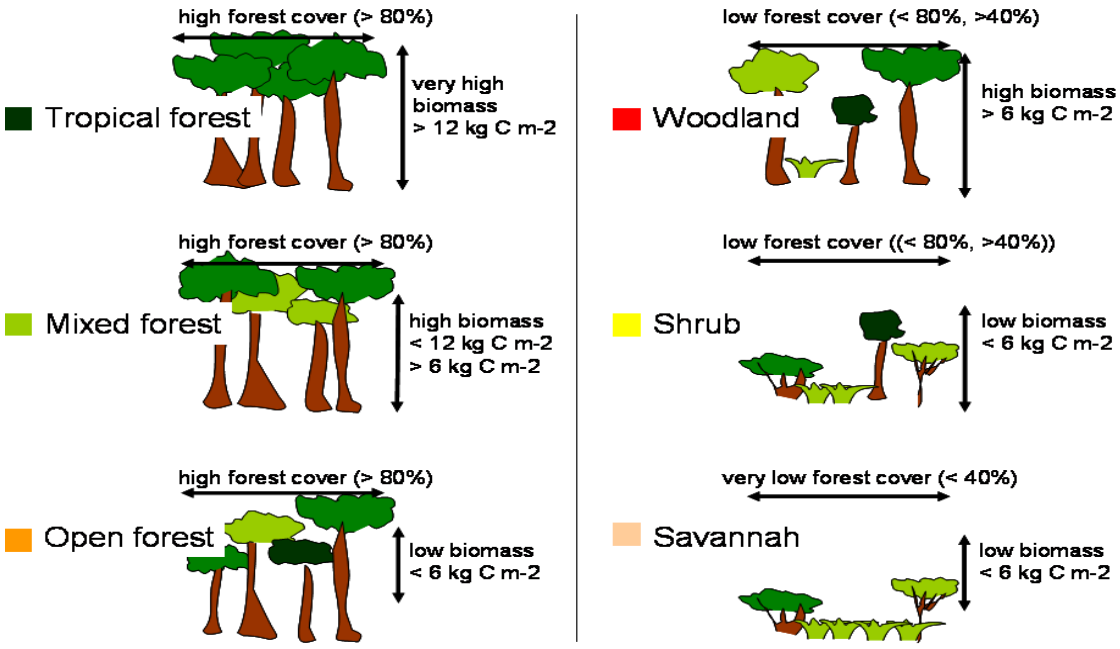

Under current climate conditions (1981–2000), the potential natural vegetation in the Amazon basin is dominated by tropical and mixed (deciduous) rainforests. LPJmL simulations of current vegetation are in accordance with other biome classification and potential vegetation maps (IBGE 1988; Salazar et al. 2007). The total estimated biomass (above- and belowground) ranges from 47 to 86 Pg C in the Amazon basin; this lies within the (broad) range of other simulation results and inventories which suggest values between 39 and 123 Pg C (Houghton et al. 2001; Cowling and Shin 2006; Malhi et al. 2006; Soares-Filho et al. 2006; Saatchi et al. 2007).

4. RESPONSE OF BIOMASS TO PROJECTED CHANGES IN RAINFALL IN THE DIFFERENT GEOGRAPHICAL DOMAINS

The biomass response as calculated from LPJmL based on the CMIP-3 multi-model climatology has been ranked according to the PDFs for rainfall (calculated in Section III). Figures IV.2 to IV.6 show the estimated model weightings and the projected changes in biomass for the time period 2070–2100 vs. 1970–2000 for the LPJmL-S1 (shallow roots and the SRES-A1B emission trajectory) simulations while deliberately excluding the potential role of CO_2 fertilization.

Current knowledge and available data seem to indicate that, provided there are no limiting water and nutrient constraints, CO_2 fertilization plays a role in the growth of stands in temperate forests (this is particularly important for young forest stands). This assumption has been at the basis of current dynamic vegetation modeling.

However, under pronounced nutrient constraints, typical of poor soil conditions in the Amazon basin, there is substantial uncertainty that CO_2 fertilization may play such an effective role in tropical, mature forest ecosystems. Thus, in the absence of solid information (such as from ecosystem CO_2 fertilization experiments), the assumption that CO_2 fertilization will be significant in the Amazon cannot presently be used as a basis for sound policy advice.

The bar plot in the top panel of Figures IV.2 to IV.6 shows the ranking of the 24 climate models for the respective geographical domain as calculated for the combined distribution over all seasons without the CO_2 effect. Models with the highest probability are best reproducing mean and distribution of rainfall patterns in the respective region. The box-and-whiskers plots in the panel below show the corresponding change in biomass, simulated by LPJmL under the SRES-A1B emission trajectory. The graphs show the difference between the average over the periods 2070–2100 and 1970–2000. Negative values indicate decrease and positive values indicate increase in vegetation cover and forest cover.

The plots indicate that the best ranking models consistently predict a reduction in the density of vegetation carbon in all geographical domains; the reductions are largest for those models with the highest ranking.

The vegetation carbon response based on the GCM weightings clearly shows that the changes in vegetation carbon vary strongly among the five regions and among the climate scenarios. The climate models having the highest probability in reproducing annual precipitation cycle differ among the five regions looked at. The vegetation response to the highest-ranked climate models is considerable and often contains a high spatial variability for a climate scenario.

When the CO_2 fertilization effect is included in the estimate of biomass response, the reductions in vegetation carbon are diminished and in some cases an increase in vegetation carbon can be observed. However, as indicated above, the CO_2 fertilization effect in mature forests, under nutrient-limiting conditions such as those prevalent in Amazonian soils, is highly uncertain; therefore, the current information scenarios without CO_2 fertilization should be used as a basis for policy decisions.

Figure IV.2. Ranking of the 24 climate models (top panel, models with highest probability are best reproducing mean and distribution of rainfall patterns in this region) for the Eastern Amazonia region (EA) as calculated for the combined distribution over all seasons.

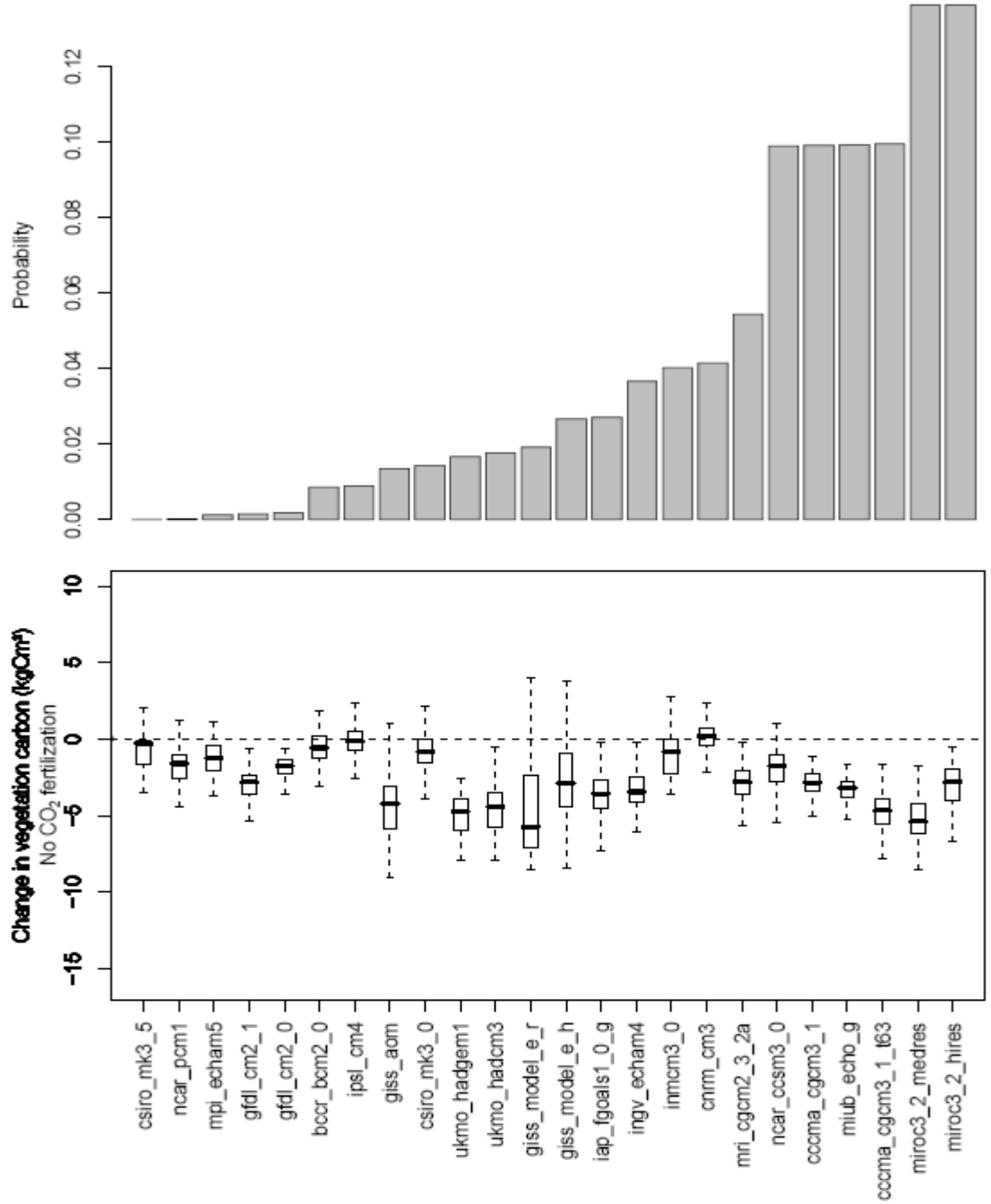

For Eastern Amazonia (EA), two models rank best (miroc3_2_hires, miroc3_2_medres). Their climatologies lead to two slightly different responses of vegetation carbon projections under future conditions. Without CO_2 fertilization both models predict a decrease of between 2 and 5 kg C m^{-2}.

Figure IV.3. Results of the regional analysis and the ranking for Northwestern Amazonia (NWA).

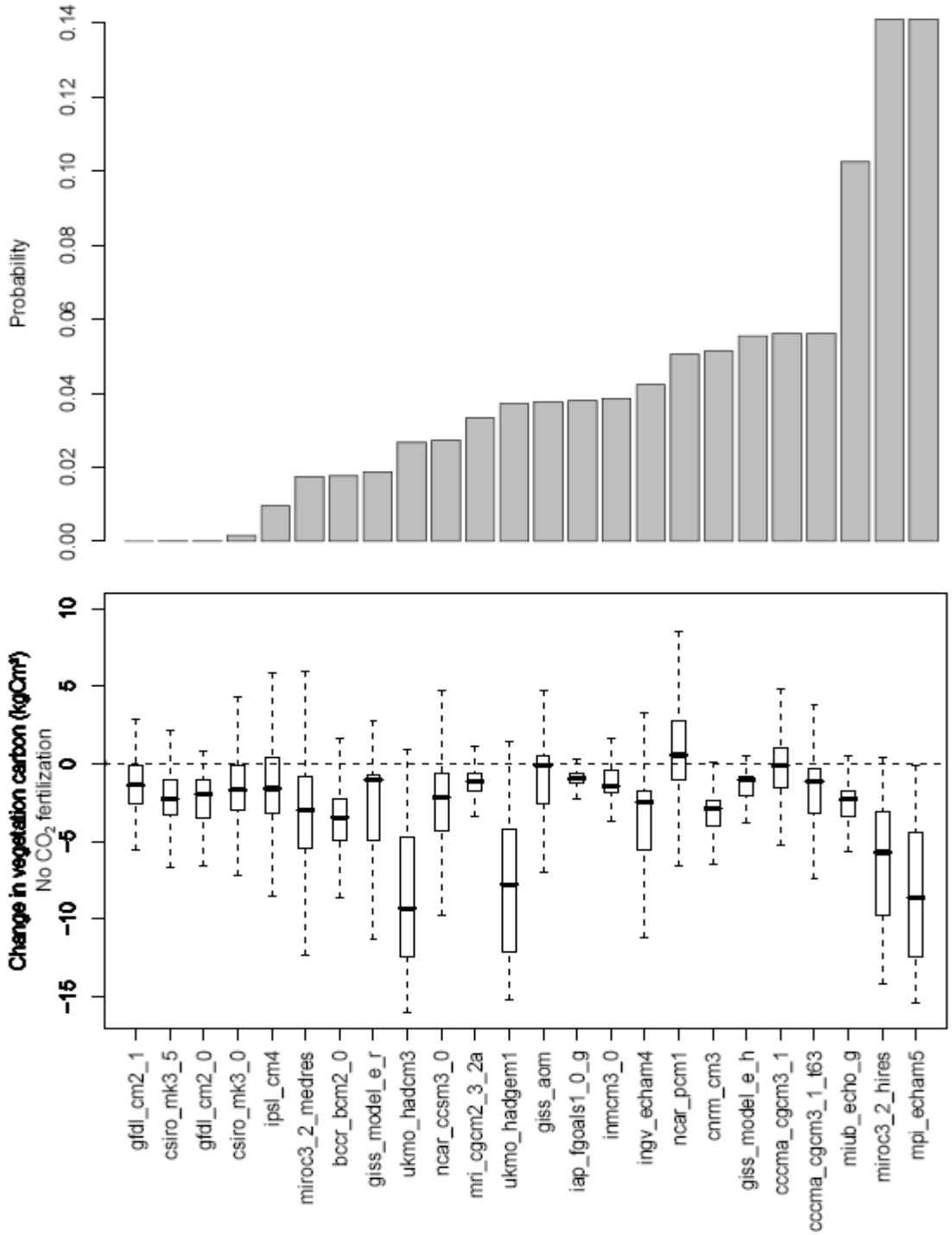

In Northwestern Amazonia (NWA), the region with the highest biomass density under current conditions, the range of potential biomass changes is very large. Again, the two highest ranked models project different responses in biomass under the no-CO_2 fertilization scenario. Under the mpi_echam5-climatology, LPJmL projects on average a loss of biomass of ~8 kg C m^{-2} in the grid cells of Northwestern Amazonia. The miroc3_2_hires-climatology leads to a projected decrease on average of ~2 kg C m^{-2}.

Figure IV.4. Results of the regional analysis and the ranking for Southern Amazonia (SAz)

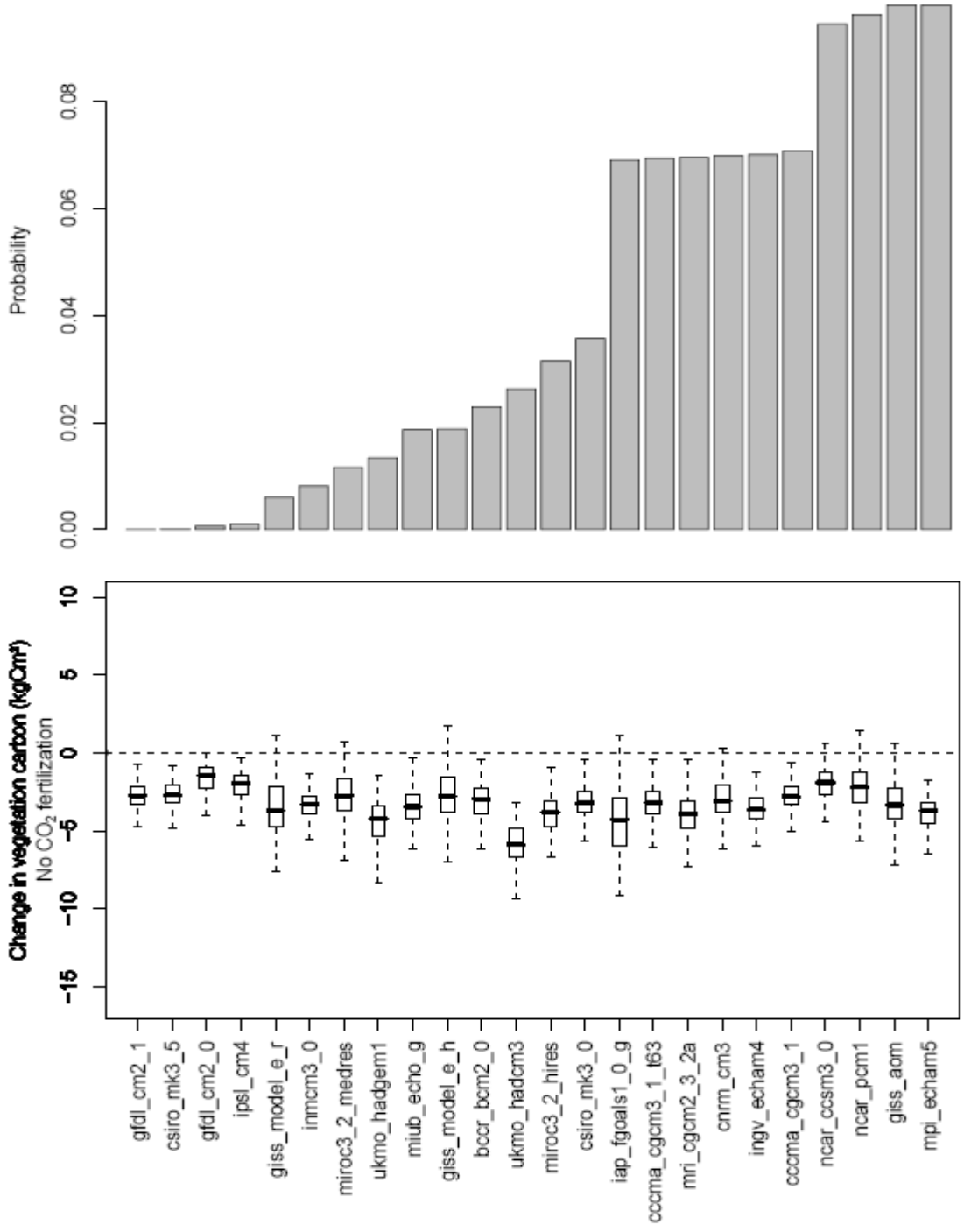

For Southern Amazonia (SAz), LPJmL projects a decrease in vegetation carbon for the four highest ranked climate models (mpi_echam5, giss_aom, ncar_pcm1, ncar_ccsm3_0).

Figure IV.5. Results of the regional analysis and the ranking for Northeastern Brazil (NEB)

.

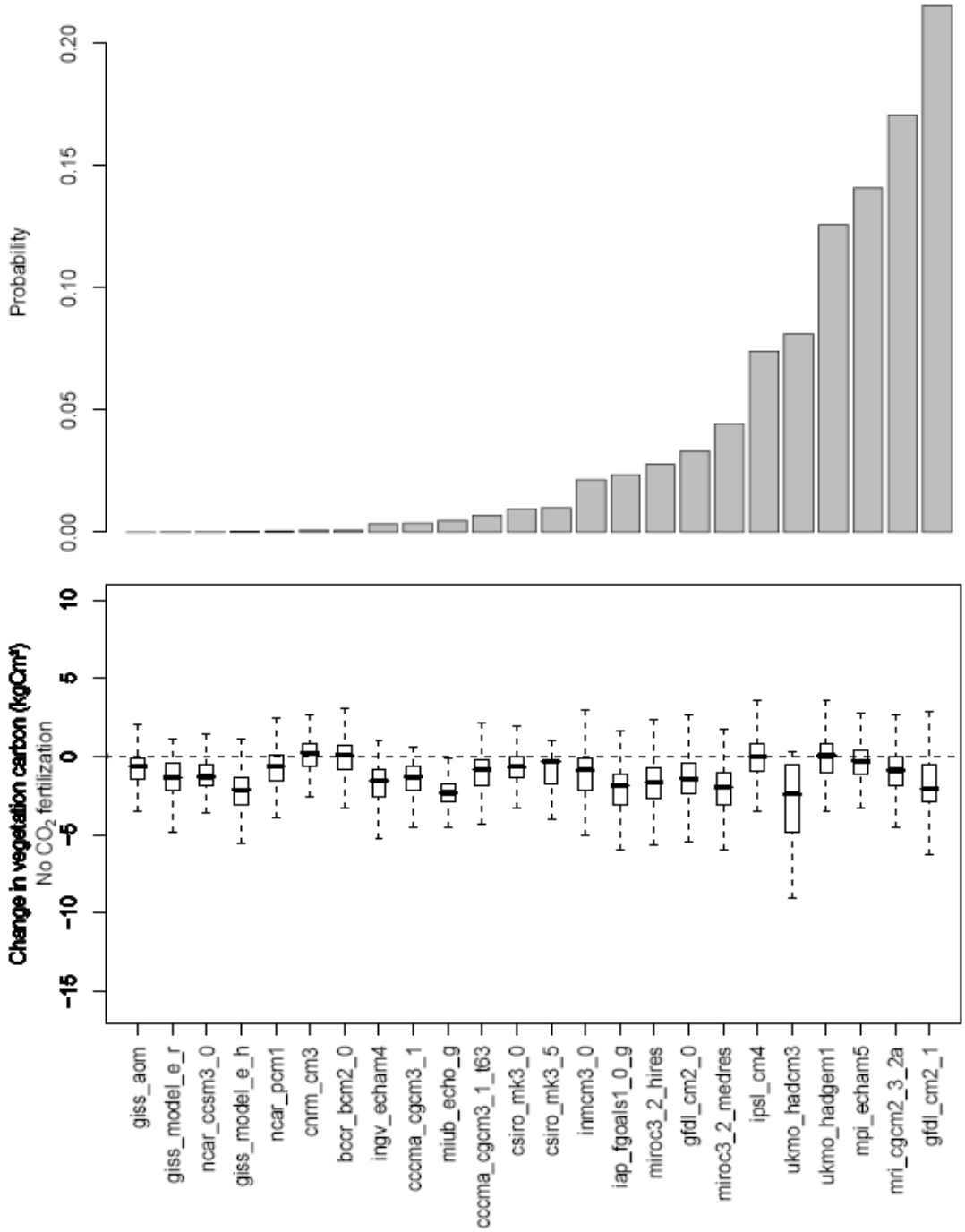

In Northeastern Brazil (NEB), the gfdl_cm2_1 climate model is highest ranked. Here, LPJmL projects a somewhat lower decrease in vegetation carbon of 0 to -2 kg C m^{-2} for the four best ranked models.

Figure IV.6. Results of the regional analysis and the ranking for Southern Brazil (SB)

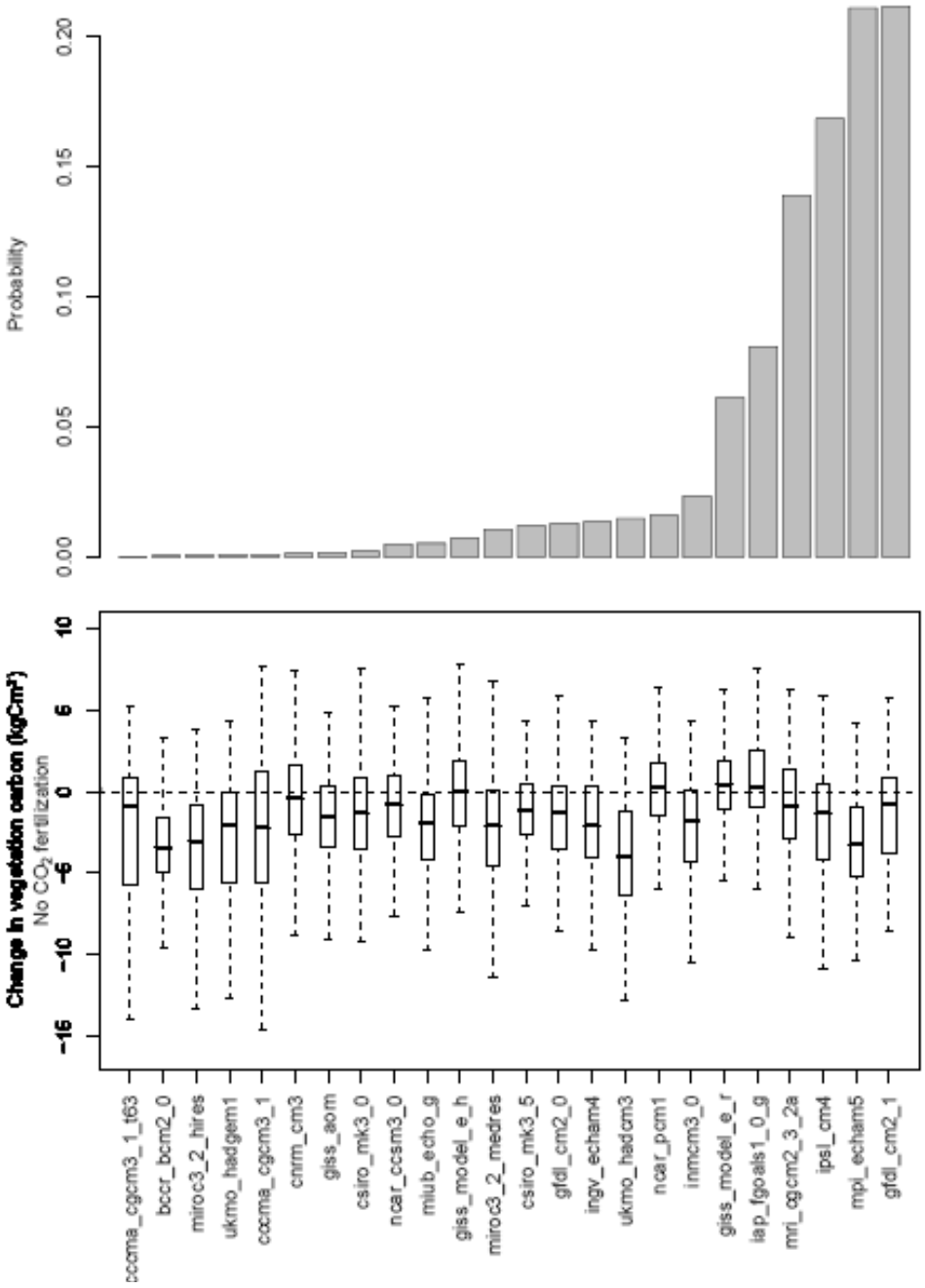

In Southern Brazil (SB), vegetation carbon is projected to decrease in most climate scenarios. With the two highest ranked models for this region (mpi_echam5, gfdl_cm2_1), LPJmL projects a "moderate" decrease in biomass.

The analysis above assumes no CO_2 fertilization. When CO_2 fertilization would be allowed in LPJmL, a number of climate models would result in increases in biomass carbon. However, as indicated before, the extent and limits of CO_2 fertilization are uncertain and subject to current scientific debate (Nowak et al. 2004; Korner et al. 2005; Norby et al. 2005).

5. PROBABILITY FUNCTION FOR AMAZON FOREST BIOMASS CHANGE

In this subsection, key outputs of Sections III and IV are combined to derive PDFs and Cumulative Distribution Functions (CDFs) for changes in vegetation carbon. The simulated changes in vegetation carbon from the LPJmL-S1 simulations (shallow roots and the SRES-A1B emission trajectory), as presented in Section IV, are weighted according to the climate model PDFs shown in Figure III.2. LPJ simulations with and without CO_2-fertilization are considered.

Figures IV.7–IV.11 show the derived distribution functions for the five study regions. In each case the inclusion of CO_2 fertilization (red lines) significantly increases the resilience of the forest to CO_2-induced climate change and therefore substantially reduces the risk of forest dieback. This is seen most clearly in the CDF plots (top panels), which show how the probability of a vegetation carbon change below some value *x* varies with *x*. Thus, for example, the probability of a reduction in forest carbon greater than 1 kg C m^{-2} (as shown by the vertical dashed line) is about 30% in Eastern Amazonia (Figure IV.7.) in the absence of CO_2 fertilization (black curve), but is essentially negligible once the default LPJ CO_2-fertilization effects are included (red curve). As mentioned above, there is still an active scientific debate about the likely level of direct CO_2 effects on mature forest ecosystems, with some scientists arguing that nutrient requirements will most likely limit the level of CO_2-fertilization in the 21st century.

On the basis of the PDF of biomass response, the probability of a 25% reduction in standing carbon induced by climate change for the different geographical domains has been estimated in the absence of the CO_2 fertilization effect and under the A1B emission trajectory. The assessment estimates a very high probability of dieback in Southern Amazonia (62%) and significant probabilities in Northeastern Brazil and Eastern Amazonia. Northwestern Amazonia appears in the analysis to be among the most resilient regions. A more rapid warming may result in more drastic dieback (see Table IV.1 below).

It is concluded that direct CO_2 effects at ecosystem level are the key unknown in assessing the risk of Amazon forest dieback under 21st century climate change. [15] Reducing this uncertainty, using a combination of estimates of the Amazonian carbon sink (Phillips et al. 2009) and trends in river runoff (Gedney et al. 2006), is therefore a priority for follow-on study. Drastic differences between the total impacts of climate change caused by CO_2 and other climate forcing agents (e.g., increases in methane or reductions in sulfate aerosols) have implications for international climate policy, which currently treats all radiative forcings as equally damaging. In contrast, this study shows clearly that the risk of Amazon forest dieback is many times greater if climate change arises from agents other than CO_2.

[15] While physiological aspects of CO_2 stimulation at leaf level are well-researched, a major challenge is to upscale CO_2 leaf-level effects to community- or ecosystem-level, which is a critical assumption in vegetation modeling. Korner (2004, 2006) for example shows that with regard to CO_2 fertilization, it is crucially important to clearly distinguish a possible stimulation of growth or NPP from any change in the carbon pool size of the ecosystem. Enhanced growth or NPP, should it occur at ecosystem level, does not translate in a change in pool size by simple terms neither in a change of the ecosystem's resilience. This in turn means that even if there was a CO_2 stimulation of growth, this cannot be taken as evidence of a change in carbon storage or increased resilience of the ecosystem. To the contrary, should there be a stimulation of fast growing, low wood density tree species or lianas (see discussion in Korner 2004), the ecosystem's carbon stock would decline despite greater NPP or growth.

Figure IV.7. Cumulative Distribution Functions (upper panel) and Probability Density Functions (lower panel) for change in vegetation carbon in Eastern Amazonia (from 1970–2000 to 2070–2100). Produced from LPJmJ-S1 simulations (shallow roots and the SRES-A1B emission trajectory) with CO_2 fertilization (red lines) and without CO_2 fertilization (black). The dotted vertical line indicates a loss of 1 kg C m^{-2}.

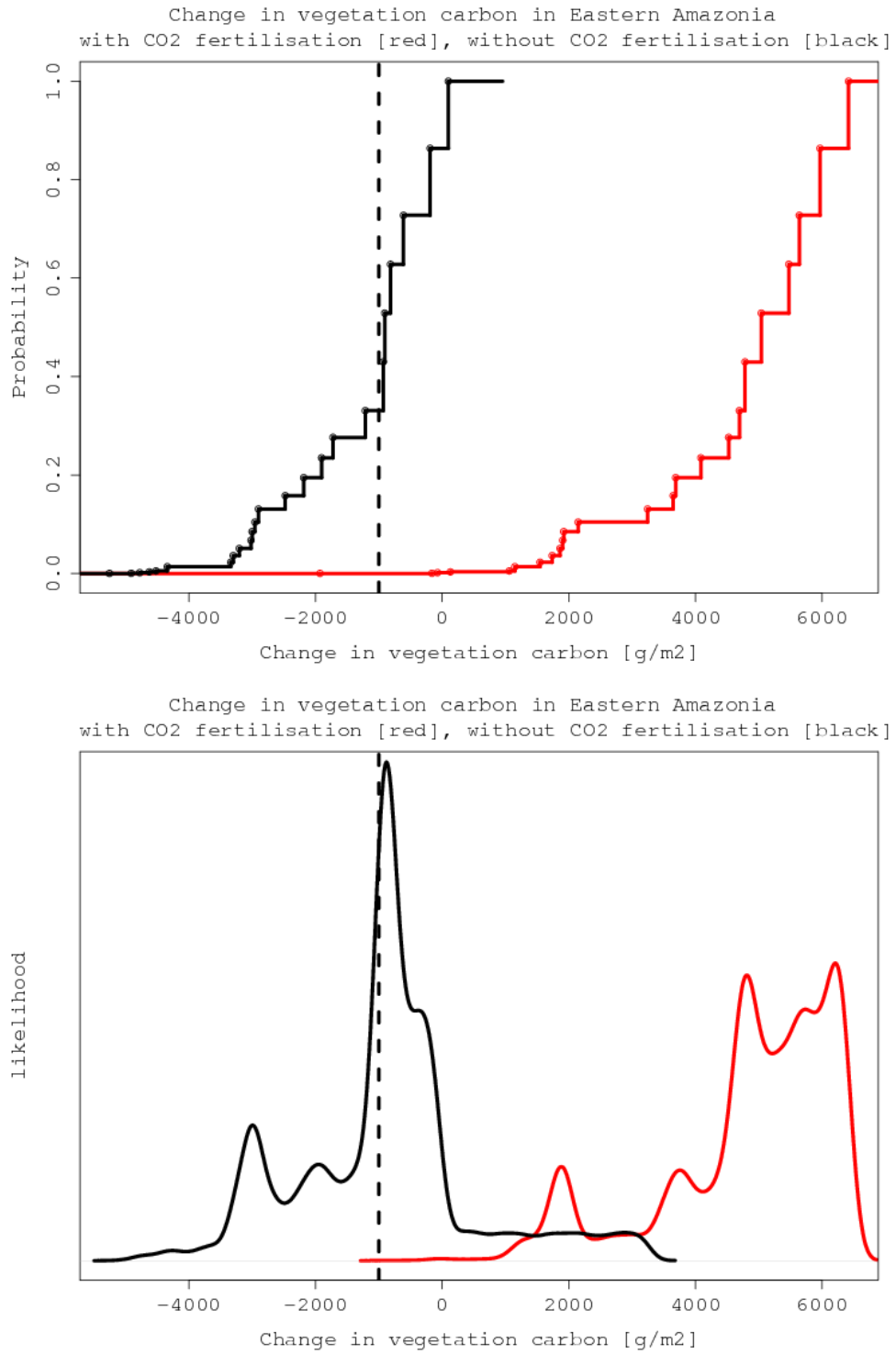

Figure IV.8. Cumulative Distribution Functions (upper panel) and Probability Density Functions (lower panel) for change in vegetation carbon in Northwestern Amazonia (from 1970–2000 to 2070–2100). Produced from LPJmJ-S1 simulations (shallow roots and the SRES-A1B emission trajectory) with CO_2 fertilization (red lines) and without CO_2 fertilization (black). The dotted vertical line indicates a loss of 1 kg C m^{-2}.

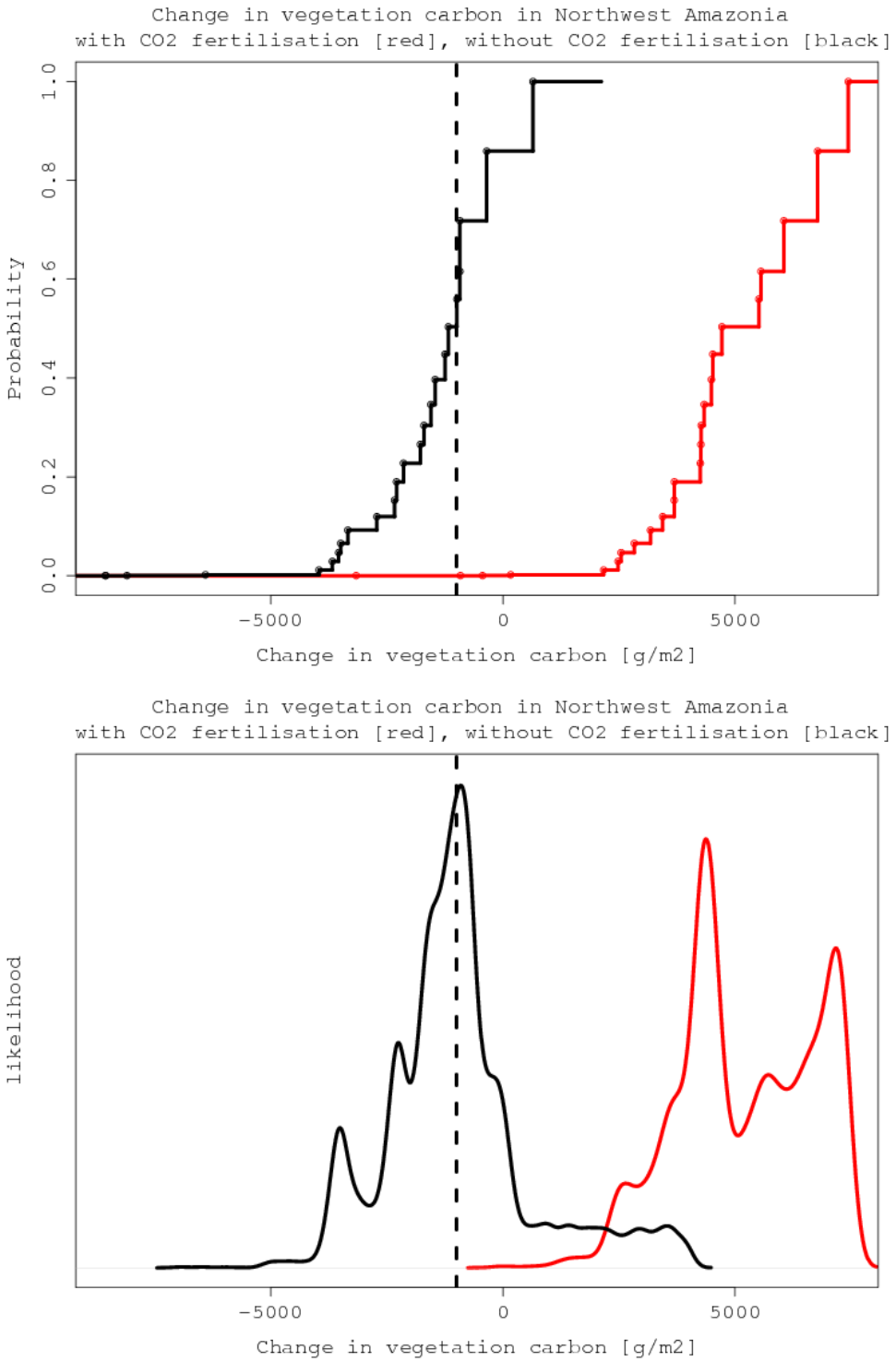

Figure IV.9. Cumulative Distribution Functions (upper panel) and Probability Density Functions (lower panel) for change in vegetation carbon in Southern Amazonia (from 1970–2000 to 2070–2100). Produced from LPJmJ-S1 simulations (shallow roots and the SRES-A1B emission trajectory) with CO_2 fertilization (red lines) and without CO_2 fertilization (black). The dotted vertical line indicates a loss of 1 kg C m^{-2}

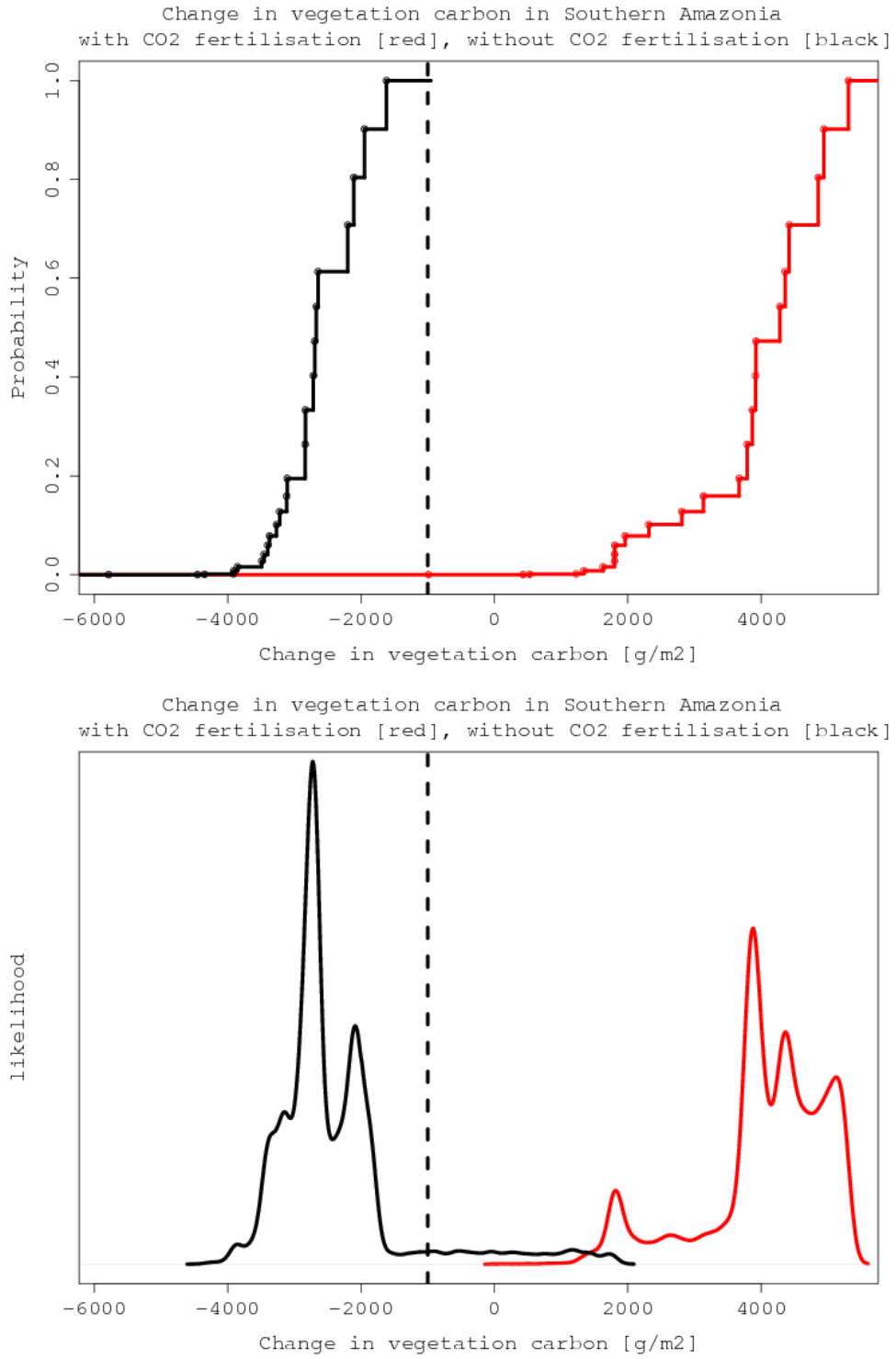

Figure IV.10. Cumulative Distribution Functions (upper panel) and Probability Density Functions (lower panel) for change in vegetation carbon in Northeastern Brazil (from 1970–2000 to 2070–2100). Produced from LPJmJ-S1 simulations (shallow roots and the SRES-A1B emission trajectory) with CO_2 fertilization (red lines) and without CO_2 fertilization (black). The dotted vertical line indicates a loss of 1 kg C m^{-2}.

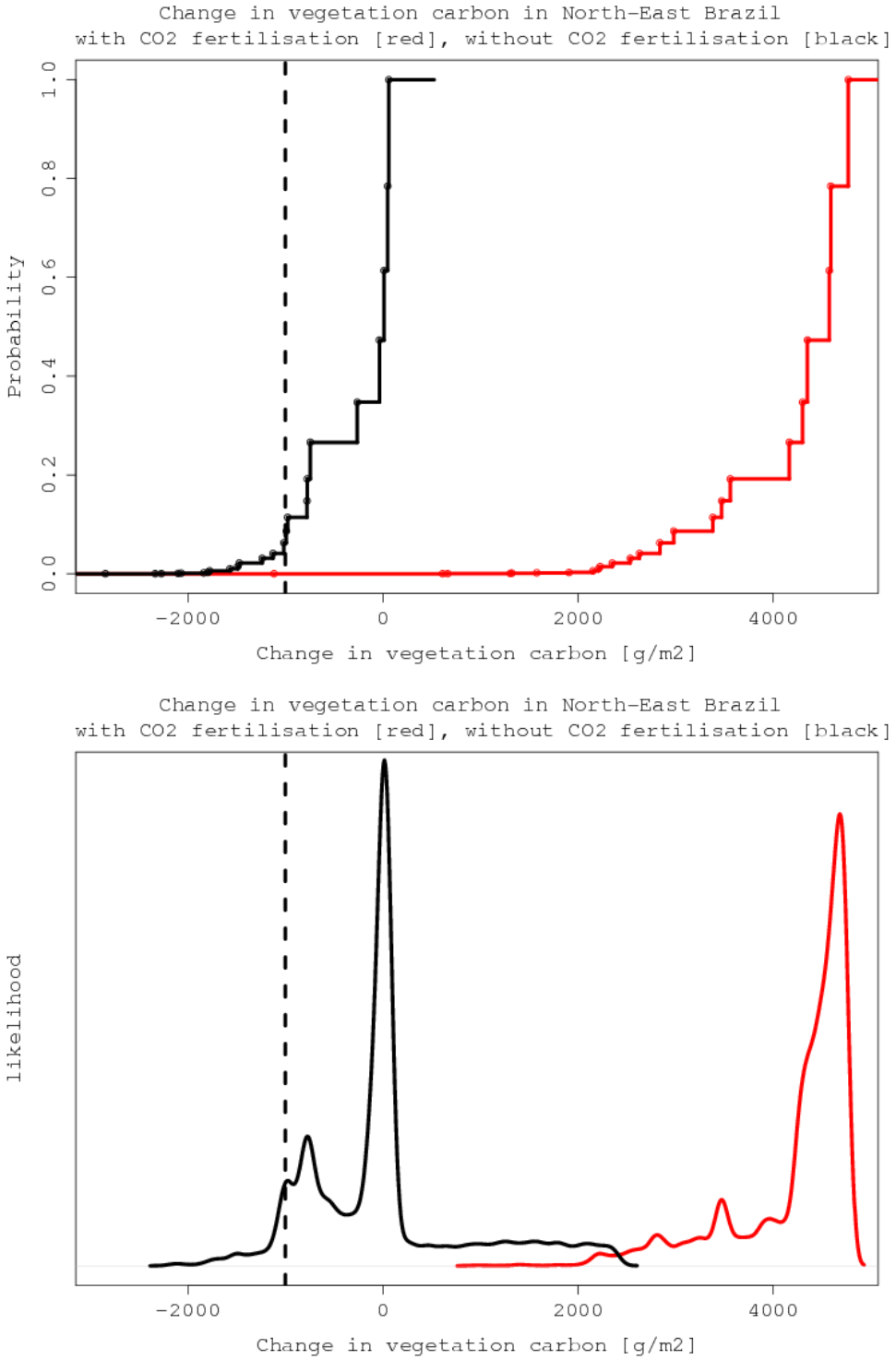

Figure IV.11. Cumulative Distribution Functions (upper panel) and Probability Density Functions (lower panel) for change in vegetation carbon in Southern Brazil (from 1970–2000 to 2070–2100). Produced from LPJmJ-S1 simulations (shallow roots and the SRES-A1B emission trajectory) with CO_2 fertilization (red lines) and without CO_2 fertilization (black). The dotted vertical line indicates a loss of 1 kg C m^{-2}.

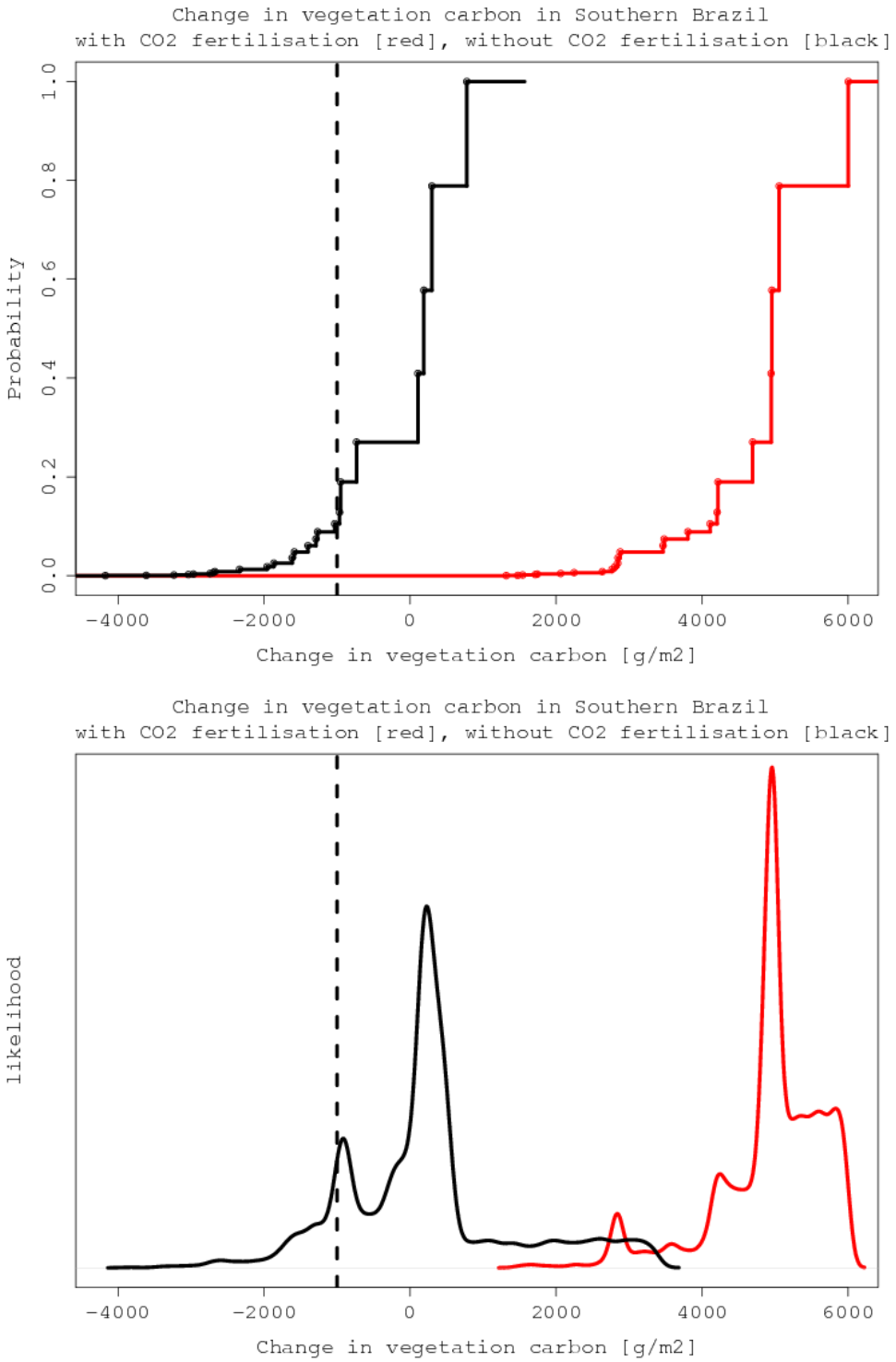

Table IV.1. Assessment of the risk of Amazon dieback, defined as 25% loss of vegetation carbon (from 1970–2000 to 2070–2100) for the five geographical domains using LPJmL-S1 simulations (shallow roots and the SRES-A1B emission trajectory) without CO2 fertilization.

Geographical domain	Average veg. carbon (kgC/m^2)	Probability of dieback w/o CO_2 fertilization in %
Eastern Amazonia	12	8
Northwestern Amazonia	15	3
Southern Amazonia	10	62
Northeastern Brazil	3	19
Southern Brazil	10	2

6. SIMULATION OF SENSITIVITY TO CO_2 AND ROOTING DEPTH

As seen above, the likelihood and extent of CO_2 fertilization and its effects at ecosystem level are critical to assess the prospects for dieback. Root depth also affects the resilience of biomass, in particular its ability to withstand droughts. To evaluate the effects of CO_2 fertilization and different rooting depths, LPJmL was run for four scenarios (Table IV.2). Scenarios S1 and S2 are run using the standard SRES-A2 emission trajectory and include the effects of climate and increasing atmospheric CO_2 conditions. Under scenarios S3 and S4, the effect of CO_2 has been removed by using constant 2000 CO_2 conditions.

Scientific studies show that the effects of elevated CO_2 on plant growth are dependent on (i) the species considered, (ii) the growth stage of the species, (iii) its photosynthetic characteristics, as well as (iv) the management regime, such as water, nitrogen (N) applications for crops and availability of micro-nutrients (Jablonski et al. 2002; Kimball et al. 2002; Norby et al. 2003; Ainsworth and Long, 2005).[16]

For trees, the measured change in biomass (i.e. growth) in young and rapidly growing parcels at 550 ppm CO_2 can be in the 0–30% range, with the higher values reported in younger trees.[17] For mature, natural forests there was no or only little response to elevated CO_2 observed (Nowak et al. 2004; Korner et al. 2005; Norby et al. 2005).[18] Norby et al. (2005) found a mean tree net primary production (NPP) response of 23% in young tree stands; however, in mature tree stands Korner et al. (2005) reported no CO_2 stimulation. In addition, it is important to note that the measured NPP response (if so) is not providing any information on net changes in carbon stock (Korner et al. 2007). Thus, the effect of CO_2 stimulation at ecosystem level on mature tropical

[16] Compared to current atmospheric CO_2 concentrations, crop yields, for example, increase at 550 ppm CO_2 in the range of 10–20% for C3 crops (e.g., wheat, barley, potatoes) and 0–10% for C4 crops such as maize (Ainsworth et al. 2004; Gifford, 2004; Long et al. 2004).

[17] However, from such data landscape wide C-stocking cannot be inferred, unless the associated tree life history (life span, turnover etc.) is known.

[18] For commercial forestry this would mean that slow-growing trees may respond little to elevated CO_2 (e.g., Vanhatalo et al. 2003), while fast-growing trees would possibly do so more strongly (Calfapietra et al. 2003; Liberloo et al. 2005;Wittig et al. 2005).

forest of the type prevalent in the Amazon basin has yet to be ascertained, particularly under soil nutrient constraints.

For assessment of the effects of rooting depth, two different model settings of LPJmL were also used. In the standard setting (scenarios S1 and S3), the soil is differentiated in two layers: the upper layer contains 50 cm of soil and the lower layer 150 cm. 85% of the roots of evergreen PFTs are located in the upper and 15% in the lower soil layer. Raingreen trees are assumed to have 60% of their roots in the upper and 40% in the lower soil layer. As a second scenario, simulating "deep roots" (scenarios S2 and S4), a rooting depth of 8 m, with a soil profile of 50 cm of soil in the upper, and 750 cm in the lower layer was assumed. It was also assumed that evergreen trees have deeper roots with only 55% of their roots in the upper and 45% in the lower layer. Raingreen trees were assumed to have 85% of their roots in the upper and only 15% of the roots in the lower layer.

Table IV.2. Simulation experiments conducted with LPJmL to investigate the role of CO_2 and deep roots. See text for detailed description of the experiments.

Scenario	Description	
S1	Climate and CO_2 effects	Shallow roots
S2	Climate and CO_2 effects	Deep roots
S3	Climate effects only	Shallow roots
S4	Climate effects only	Deep roots

LPJmL simulates the coupled terrestrial carbon and water cycles, which are linked through vegetation with roots growing to a certain depth in the soil layer. However, only a few observations on rooting depth and distribution exist. Recent investigations have outlined the importance of deep roots to maintain a close canopy during the dry season, where they are needed to obtain sufficient water supply from deep soil water. Standard LPJmL simulations assume a soil depth of 2 m but root systems of up to 18 m deep have been found in Northeastern Pará (Nepstad et al. 1994; Kleidon and Heimann 2000). In order to better understand the associated uncertainty, a simulation experiment was conducted in which the effect of deep and shallow roots was tested (Table IV.3).

In a similar way, the effects of rising atmospheric CO_2 concentrations on vegetation are uncertain. CO_2 plays a major role as a limiting resource for carbon assimilation by plants (Farquhar et al. 1980). Several small-scale and chamber experiments have shown an enhancement of photosynthesis in C_3-plants under elevated CO_2 concentrations, leading to increased NPP (Curtis and Wang 1998; Norby et al. 1999). However, the long-term effects on real ecosystems are unclear (Norby et al. 1999). Large-scale ecosystem models such as LPJmL generally suggest a substantial impact of CO_2 on NPP (Cramer et al. 2001). Measurements from large-scale free-air CO_2 enrichment (FACE) experiments in temperate forests (Norby et al. 2005) have been compared to LPJ model simulations, and have shown that the model reproduced the overall response of forest productivity to elevated CO_2 (Hickler et al. 2008). In the model assumptions, elevated CO_2 concentrations reduce the negative effects of drought on plant growth (Gerten et al. 2005), which increase plant productivity. In the current assessment, the effects of

CO_2 were tested using a constant CO_2 scenario (Table IV.3) for a model that predicts severe rainfall reduction and Amazon dieback (HadCM3).

Table IV.3. Percentage of forest cover of the classified vegetation types in the Amazon basin under HadCM3-A2 scenario. Results for the factorial experiments, in which the effects of climate and CO_2 and the effects of shallow and deep rooting trees were tested.

Scenario	Forest cover (%)					
	1991–2000					
	tropical	deciduous	open forest	woodland	shrubland	savanna
S1	45.5	46.5	0.6	1.5	0.2	5.8
S2	75.3	16.8	0.3	1.5	0.2	5.8
S3	45.5	46.5	0.6	1.5	0.2	5.8
S4	75.3	16.8	0.3	1.5	0.2	5.8
	2041–2050					
	tropical	deciduous	open forest	woodland	shrubland	savanna
S1	32.0	60.8	0.2	1.2	0.1	5.8
S2	69.4	23.1	0.2	1.5	0.1	5.8
S3	25.3	27.8	20.1	5.0	15.9	5.8
S4	45.5	20.1	3.4	13.7	11.4	5.8
	2091–2100					
	tropical	deciduous	open forest	woodland	shrubland	savanna
S1	15.2	55.7	2.7	8.2	10.3	7.7
S2	36.9	38.9	2.9	9.0	5.9	6.4
S3	0.5	5.8	6.9	1.9	67.6	17.3
S4	0.8	2.5	2.8	3.1	74.7	16.1

Varying rooting depth and CO_2 effects produced strong effects on the degradation of Amazon forests under climate change (Table IV.3). Under current conditions, the vegetation of the Amazon basin is dominated by "tropical" and "mixed" deciduous forests. Assuming a forest with shallow rooting trees (scenario S1), 45% of the Amazon basin is covered with tropical forests (HadCM3-A2 scenario). With the assumption of deeper rooting trees (scenario S2), a 75% cover with tropical forests is projected for current climate conditions, due to better accessibility of trees to deep soil water.

With increasing atmospheric CO_2 concentrations (SRES-A2), the degradation of tropical forests is moderate until the middle of the 21st century, with 32% and 69% of the Amazon basin still covered by tropical forests in the S1 and S2 scenarios, respectively. Removing the drought-buffering and growth-stimulating effects of CO_2 from the simulations leads to a different picture. In the S3 scenario, about half of the former "mixed" forests are degraded to "open" forests, containing lower amounts of biomass. Shrublands increase by 15%. In the deep roots scenario, woodland and shrubland increase by 10%.

By the end of the century, under the assumed climate and CO_2 effects, only 37% of tropical forests remain in the S1 Scenario and 15% in the S2 Scenario. In the extreme case of the S3 Scenario, tropical forests disappear. The vegetation in the basin is converted to 68% shrubland and 17% savanna-like vegetation. The remaining 15% consists of mixed and open forests. Similar patterns are found in the S4 Scenario.

These results lead to the conclusion that the extent of a potential Amazon forest dieback is highly dependent on the model assumptions made on vegetation structure and response to environmental factors. The evaluation of the two assumptions on (1) the effects of CO_2 buffering on drought and (2) different rooting depth showed that an estimate of the strength of a potential dieback and the direction of forest degradation is strongly dependent on these assumptions.

Evidence from field measurements for these processes is lacking and estimates on the potential effects of CO_2 or on rooting depth distribution over the Amazon basin are not yet available. These crucial aspects for the ecosystem's resilience would certainly have to be part of any follow-up analysis. A substantial impact of CO_2 fertilization in mature stands of tropical forest under nutrient limited conditions is uncertain and should not be used as the basis for policy decisions.

Figure IV.12. Scenario analysis of the influence of deep and shallow roots under climate and CO_2 effects and climate-only effects. Simulation results for the HadCM3-A2 climate scenario.

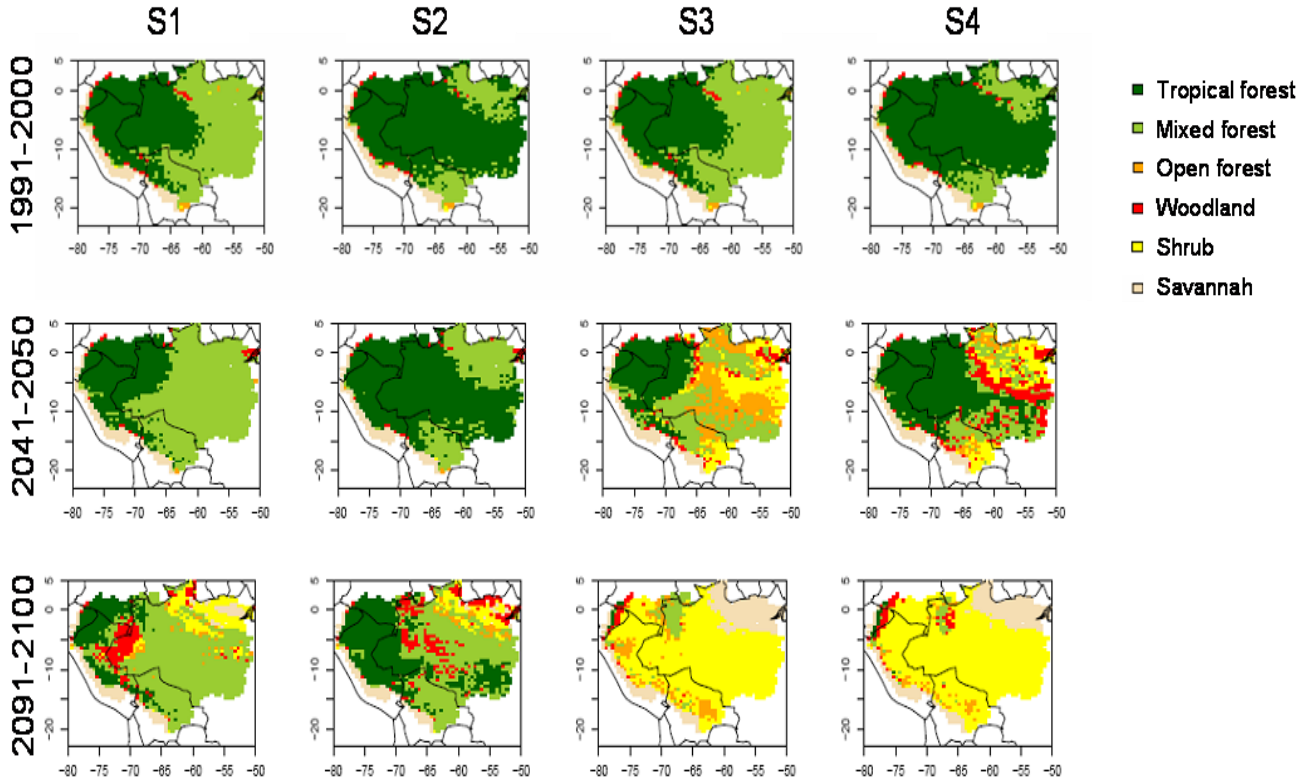

7. CHANGES IN TRANSPIRATION

Another aspect of vegetation changes in the Amazon basin is the contribution of forest to the convective precipitation that plays an important role in the region for water supply (Malhi et al. 2008). Vegetation in Amazonia is dominated by tropical and mixed forests that maintain high transpiration rates of ~850 mm yr^{-1} (~2.3 mm d^{-1}) under current climate conditions, with annual precipitation of 1200–3000 mm and temperatures of 20–28°C. This figure illustrates that tropical forests have a lower plasticity when it comes to adaption to drier conditions. They remain only in areas with still high precipitation and maintain high transpiration rates. Mixed forests are able to adapt to drier conditions and their transpiration rates decrease under drier conditions and with higher temperatures. However, the ecosystem shifts toward degraded forest types with less forest cover and lower biomass, such as woodland and shrubs. These types transpire less and therefore reduce the contribution to convective precipitation.

Figure IV.13. Transpiration (in mm yr-1) for the different vegetation types is dependent on precipitation and temperature. Under future conditions, with changing precipitation and temperature patterns and shifts in vegetation, transpiration changes.
Results from LPJmL simulations with HadCM3-A2 climatology.

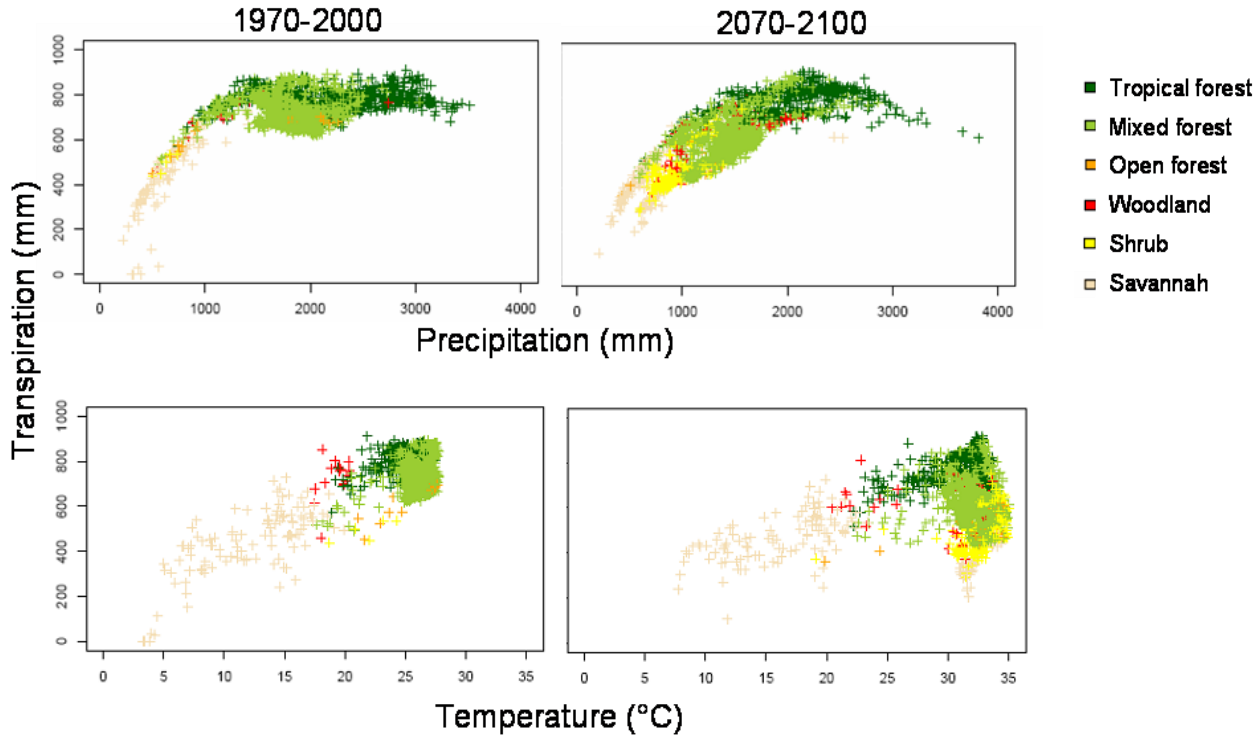

8. MECHANISMS OF POTENTIAL AMAZON DIEBACK

The mechanism of the potential forest dieback is illustrated best by the development of forest and grass cover over time in regions with severe drought simulated by the climate model. This is

illustrated for one example grid cell located in the northeastern part of Amazonia, at 51.25°W and 0.25°S (Figure IV.14), using one of the models that predict rainfall reductions.

The overall driver of the climate-caused collapse of forest in the northeastern part of Amazonia under the HadCM3-A2 climatology is a general decrease in mean precipitation accompanied by several extreme drought events starting after 2050. High transpiration rates first lead to a depletion of soil water in the upper and then the lower soil layer, causing high water stress in the plants. This is followed by a strong reduction in NPP and quickly increasing mortality of trees.

In this particular example, forest cover recovers during the following years back to 80–95%. This can be explained by a quick response of woody-vegetation regrowth. The response of the vegetation may be severely overestimated in LPJmL since no soil erosion or other degradation is assumed to take place. The structure of the forest changes, with a result of more grass vegetation than before the drought events. In the case of the S1 and S3 Scenarios, the high amount of these highly flammable grasses triggers frequent fire events. These effects are stronger under the climate-effects-only assumption. The system may at this point change to a fire-driven ecosystem state that can be characterized as savanna.

Figure IV.14. Vegetation change at local scale in a grid cell in Northeastern Amazonia. (a) Mean annual temperature and sum of annual precipitation from 1980 to 2100 from the HadCM3-A2 climate scenario. (b-e) Factorial analysis of the influence of deep/shallow roots and simulations with influence of climate+CO_2 and climate change effects only (Scenarios S1-S4).
The light blue line is soil water content as a fraction of soil water holding capacity (in %) for upper (plain line) and lower (dashed line) soil levels.

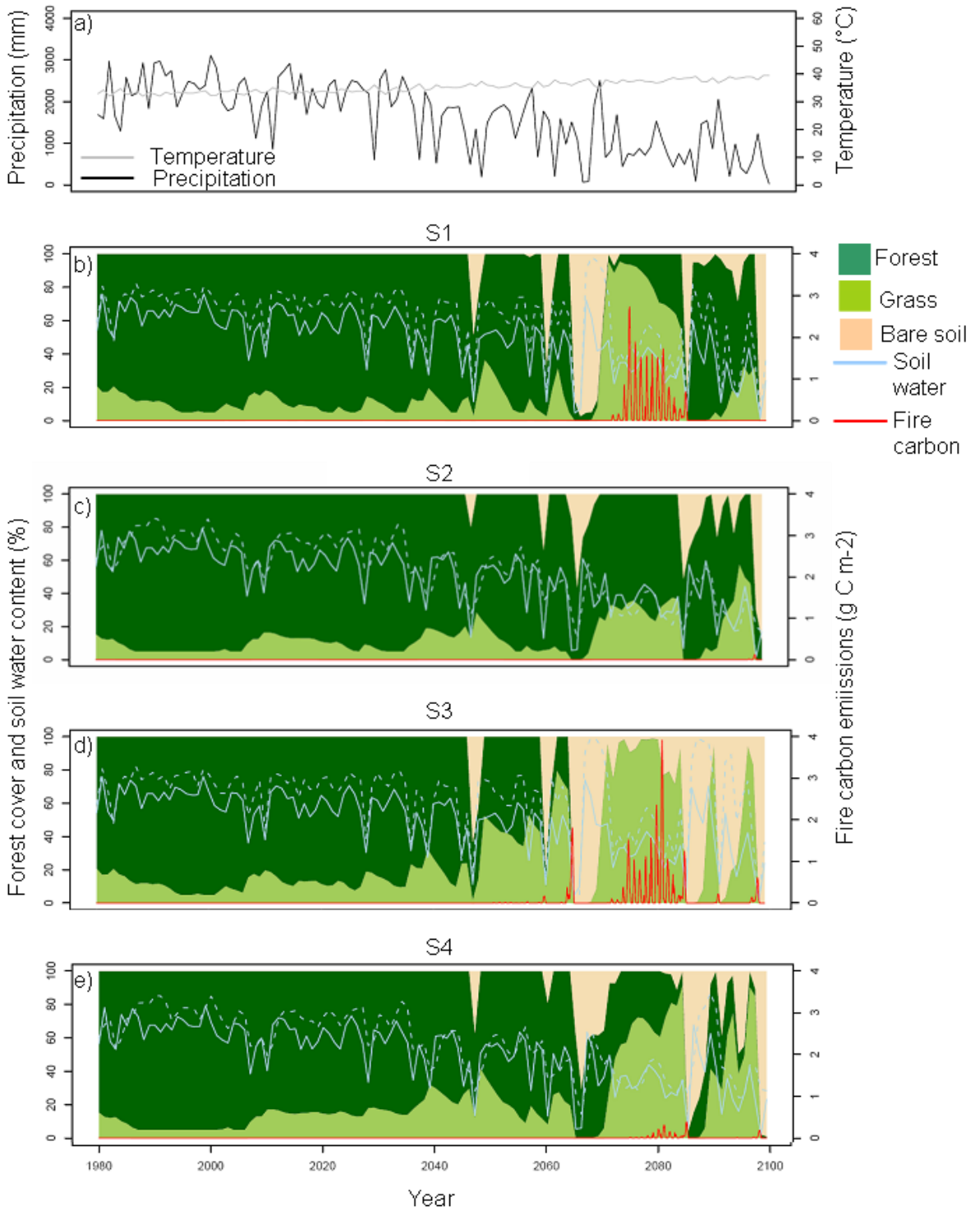

9. CHANGES IN LIGHTNING-CAUSED WILDFIRES

Fires are rare events under undisturbed conditions in tropical forest ecosystems. They have been observed historically either as part of small-scale slash-and-burn activity (Kauffman and Uhl 1990), or due to lightning-caused ignitions in occasional drought years (Cochrane and Laurance 2008). Thus, besides physiology-driven growth and mortality responses, another important indicator for the effects of climate change on the Amazon rainforest could be changes in the occurrence of actual fires or fire danger.

Climatic fire danger, based on LPJmL-SPITFIRE, was analyzed. The fire danger index is projected to increase significantly under the dry and hot HadCM3-A2 Scenario. The interannual variability increases remarkably after 2060, when the projected precipitation starts to decline in the HadCM3 model. Under the wetter scenario of the MRI CGCM 2.3.2a, the climatic fire risk remains variable but relatively constant over the two centuries (Figure IV.15).

Figure IV.15. Projected climatic fire danger for the HadCM3 (blue) and the MRI CGCM 2.3.2a (red) under the SRES-A2 Scenario simulated by LPJmL-SPITFIRE for the 20th and 21st century.

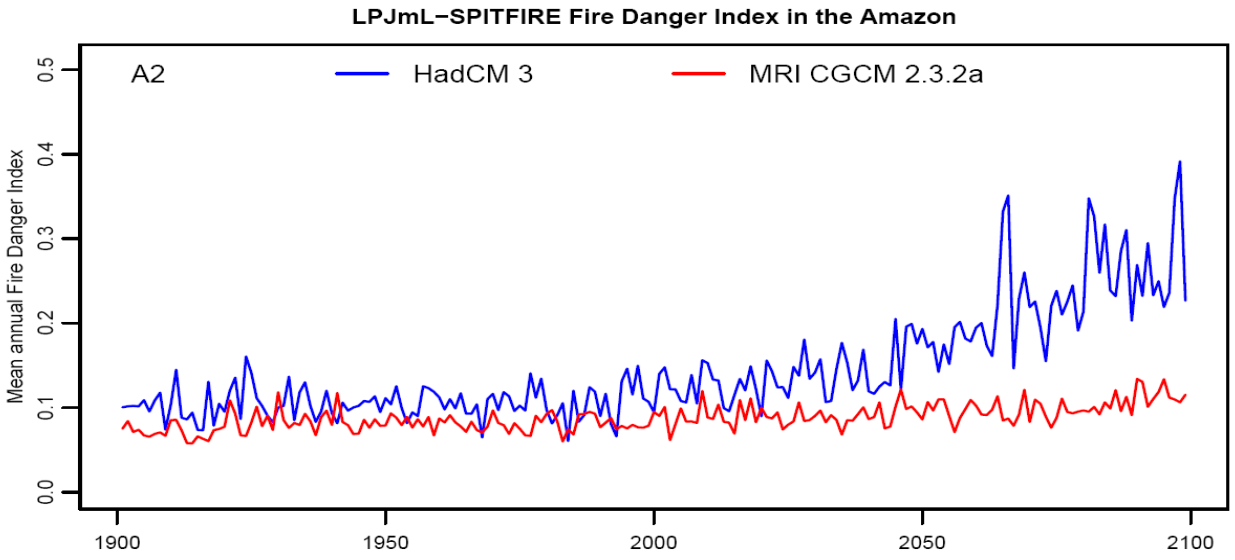

Using the HadCM3-A2 Scenario, the simulated climatic fire danger is still low under current climate conditions, but already higher than under the MRI CGCM. Changed climatic conditions by the end of the 21st century lead to an increased fire danger, with very high danger levels in Northeastern Amazonia in the HadCM3-A2 Scenario. In the wet scenario (MRI CGCM 2.3.2a), climatic fire danger increases from very low to low fire danger levels, mainly in the southeast of the basin.

Figure IV.16. Simulated climatic fire danger under the MRI CGCM 2.3.2a (top) and the HadCM3 (bottom) climate scenario using the SRES A2 emission scenario.
Top-left and bottom-left maps show contemporary average (1970–2000); top-right and bottom-right maps show the average over 2070–2100.

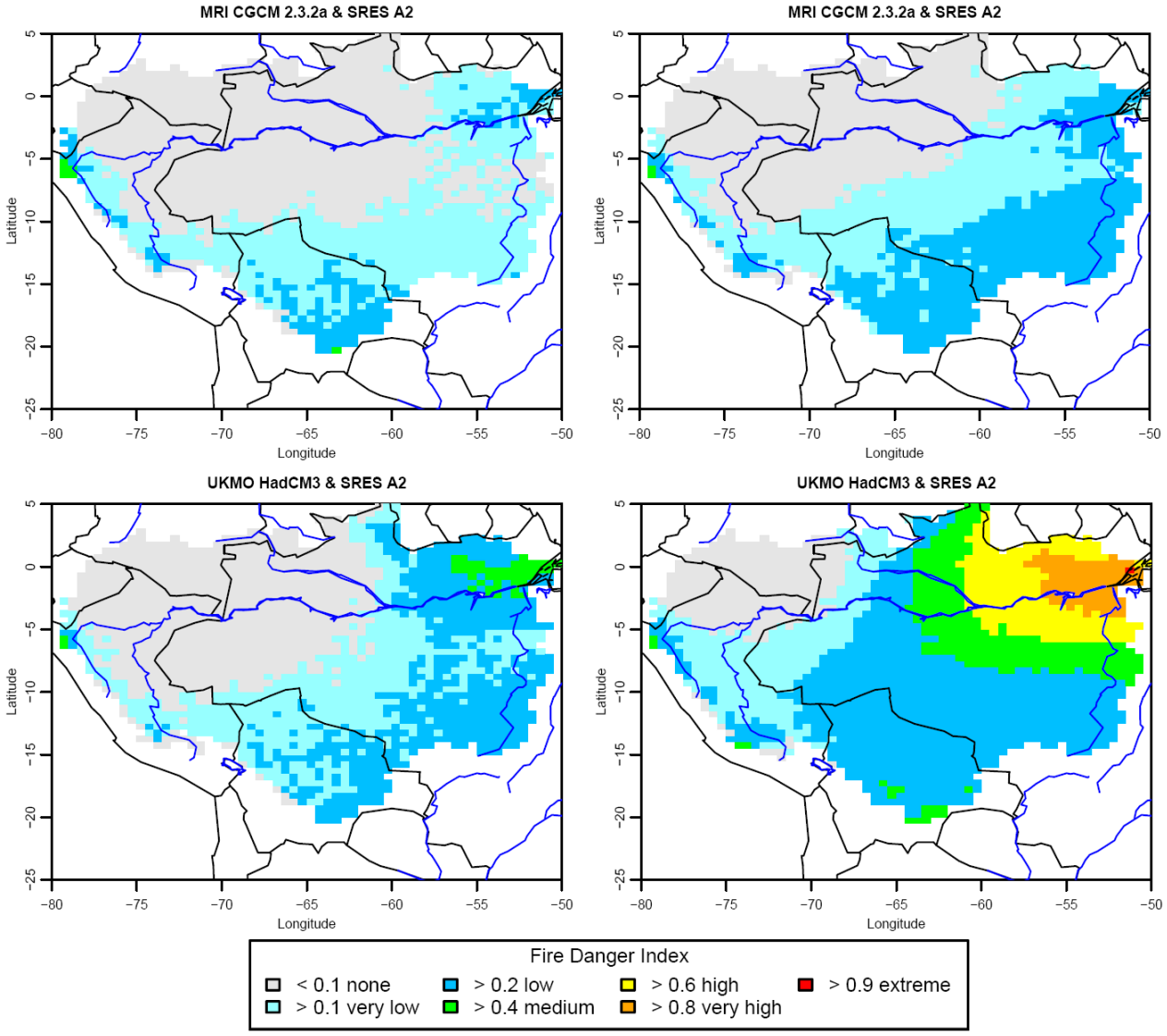

The elevated fire danger index is not automatically leading to increased fire frequency. Fires can start after lightning events only if sufficient fuel load is available. Thus, after a significant increase of flammable grasses, e.g., as a result from drought-induced forest degradation (see

Figure IV.16), increases in climatic fire danger in the Northeastern Amazon lead to an increase in burned area, thus the fire-related carbon emission (Figure IV.17) in the HadCM3-A2 scenario. Low climatic fire danger levels do not allow the development of sufficient surface energy which could sustain burning. Therefore, no carbon emissions are simulated under the wet MRI-CGCM 2.3.2a climate scenario.

Figure IV.17. Annual total carbon emission from wildfires as simulated by LPJmL-SPITFIRE for the Eastern Amazon Region (for HadCM3, MRI CGCM 2.3.2a and SRES-A2).

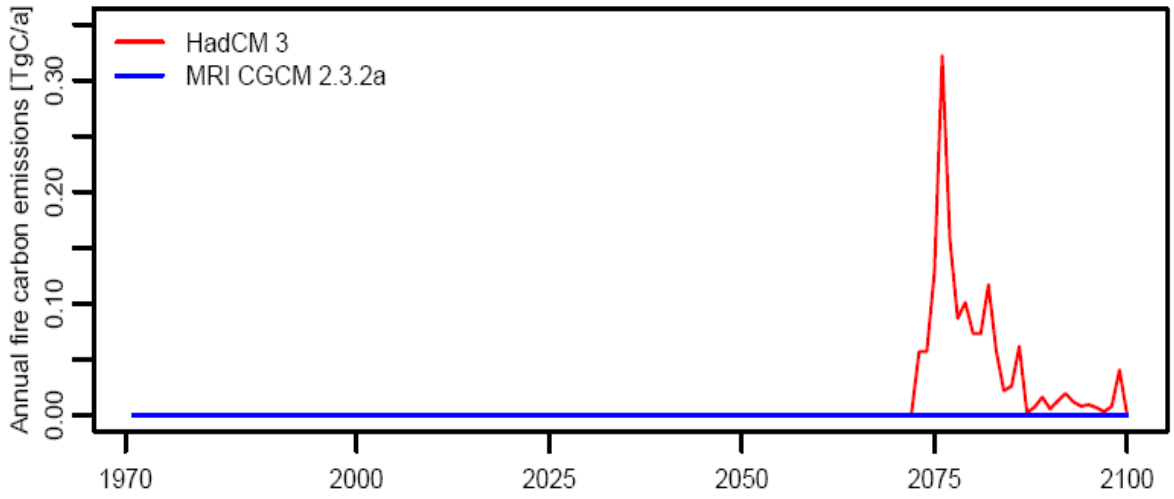

V. Interplay of climate impacts and deforestation in the Amazon

1. REGIONAL LAND USE AS A DRIVER IN THE STABILITY OF THE AMAZON RAINFOREST

The previous analysis was made on the basis of no land use change and in response to climate-induced changes in rainfall through a dynamic (LPJmL) vegetation model. However, regional land use changes, such as deforestation, biomass burning and forest fragmentation, affect local and regional climate and may compound the effects of global climate change on the stability of the Amazon rainforest by redefining bioclimatic conditions and thus the biome-equilibrium state of the basin.

For example, field observations (e.g., Gash and Nobre 1997) and numerical studies (e.g., Sampaio et al. 2007, Nobre et al. 1991) have revealed that large-scale deforestation in Amazonia could alter the regional climate significantly. Evapotranspiration and precipitation are reduced and soil temperature is increased where there is no forest canopy. That effect might lead to a biome shift toward "savanna" of portions of the tropical forest domain.[19]

A coupled climate-vegetation model (CPTEC-CPVM, described later in the report) is used to estimate these combined effects.[20] The advantage of being coupled with a climate model is that the feedbacks of vegetation change to the climate can be investigated. Thus, the model can simulate biome distribution (one biome per grid cell) based on bioclimatic limits as these are affected by climate change.

The current vegetation in the Amazon basin, including its deep root system, is efficient in recycling water vapor, which may be an important mechanism for the forest's maintenance and contributes to the overall water cycle in the region. Thus, deforestation and forest fragmentation can alter the hydrological cycle and cause other impacts as well. For instance, in the event of severe droughts the forest can become highly susceptible to fires due to soil water deficits (Nepstad et al. 2001). Soares-Filho et al. (2006) have shown that if the current high deforestation rates are to continue into the future, about 40% of the Amazonian tropical forests will have disappeared by 2050. In principle, deforestation and global warming acting synergistically could lead to drastic biome changes in Amazonia.

In this section, analyses are made to quantify how deforestation and climate change may combine to affect the distribution of the Amazon ecosystem. To this end, simulations of climate (temperature, precipitation) and vegetation change in tropical South America were performed in the five selected geographical domains. The simulations account for land use change, global warming and vegetation fires. Changes in land use consider deforestation scenarios of 0%, 20%, 50% and 100%, with and without fires, under scenarios B1 and A2 from IPCC AR4.

[19] Oyama and Nobre (2003) showed that it is possible to have two biome-climate equilibrium states in tropical South America. One equilibrium state corresponds to the current vegetation distribution where the tropical forest covers most the Amazon Basin and the second corresponds to stable biome-climate equilibrium with savannas covering eastern Amazonia and semi-deserts in Northeastern Brazil.

[20] There is no model that combines the dynamic and coupled features of LPJmL and CPTEC-CPVM and thus these two tools are used, where they can best be applied.

In addition, results of the use of the CPTEC land vegetation model (CPTEC-PVM) with the Earth Simulator MRI-GCM outputs, with particular focus on the regional impacts in the five selected domains and the La Plata basin, are also reported.

2. SCENARIOS

2.1 Deforestation

In the simulated deforestation scenarios, rainforest was converted to degraded grass (with deforested areas equal to 20%, 50% and 100% of the original extent of the Amazon forest). The land cover change scenarios are from Sampaio et al. (2007) and Soares Filho et al. (2006), and consider that recent deforestation trends will continue; highways currently scheduled for paving will be paved; compliance with legislation requiring forest reserves on private land will remain low; and protected areas will not be enforced. Although extreme, it is important to evaluate scenarios of complete deforestation.

2.2 Climate Change

This study uses standard output, available through the Coupled Model Intercomparison Project phase 3 (CMIP3) multimodel dataset, from Coupled Ocean-Atmosphere GCMs for the IPCC AR4. (See details in Table V.1.)

Biome distribution was examined for the 21st century under emission scenarios A2 and B1,[21] which provide an outer envelope to the A1B scenario on the upper and lower bounds. Climate simulation for the end of the 20th century (20CM3) of each model is used to evaluate the models' anomalies. The precipitation and surface temperature monthly climatology for the Amazon (1961–1990) is obtained from work by Willmott and Matsuura (1998).

[21] These represent a plausible range of conditions over the next century. In scenario B1, the atmospheric CO_2 concentration in year 2100 (2025, 2075) reaches a level of 550 ppm (410 ppm, 480 ppm); in A2 the corresponding value is 730 ppm (410 ppm, 520 ppm) (Intergovernmental Panel on Climate Change, 2000).

Table V.1. The climate models referred to in this analysis. The models are selected from those in the Coupled Model Intercomparison Project phase 3 (CMIP3) multi-model dataset.

Model	Institute (Country)	Resolution (Atmospheric component)
BCCR-BCM2.0	Bjerknes Centre for Climate Research (Norway)	T42L31 (approx. 2.8° lat/lon)
CCSM3	National Center for Atmospheric Research (USA)	T85L26 (approx. 1.4° lat/lon)
CGCM3.1(T47)	Canadian Centre for Climate Modelling and Analysis (Canada)	T47L31 (approx. 3.75° lat/lon)
CNRM-CM3	Météo-France/Centre National de Recherches Météorologiques (France)	T42L45 (approx. 2.8° lat/lon)
CSIRO-Mk3.0	CSIRO Atmospheric Research (Australia)	T63L18 (approx. 1.875° lat/lon)
ECHAM5/MPI-OM	Max Planck Institute for Meteorology (Germany)	T42L31 (approx. 2.8° lat/lon)
ECHO-G	Meteorological Institute of the University of Bonn (Germany), Institute of KMA (Korea)	T30L19 (approx. 3.75° lat/lon)
GFDL-CM2.0	US Dept. of Commerce/NOAA/ Geophysical Fluid Dynamics Laboratory (USA)	2.° lat. x 2.5° lon., L24
GFDL-CM2.1	US Dept. of Commerce/NOAA/ Geophysical Fluid Dynamics Laboratory (USA)	2.° lat. x 2.5° lon., L24
GISS-ER	NASA/Goddard Institute for Space Studies (USA)	4° lat x 5° lon., L15
INM-CM3.0	Institute for Numerical Mathematics (Russia)	5° lat. x 4° lon, L21
IPSL-CM4.0	Institut Pierre Simon Laplace (France)	2.5° lat x 3.75° lon., L19
MIROC3.2(medres)	Center for Climate System Research (Univ. of Tokyo), National Institute For Environmental Studies, and Frontier Research Center For Global Change (Japan)	T42L20 (approx. 2.8° lat/lon)
MRI-CGCM2.3.2	Meteorological Research Institute (Japan)	T42L21 (approx. 2.8° lat/lon)
UKMO-HadCM3	Hadley Centre for Climate Prediction and Research/Met Office (UK)	2.5° lat. x 3.75° lon. L19

The climate change scenarios at regional scale (60-km resolution) were projected by the high-resolution MRI-JMA AGCM for the present time (1989–1999), near future (2015–2039) and future (2075–2099) for the IPCC SRESA1B emission scenario.

3. MODELS USED

3.1 The CPTEC AGCM Model

Although the vegetation response was estimated using the LPJmL model referred to in Section IV, there is a need to estimate biome shifts and not merely biomass response. The latter is achieved with a coupled vegetation model (a model that links climate forcing and biome equilibrium states in the Amazon basin). The CPTEC-INPE global atmospheric model (Cavalcanti et al. 2002) is used for the numerical simulations, at T062L42 spectral resolution (42 vertical levels, ~2° lat/lon horizontal resolution).[22] The land surface scheme is the SSiB (Xue et al. 1991). For each land grid point, a vegetation type (biome) is prescribed following the classification by Dorman and Sellers (1989) along with a set of physical, morphological and physiological parameters.

3.2 Non-dynamic Potential Vegetation Model CPTEC-PVM2.0

The CPTEC-PVM2.0 (Lapola et al. 2009), a new version of the CPTEC (global) Potential Vegetation Model (Oyama and Nobre 2004), was used. It shows a particularly good performance over South America due to the consideration of seasonality as a determinant for the delimitation of forests and savannas. It also takes into account plants' physiological responses to seasonality (such as primary productivity) under varying atmospheric CO_2. The biome allocation relies mainly on the optimum net primary productivity (NPP) values for a given grid cell.

The determination of biome distribution through NPP is done based on numerous studies showing that different biomes have different average NPP (e.g., Sahagian and Hibbard 1998; Turner et al. 2006). However, in some cases NPP can be quite similar among biomes (such as for boreal forest and grassland) and in these cases variables other than NPP (e.g., coldest month temperature) are used for biome allocation. As a non-dynamic model, it calculates only equilibrium solutions based on long-term mean monthly climate variables. This is done concomitantly with a water balance submodel using climatologies of surface temperature and precipitation (1961–1990: Willmott and Matsuura 1998), intercepted photosynthetically active radiation (IPAR) (1986–1995: Raschke et al. 2006) and atmospheric CO_2 (1961–1990: 350 ppmv) as inputs.[23]

[22] The CPTEC-INPE AGCM (atmospheric global circulation model) available at INPE was developed at the Brazilian Center for Weather Forecast and Climate Studies (CPTEC) based on the CPTEC/COLA (Center for Ocean-Land-Atmosphere Studies) GCM described by Cavalcanti et al. (2002). It has been shown that the model simulates reasonably well the main features of global climate, as well as the seasonal variability of the main atmospheric variables.

[23] Water balance routine is nearly the same as in CPTEC-PVM (Oyama and Nobre 2004) based on Willmott et al. (1985), although canopy resistance r_c (1/canopy conductance g_c) is calculated in terms of NPP and atmospheric (CO_2), based on the formulation by Collatz et al. (1991), which is used by several DGVMs (Sitch et al. 2008) and GCM surface schemes (e.g., Sellers et al. 1996)). The canopy resistance is used to calculate evapotranspiration (hereafter E) according to Penman-Monteith's equation. This formulation enables a two-way interaction of water cycle and plant physiology. CPTEC-PVM2 also considers a simple parameterization of lightning-induced fires in savannas based on the study by Cardoso et al. (2008). Fire occurrence is regarded as dependent on the availability of natural ignition source (using 850 hPa zonal wind as a proxy to lightning) and fuel moisture (through soil water level). The fertilization effect in this model is considered 25% of the total CO_2 atmospheric concentration for each emission scenario (A2 and B1). Global and regional NPP simulated by CPTEC-PVM2 are quite comparable to that

CPTEC-PVM2.0 is forced by monthly precipitation, surface temperature and zonal wind inputs derived from ocean-atmosphere global climate models of the IPCC AR4, for the 1961–1990 period (actual climate) and three time slices in the 21st century (2010–2039, 2040–2069 and 2070–2099).

4. SIMULATIONS

4.1 Deforestation-only forcing

To evaluate the impact of a specific deforestation scenario, the climate and vegetation model results are used in sequence, according to the following steps. The climate model is run first, under the new deforestation scenario, and a climate condition is found that corresponds to this new surface configuration. Then, assuming that this resulting climate condition is sustained, the potential vegetation model is applied to find the new vegetation distribution in equilibrium with this climate. The resulting vegetation distribution will not necessarily reflect exactly the patterns in the deforestation scenario. That may happen because the new climate could support forest recovery or further savanna expansion, for example.

The CPTEC AGCM was integrated for 87 months, with five different initial conditions derived from five consecutive days of NCEP analyses, from October 14 to 18, 2002. Climate boundary conditions, including sea surface temperature, for experiments and control were used. The simulated deforestation was converted to degraded grass (for land cover change scenarios with deforested areas equal to 20%, 50% and 100% of the original extent of the Amazon forest).

4.2 Climate-change-only forcing

The CPTEC-PVM2.0 was used in three 20-year time slices of the 21st century: 2015–2034, 2060–2079 and 2085–2099 ("2025," "2075," and "2100" time slices, respectively), for the A2 and B1 scenarios of Greenhouse Gas Emissions (GHG) from 15 IPCC models.

4.3 Climate change and deforestation

The CPTEC-PVM2.0 was used by combining the methodology in paragraphs 4.1 and 4.2 above. A supposed deforestation of 20% is assumed in the "2025" time slice and a deforestation of 50% in the "2075" time slice. The climate anomalies from deforestation were combined with the anomalies of the IPCC scenarios, for each time slice. The total (100%) deforestation was not evaluated together with climate projections because of the major uncertainties associated with both extreme scenarios, and the lack of results from some of the climate models beyond the 21th century, when total deforestation would be assumed.

4.4 Climate change, deforestation and fire

The CPTEC-PVM2.0 was used as in paragraph 4.3, adding to the potential for occurrence of land use fires according to the method described in the section above.

---

from observations and also from other NPP models. Biome distribution is evaluated against an analysis of natural vegetation (Lapola et al. 2008) and results in a global kappa statistic (Monserud and Leemans 1992) of 0.53, and an agreement fraction of 57% (Lapola et al. 2009).

5. BIOME RESPONSE TO DIFFERENT FORCINGS

5.1 Deforestation only

The results from deforestation only simulations are summarized in Figure V.1. In the case of 20% deforestation (Figure V.1a), the biome-climate equilibrium state shows a reduction of forest area in Eastern and Southern Amazonia with savannas and tropical seasonal forest covering this region, and semi-desert area in Northeastern Brazil.

With 50% deforestation (Figure V.1b), the savannas and tropical seasonal forest areas cover a large part of Amazonia. The original forest cover is replaced by savannas and tropical seasonal forest and there is an expansion of the semi-desert area in Northeastern Brazil.

For the extreme case of 100% deforestation, the biome-climate equilibrium shows that most of Amazonia is covered by savannas and tropical seasonal forest (Figure V.1c). In Northeastern Amazonia there appears an area with dry shrubland (*caatinga*) and in Northeastern Brazil a large expansion of the semi-desert area. In general for the Amazon and Northeastern Brazil, there is replacement by drier climate biomes: savannas replacing forests, caatinga replacing savannas and semi-desert vegetation replacing dry shrubland. In these regions, the decrease in precipitation is more distinct in the dry season (June–October). In all cases, the average temperature near the surface increases with deforestation.

Figure V.1. Biome-climate equilibrium states in South America for 20% (a), 50% (b) and 100% (c) Amazon deforestation scenarios

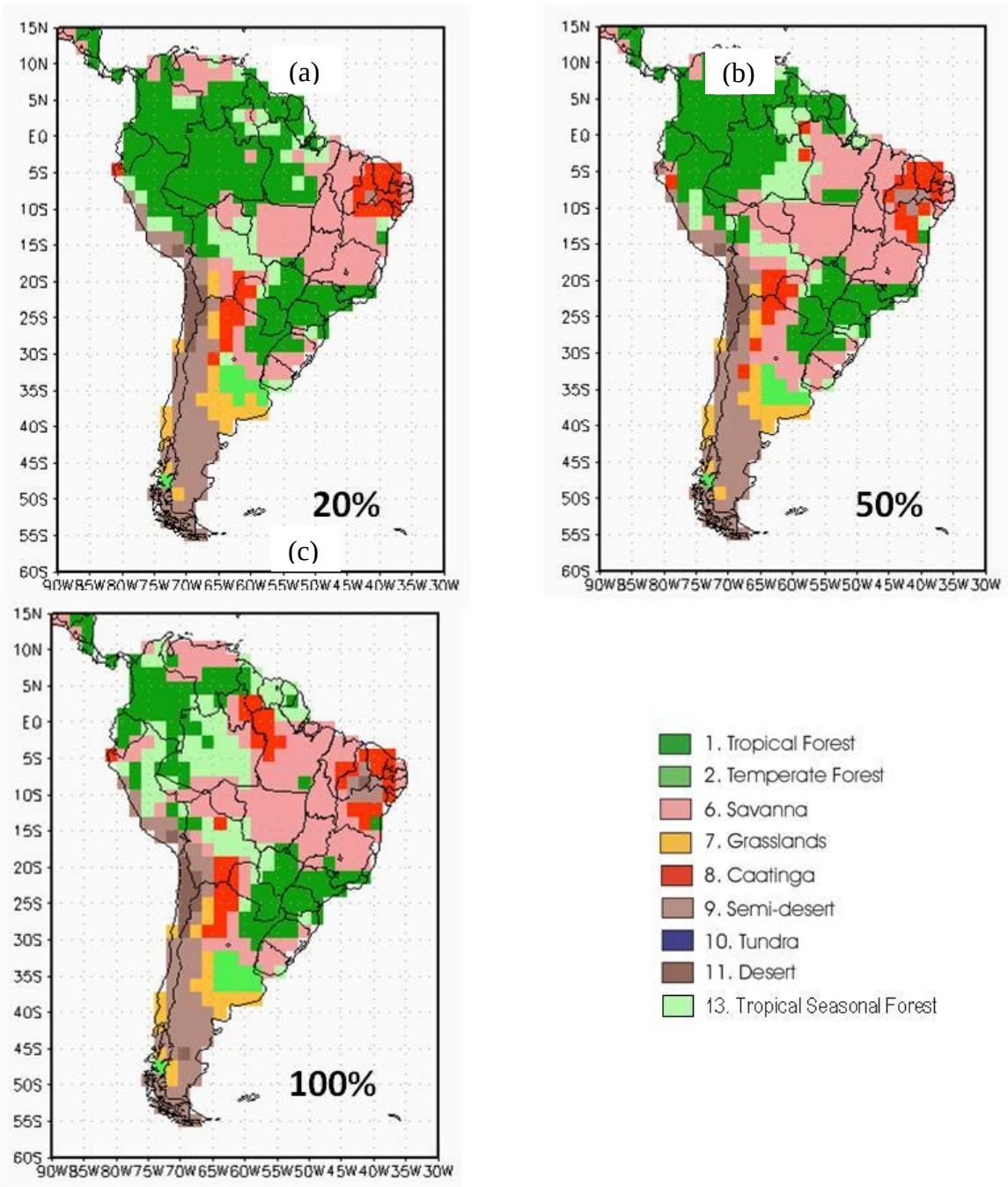

The implications of deforestation at these levels are serious and drastically affect the viable biomes in the region. The results for the specific regions are shown in Figure V.2.

For Eastern Amazonia (Figure V.2a), the remaining area of tropical forest decreases with the expansion of the altered area at the initial condition. The remaining area of seasonal forest

increases for 0–20% deforestation, decreases for 20–50%, and stabilizes for further deforestation. Savannas expand in all cases, but their rate of expansion is substantially higher, between 0 and 50% deforestation.

For Northwestern Amazonia (Figure V.2b), the decrease of the remaining area of tropical forest is higher after 50% deforestation. The expansion of the remaining area of seasonal forest exhibits a similar but inverse pattern, with pronounced expansion for deforestation fractions greater than 50%. The change in the remaining savanna area is less pronounced, and is greater for deforestation higher than 50%.

The patterns of change in Southern Amazonia (Figure V.2c) are similar to the patterns in the eastern part of the region, with tropical forests always decreasing with deforestation; savanna expansion is pronounced for percentages of altered area in the initial condition smaller than 50%. However, savannas show a slight decrease for higher values of altered initial areas.

For the entire region (Figure V.2d), the remaining area of tropical forest decreases almost linearly with deforestation. The other biomes expand in all cases; however, the expansion of savannas is more intense for 0–50% deforestation but stabilizes for higher values.

In Northeastern Brazil (Figure V.2e), there is a noticeable expansion of the semi-desert and a decrease of the remaining areas of savanna and caatinga. For Southern Brazil (Figure V.2f), the areas of all major biomes analyzed remain virtually unchanged.

Figure V.2. Remaining area (10^6km²) of potential tropical forest, seasonal tropical forest, savanna, caatinga and semi-desert biomes for Eastern Amazonia (a), Northwestern Amazonia (b), Southern Amazonia (c), Amazonia as a whole (d), Northeastern Brazil (e) and Southern Brazil (f), for land cover change scenarios with deforested areas equal to 20%, 50% and 100% of the original extent of the Amazon forest

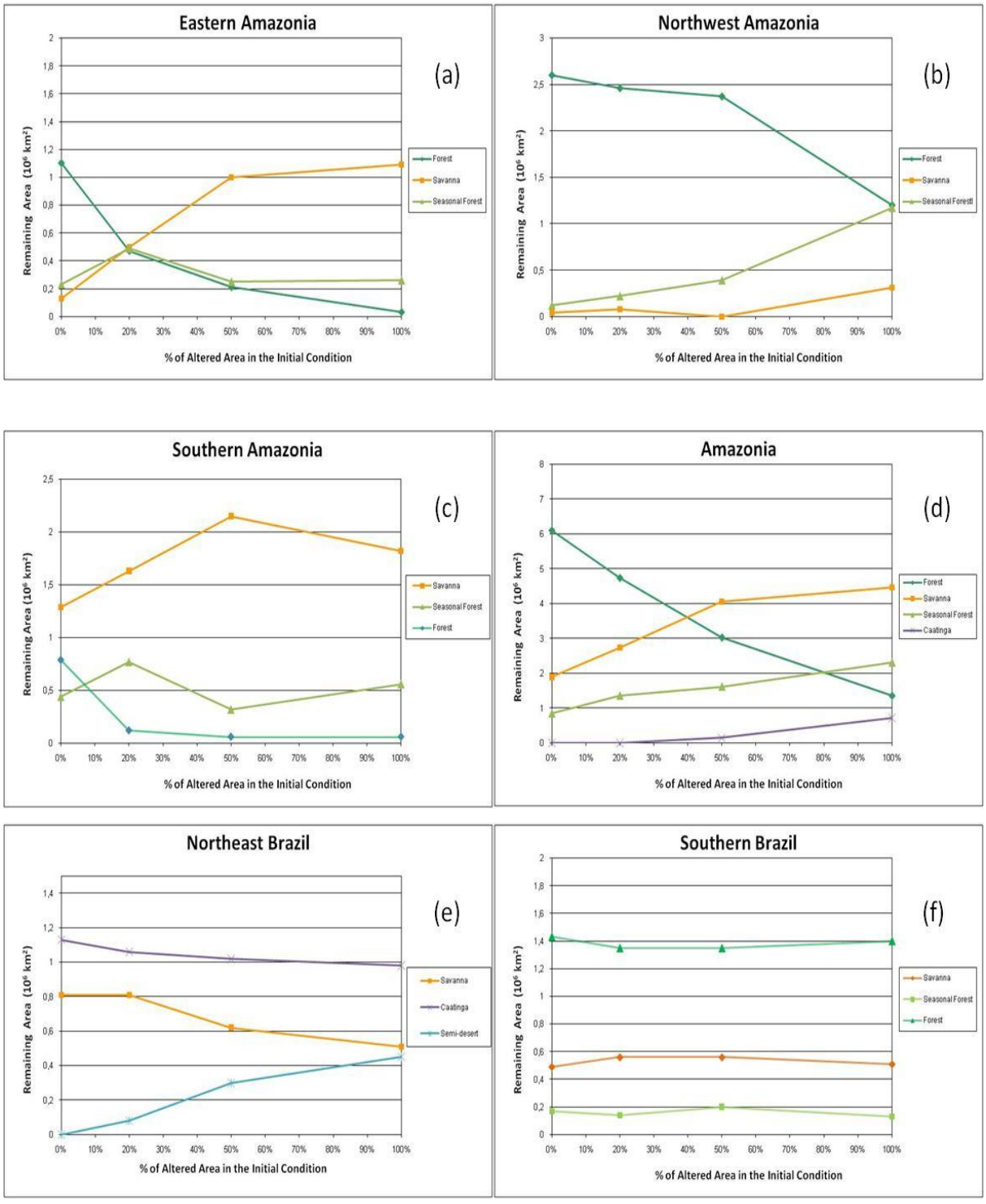

5.2 Climate change only

The results of climate only impacts on biome equilibrium shifts are shown in Figure V.3 The results in Figures V.3 to V.5 show grid points where more than 75% (at least 12) of the models coincide in projecting the future condition of biomes in relation to the current potential vegetation (75% consensus) for the different experiments. In these maps, "no consensus" means that fewer than 12 models agree with the transition. "Loss" means consensus for substitution of that biome class.

Climate change will potentially have important effects on the spatial patterns of the biomes' distribution in South America. The results for the Amazon under scenario A2 indicate consensus for change from tropical to seasonal forest by 2075, and from tropical to other biomes by 2100. In this region, for climate scenario B1, the results are less severe.

5.3 Climate change and deforestation

Combined global climate change and deforestation in Amazonia compound the effects on the spatial patterns of biome distribution in South America. The results of these interactions are shown in Figure V.4. Relative to the previous climate-change-only analysis, the results here generally show a larger area of tropical forest loss and noticeable savanna expansion for scenario B1 by 2075, under 50% deforestation. In Northeastern Brazil, for both climate scenarios, the area of consensus for changes from caatinga to other biomes is larger than in the previous results with expansion of caatinga to the North and Northwest. In Southern Brazil, the results are similar to the climate-change-only analysis, and project consensus for expansion of tropical forest over areas of potential savannas.

Figure V.3. Grid point for 75% consensus on future condition of tropical South American biomes in relation to current potential vegetation, for time slices (A) 2025, (B) 2075 and (B) 2100 for the A2 GHG emissions scenario, and (D), (E), (F) similarly for the B1 GHG emissions scenario. In these maps, "no consensus" means that fewer than 12 models agree with the transition. "Loss" means consensus for substitution of that biome class. SD means semi-desert.

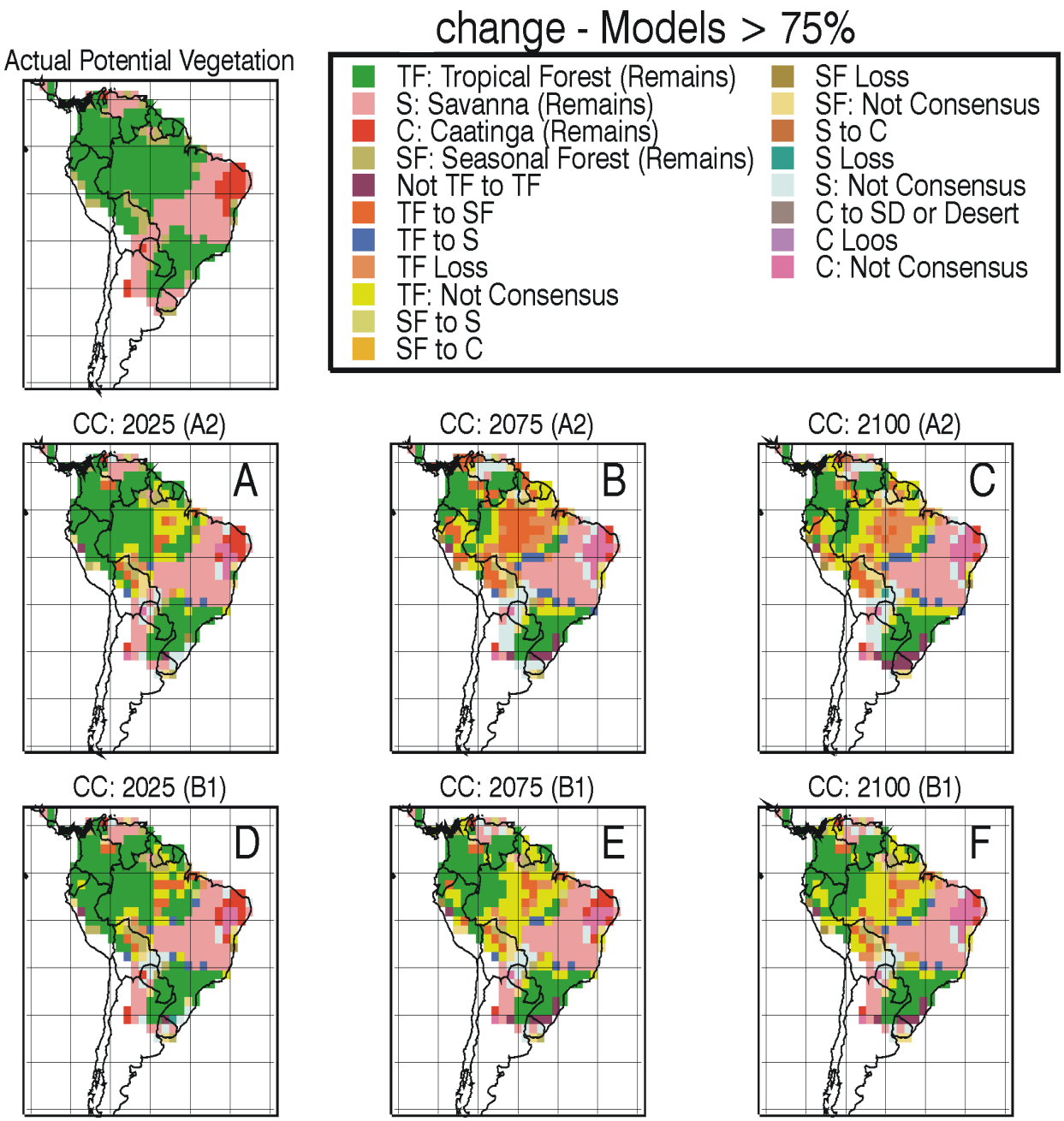

Figure V.4. Grid point for 75% consensus on projecting the future condition of tropical South American biomes in relation to current potential vegetation, for time slices (A) 2025 + 20% deforestation and (B) 2075 + 50% deforestation for the A2 GHG emissions scenario, and (C), (D) similarly for the B1 GHG emissions scenario. In these maps, "no consensus" means that fewer than 12 models agree with the transition. "Loss" means consensus for substitution of that biome class.

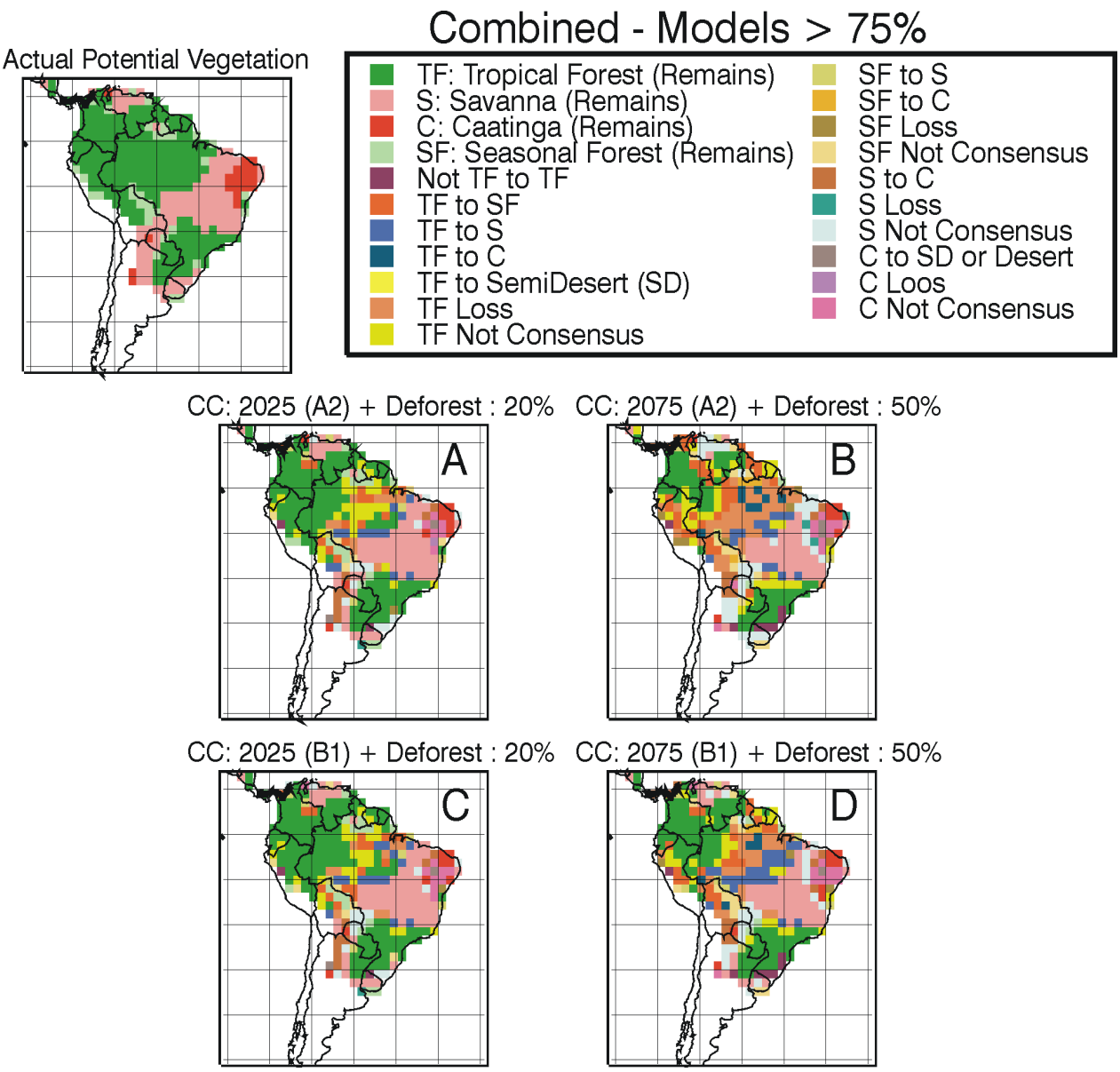

5.4 Climate change, deforestation and fire

Figure V.5 displays results considering the combination of global climate change, deforestation and fires. An important feature in these results is that the effect of including the potential for fire occurrence is greater in the period before 2025 for both climate scenarios. For Amazonia as a whole, the remaining tropical forest area for time slice 2025 progressively reduces as climate

change impacts, deforestation and fire are combined relative to its original extension. The projected remaining Amazon rainforest biome by 2100, under scenario A2, is about one third of the original.

Major impacts are projected in Eastern Amazonia. The combined effects of climate and deforestation result in a severe decrease of the rainforest biome, in relation to its original extension for forest area. The remaining forest biome, by 2075, accounting for 50% deforestation and or the effects of fires, is about 5%. This is the largest relative decrease in the entire basin.

The Northwest projections indicate the smallest relative decrease of tropical forest biome for the entire basin. The impact of fires was found to be not significant. The decrease of the tropical forest area is smaller than 10% for time slice 2025. However, even for this region, under scenario A2 there would be a significant decrease by 2100 (about 60% of remaining biome).

For Southern Amazonia, the analysis indicates a relative increase in the area of savanna. Deforestation contributes to this configuration with a drier and hotter climate, favoring savanna expansion in replacement of tropical forests. In this region, fire has an important effect. For scenario A2 (and B1), and time slices 2025 and 2075, the projection indicates a net increase in the area of savanna, ranging from 30% to 80%.

For the Northeast the analysis indicates a slight relative increase (4%–7%) in caatinga, resulting from hotter and drier climate.

In Southern Brazil the combination of factors leads to a decrease in the forest area, with a strong effect derived from forest fires. In general, fire potential strengthens the consensus for transitions from tropical forest to savanna in the Southern and Southeastern regions of Amazonia.

Table V.2 Consensus results for remaining share of reference biome compared to baseline (=100) by geographical domain, from 2025 to 2100 under scenario A2*

Domain	Reference biome	Climate change impact by 2025	+20% deforestation	+ fire impact	Climate change impact by 2075	+50% defor.	+ fire impact	Climate change impact by 2100
EA	**Rainforest**	**56**	**29**	**26**	**37**	**5**	**5**	**26**
NWA	**Rainforest**	**92**	**89**	**89**	**80**	**74**	**74**	**60**
SAz	**Savanna**	**130**	**136**	**138**	**125**	**145**	**180**	**134**
NEB	**Caatinga**	**92**	**91**	**91**	**90**	**105**	**105**	**82**
SB	**Rainforest**	**110**	**108**	**107**	**118**	**116**	**108**	**128**
Amazonia	**Rainforest**	**74**	**59**	**56**	**57**	**33**	**32**	**37**

(*) Similar but smaller transitions are found for scenario B1.

Figure V.5. Figure 3 - Future condition of tropical South American biomes, plots of results for which more than 75% of the models coincide[24] as in relation to current potential vegetation, for time-slices:

(A) A2 GHG emissions scenario 2025 + 20% deforestation + fire;
(B) A2 GHG emissions scenario 2075 + 50% deforestation + fire
(C) B1 GHG emissions scenario 2025 +20% deforestation + fire
(D) B1 GHG emissions scenario 2075 + 50% deforestation + fire

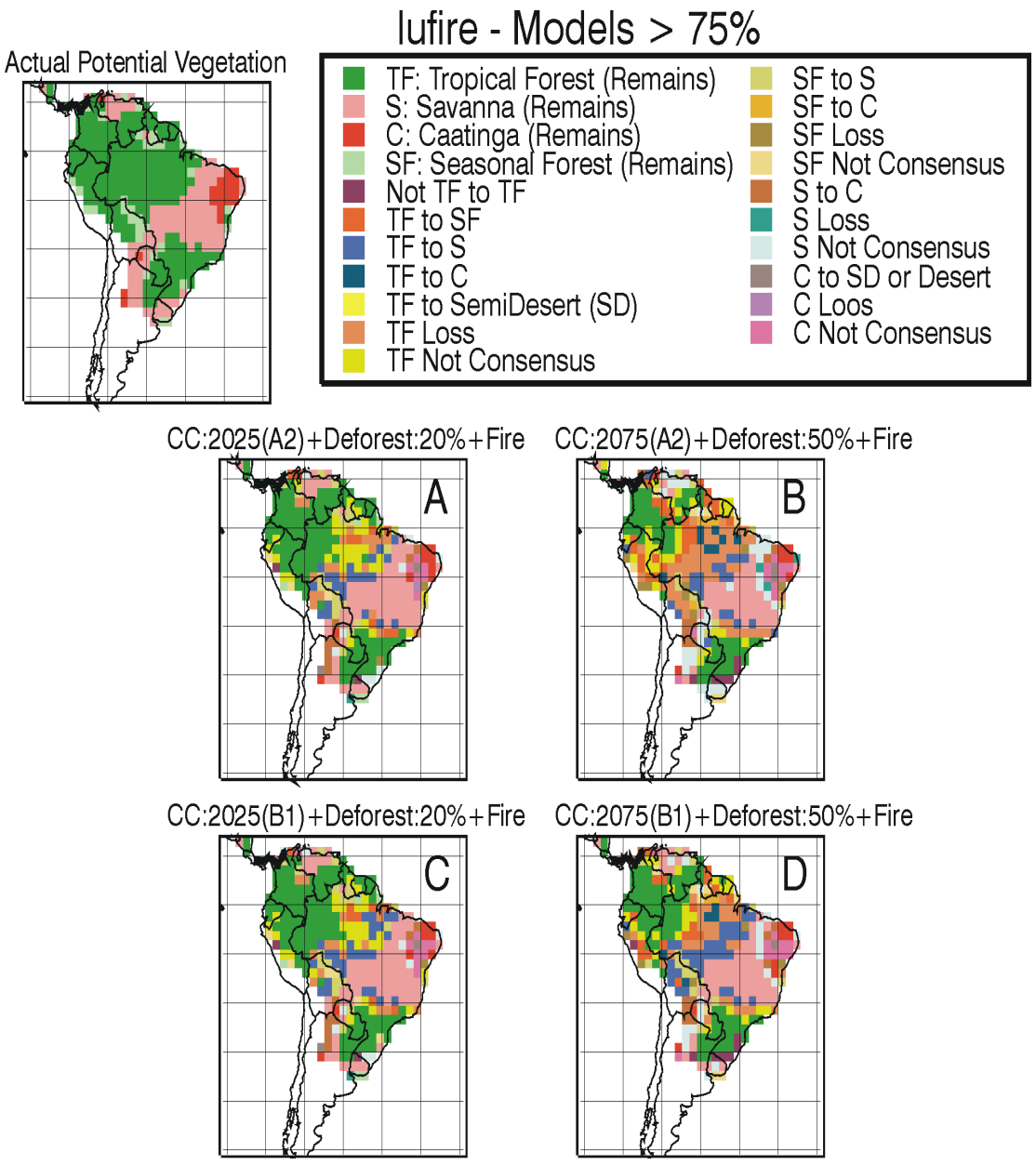

[24] In these maps, "no consensus" means that fewer than 12 models agree with the transition. "Loss" means consensus for substitution of that biome class

5.5 Summary of regional results

Table V.2 summarizes the results by region under analysis (geographical domains, as defined in Section I) including the net changes in vegetation carbon and the risk of Amazon dieback induced by climate forcing under A1B scenario. The summary portrays the different momentums of land use change driven by the changes in vegetation carbon and anticipated shifts in biome driven by changes in bioclimatic conditions. It also presents the elements of a preventing response to the anticipated combined impacts of climate, deforestation and fire events.

Table V.2 Regional Impacts and Elements of an Ameliorating Response

Geographic domain (defined in Figure 1.1)	Current vegetation carbon density (kg C m^{-2})	Risk of dieback (%) (probability of a 25% reduction in veg. carbon)	Change in vegetation carbon by two best-ranked models (kg C m^{-2}) (*)	Potential biome shift caused by climate change with deforestation at 50% and occurrence of fires by 2075 [CPTEC-PVM]	Elements of an ameliorating response
EA - Eastern Amazonia	12	8	-2 to -6	Savanna from 20% to 40% of area; Significant reduction in Tropical Rainforest.	a) Prevent further deforestation, conserve remaining stands of rainforest; b) launch further reforestation efforts to prevent savannization in border areas with remaining forests.
NWA - North Western Amazonia	15	3	-5 to -6	No significant change in cover of Tropical Rainforest or Seasonal Forest.	Maintain momentum of strong conservation policies through increased financing of existing protected areas to prevent encroachment.
SA - Southern Amazonia	10	62	-4 to -5	No major change in cover of Savanna; further reduction in Tropical Rainforest biome from 10% to less than 5%; slight increases in Seasonal Forest.	Assign high priority to preventing deforestation of remaining rainforest stands.
NEB - Northeastern Brazil	3	19	-1 to -2	Reduction of Seasonal Forest from 5% to less than 1%, and transitions of Savanna to Caatinga and Caatinga to desert.	a) Prevent further losses of forest cover through aggressive efforts to avoid deforestation. b) Launch further reforestation efforts.
SB - Southern Brazil	10	2	-1 to -3	Reduction in cover of grasslands and corresponding increase in Savanna and Rainforest.	Maintain current level of reforestation efforts.

From the results of the analysis, the combined effects of climate change, deforestation and fire events will have very serious impacts on the rainforest biome throughout the Amazon basin. While the impacts from climate change result from global contributions, the deforestation and induced fires are aspects that can be addressed within the country.

In fact, the results support the view that there is a need to arrest the deforestation of the Amazon basin as it reinforces the stress induced by the anticipated impacts from climate change. The urgency of these actions is highlighted by the results under scenarios that already well surpassed by current emission trajectories. However, implications are somewhat different depending on the geographical domain under analysis.

Clearly the priority response should be focused on Eastern Amazonia, where combined impacts of Amazon dieback and deforestation result in significant decreases in the area of forest biome, already in the near future (2025). These impacts would require immediate and significant efforts to arrest deforestation and would benefit from an ambitious reforestation program.

Northwestern Amazonia is the region that fares relatively better but even there long-term impacts (by 2100) are anticipated. The priority for this region lies in strengthening conservation efforts by maintaining current forest cover.

Southern Amazonia is the region with the highest risk of Amazon dieback and also where a significant substitution of forest biome by savanna is projected. The region requires urgent measures to deter the deterioration of remaining forest stands.

In Northeastern Brazil, the anticipated relative increase in the area of caatinga foreshadows a drier and hotter climate. Efforts to reforest, restore and maintain remaining ground cover are required.

The only biome shift that favors rainforest, observed in the projections, takes place in Southern Brazil, enabling conditions for successful reforestation efforts.

VI. Qualification of potential consequences for Brazil from climate-induced damage in the Amazon

1. OBJECTIVE

This section provides a description of the potential impacts of climate change and climate-change-induced Amazon dieback. Attempts to quantify all economic impacts from Amazon dieback were inconclusive. There is too much uncertainty about the value of the natural capital lost. Further preparation and analysis are required on this matter.

2. SCOPE OF THE ASSESSMENT

In terms of type of impacts to be considered, the following should be included:

a) Direct economic losses linked to Amazon dieback include those induced by economic activity related to agriculture, forestry and power generation. Climate impacts are expected to affect the yields and areas for specific crops in tropical areas, as temperatures increase and rainfall patterns are modified, and the ideal areas for different crops shift. Amazon dieback may reduce rainfall in agricultural areas in southern Brazil because more radiation would be absorbed by bare soil instead of being used to evaporate moisture from the forest canopy, thus reducing the moisture available for rainfall from moisture generated in the Amazon.

   Sustainable forestry would also be affected by the reduction in biomass density, which would affect timber yields. The magnitude of the carbon sink would likewise be diminished. In addition, weather extremes, longer dry periods, disappearance or reduction of dry-period rainfalls and increased intensity during rainy periods would all affect stream-flow regulation. This would have an impact on the firm capacity of existing hydropower plants and on the water storage capacity of future investments.

b) Other losses are associated with the lost services to the biosphere. The Amazon rainforest plays a key role in the water and carbon cycles, but also as a depository of life. It is essential to the functioning of the global ecosystem. However, these roles and functions are not currently included in formal GDP accounting. With 2.5 million square miles of rainforest, the Amazon represents 54% of the total rainforests left on earth. More than 20% of the world's oxygen is produced in the Amazon rainforest.[25] The Amazon also produces one-fifth of the world's fresh water flows into the oceans.[26]

   Likewise, the Amazon rainforest contains the world's largest collection of living plant and animal species and the loss of habitat would unavoidably result in the reduction of

[25] http://www.rain-tree.com/facts.htm
[26] http://www.rain-tree.com/facts.htm

populations and even extinctions of many species. This would result in an impoverishment of global biodiversity.[27] There is also an intrinsic value to be lost in the genetic material stored in the Amazon ecosystem, which contains information and may be of value for future economic activities and human welfare. This intrinsic value is not amenable to easy quantification.

[27] It is estimated that a single hectare of Amazon rainforest contains about 900 tons of living plants, including more than 750 types of trees and 1,500 other plants. A single pond in Brazil can sustain a greater variety of fish than is found in all of Europe's rivers; more than 2,000 species of fish have been identified in the Amazon Basin—more species than in the entire Atlantic Ocean. The Andean mountain range and the Amazon jungle are home to more than half of the world's species of flora and fauna; for example, one in five of all birds in the world live in the Amazon rainforest. To date, some 438,000 species of plants of economic and social interest have been registered in the region, and many more have yet to be catalogued or even discovered.

VII. Conclusions

The effects of climate change will change the functioning and structure of the Amazon basin.

With rising atmospheric CO_2 concentrations, climate change will lead to a substantial warming in Amazonia during the current century, reaching levels that are highly likely to affect the remaining forests throughout the region.

It is expected that the Amazon region will experience an intensification of the water cycle with increased occurrence of heavy rainfall and consequent flooding and a lengthening of drought periods. Specific projections for indexes reflecting increased rainfall and dry period extremes, prepared through the application of the high-resolution MRI AGCM with the use of the Earth Simulator for the Amazon basin, are included in the report. Likewise, the region's hydrology will be affected, with increased stream flows during wet periods and lower than current stream flows for dry periods in major rivers of the region.

However, there is considerable uncertainty over future rainfall. Most climate models project substantial changes in rainfall patterns, but these do not coincide: some models project increases, others project decreases, and the spatial pattern of these changes also varies between the models.

To estimate the risk of Amazon drying, probability density functions for future rainfall were derived using two procedures described in the report. These indicate a strong likelihood of Northwestern Amazonia becoming wetter in the December to May period, and an increased probability of 2005-like drought conditions in Southern Amazonia (from 1 event in 100 years currently, to 1 in 17 years) toward the end of the century. In other regions the probability of change is less significant due to continuing discrepancies among climate model simulations in this region.

The climate model PDFs based on rainfall were combined with forest simulations to produce PDFs of changes in vegetation carbon in the 21st century. In the absence of CO_2 fertilization, a reduction in vegetation carbon is anticipated in most of the geographical domains. The analysis concludes that there is a substantial probability of Amazon dieback.

When leave physiology-based CO_2 fertilization default factors are used, the likelihood of this reduction is substantially lower, and the probability of increases in vegetation carbon is non-negligible. However, in tropical, mature forest ecosystems, under pronounced nutrient constraints typical of poor soil conditions in the Amazon basin, there is great uncertainty that CO_2 fertilization may play such an effective role; and in the absence of solid information, such as ecosystem-wide CO_2 fertilization experiments, the assumption that CO_2 fertilization will be an important factor positively-affecting ecosystem resilience of the Amazon cannot be used presently as a basis for sound policy advice. Reducing this uncertainty, using a combination of estimates of the Amazonian carbon sink and trends in river runoff, is therefore a priority for a follow-on study.

The impacts of deforestation, climate change and fires were estimated using the outputs of 15 GCMs and the CPTEC-PVM, using a consensus approach, where only changes in biome with 75% or higher agreement are identified. When the effects of climate change, deforestation and fire are combined, using a potential vegetation model (CPTEC-PVM) specifically developed and applied in the South American context, major shifts in biomes are predicted.

For Amazonia as a whole, the remaining tropical forest area relative to its original extension is progressively reduced as climate change impacts, deforestation and fire effects are combined. Substantial impacts are already projected by 2025 and the situation worsens by 2050. The effect of climate change alone would contribute to reduce the extent of the rainforest biome by one third by the end of the century.

Major impacts are projected in Eastern Amazonia. The combined effects of climate and deforestation result in a severe decrease of the rainforest biome, in relation to its original extension for forest area. The remaining forest biome, by 2075, accounting for 50% deforestation and/or the effects of fires, is about 5%. This is the largest relative decrease in the entire basin.

The Northwest projections indicate the smallest relative decrease of tropical forest biome for the entire basin. The impact of fires was found to be not significant. The decrease of the tropical forest area is smaller than 10% for time slice 2025. However, even for this region, under scenario A2 there would be a significant decrease by 2100 (about 60% of the remaining biome).

For Southern Amazonia, the analysis indicates a relative increase in the area of savanna. The deforestation contributes for this configuration with a drier and hotter climate, favoring savanna expansion in replacement of tropical forests. In this region, fire has an important effect. For scenario A2 (and B1) and time slices 2025 and 2075, the projection indicates a net increase in the area of savanna, ranging from 30% to 80%.

For the Northeast the analysis indicates a slight relative increase (4%–7%) in caatinga, resulting from hotter and drier climate.

In Southern Brazil the combination of factors leads to a decrease in the forest area, with a strong effect derived from forest fires. In general, fire potential strengthens the consensus for transitions from tropical forest to savanna in Southern and Southeastern Amazonia.

Losses linked to Amazon dieback would show up in agriculture, forestry and power generation, among other sectors of economic activity. However, a full accounting of losses would need to include those incurred in environmental services (fresh water, oxygen, biodiversity, ecosystem integrity, services to other species) or the intrinsic value of the lost genetic information through a major collapse of the system. The loss of the Amazon rainforest and its associated ecosystems has an intrinsic value that is not amenable to quantification but that certainly exceeds any accounting made with current economic tools. Nevertheless, a better valuation of the financial and natural capital represented by the Amazon ecosystem is required as well as a more comprehensive assessment of the economic implications of its potential dieback; this should also be part of a follow-up.

All of these results indicate the need to avoid reaching a point of GHG emissions that would result in an induced Amazon loss. The current emissions trajectory may result in a high risk of incurring in these losses during this century. Thus, Amazon dieback should be considered a threshold for dangerous climate change. Likewise, the estimated combined effects of climate

impacts and deforestation on the integrity of the Amazon strongly suggest that deforestation should be rapidly reduced.

There are four major, non-linear, positive-feedback responses to global warming with the potential to create major disruptions in global climate. These are the slowing of the North Atlantic Thermohaline Circulation, the breakup of the West Antarctic Ice Sheet, methane emissions from melting permafrost, and Amazon forest dieback. The pace and severity of all four depend on poorly understood physical processes. Of the four, only Amazon forest dieback can to some extent be mitigated by deliberate intervention at a global scale through the reduction in greenhouse gas emissions combined with efforts to avoid further deforestation.

Next steps

The conclusions reached in the report have significant implications for forest and climate policy in Brazil and elsewhere. The risk of Amazon dieback, in the absence of any significant CO_2 fertilization effect at ecosystem level, has been found to be substantial for key regions of the Amazon basin. The potential shift of equilibrium state of the basin toward biomes with less biomass should be of great concern. This potential shift is likely to be exacerbated by the combined effects of deforestation, climate change and associated increases in the likelihood of fires.

These conclusions and the supporting material should be discussed as soon as possible with climate specialists and government policy makers in the Government of Brazil.

In addition, it is recommended that additional efforts be made to ascertain the potential role, if any, of CO_2 fertilization and its effect on growth, carbon stocking, and resilience at ecosystem level for the Amazon basin. Direct CO_2 effects at ecosystem level are the key unknown in assessing the risk of Amazon forest dieback under 21st century climate change. Reducing this uncertainty, using a combination of estimates of the Amazonian carbon sink (Phillips et al. 2009) and trends in river runoff (Gedney et al. 2006), is therefore a priority for a follow-on study.

Furthermore, the findings indicate that differences between the total impacts of climate change caused by CO_2 and other climate forcing agents (e.g., increases in methane or reductions in sulfate aerosols) have implications for international climate policy, which currently treats all radiative forcings as equally damaging. In contrast, this study shows clearly that the risk of Amazon forest dieback is many times greater if climate change arises from agents other than CO_2; this differential effect should also be further assessed.

Finally, the quantification of the potential economic consequences of Amazon dieback require additional efforts to monetize all the implications derived from major changes in the global and regional environmental and economic services provided by the Amazon basin. A more comprehensive evaluation would certainly substantiate the justification of any remedial actions.

REFERENCES:

Alencar A, Nepstad D and Diaz MCV (2006): Forest understorey fire in the Brazilian Amazon in ENSO and non-ENSO years: area burned and committed carbon emissions. Earth Interactions 10: 1-17

Bondeau A, Smith PC, Zaehle S, Schaphoff S, Lucht W, Cramer W, Gerten D, Lotze-Campen H, Müller C, Reichstein M and Smith B (2007): Modelling the role of agriculture for the 20th century global terrestrial carbon balance. Global Change Biology 13: 679-706.

Cardoso, M. F., C. A. Nobre, D. M. Lapola, M. D. Oyama, and G. Sampaio (2008): Long-term potential for fires in estimates of the occurrence of savannas in the tropics, Global Ecol. Biogeogr., 17(2), 222-235, doi: 10.1111/j.1466-8238.2007.00356.x.

Cavalcanti, I.F.A., J.A. Marengo, P. Satyamurti, C.A. Nobre, I. Trosnikov, J.P. Bonatti, A.O. Manzi, T. Tarasova, L.P. Pezzi, C. D'Almeida, G. Sampaio, C.C. Castro, M.B. Sanches, M.B., and H. Camargo (2002) : Global Climatological Features in a Simulation Using the CPTECCOLA AGCM. Journal of Climate, v.15, n.21, p. 2965-2988.

Christian HJ, Blakeslee RJ, Boccippio DJ, Boeck WL, Buechler DE, Driscoll KT, Goodman SJ, Hall JM, Koshak WJ, Mach DM and Stewart MF (2003): Global frequency and distribution of lightning as observed from space by the Optical Transient Detector. Journal of Geophysical Research-Atmospheres 108.

Cochrane MA and Laurance WF (2008): Synergisms among fire, land use, and climate change in the Amazon. Ambio 37: 522-527.

Collatz et al. 1991

Condit R, Hubbell SP and Foster RB (1995): Mortality rates of 205 neotropical tree and shrub species and the impact of a severe drought. Ecological Monographs 65: 419-439

Condit R, Aguilar S, Hernandez A, Perez R, Lao S, Angehr G, Hubbell SP and Foster RB (2004): Tropical forest dynamics across a rainfall gradient and the impact of an El Nino dry season. Journal of Tropical Ecology 20: 51-72

Cowling SA and Shin Y (2006): Simulated ecosystem threshold responses to co-varying temperature, precipitation and atmospheric CO_2 within a region of Amazonia. Global Ecology & Biogeography 15: 553-566.

Cox PM (2001): Description of the TRIFFID Dynamic Global Vegetation Model. UK, Hadley Centre, Met Office: 16

Cox PM, Betts RA, Collins M, Harris PP, Huntingford C and Jones C (2004): Amazonian forest dieback under climate-carbon cycle projections for the 21st century. Theor. Appl. Climatol. 78: 137-156

Cox, PM, Harris, PP, Huntingford, C, Betts, RA, Collins, M, Jones, CD, Jupp, TE, Marengo, JA, Nobre, CA (2008): Increasing risk of Amazonian drought due to decreasing aerosol pollution. Nature(453): 212 - 216.

Cox, PM, Jupp, TE (2008): The sensitivity of Amazonian rainfall to SST indices on interannual timescales, and predicted rainfall change in the 21st century. World Bank PROJECT P109761, Discussion Paper 1.

Cramer W, Bondeau A, Woodward FI, Prentice IC, Betts RA, Brovkin V, Cox PM, Fisher V, Foley JA, Friend AD, Kucharik C, Lomas MR, Ramankutty N, Sitch S, Smith B, White A and Young-Molling C (2001): Global response of terrestrial ecosystem structure and function to CO_2 and climate change: results from six dynamic global vegetation models. Global Change Biology 7: 357-373

Cramer W, Bondeau A, Schaphoff S, Lucht W, Smith B and Sitch S (2004): Tropical forests and the global carbon cycle: Impacts of atmospheric carbon dioxide, climate change and rate of deforestation. Philosophical Transactions of the Royal Society of London 359: 331-343

Curtis PS and Wang XS (1998): A meta-analysis of elevated CO_2 effects on woody plant mass, form, and physiology. Oecologia 113: 299-313

Dirzo R and Raven PH (2003): Global state of biodiversity and loss. Annual Review of Environment and Resources 28: 137-167

Dorman and Sellers 1989

Essery RLH, Best MJ and Cox PM (2001): MOSES 2.2 Technical Documentation. UK, Hadley Centre, Met Office: 30.

Farquhar GD, von Caemmerer S and Berry JA (1980): A biochemical model of photosynthesic CO_2 assimilation in leaves of C3 plants. Planta 149: 78-90

Foley JA, Prentice IC, Ramankutty N, Levis S, Pollard D, Sitch S and Haxeltine A (1996): An integrated biosphere model of land surface processes, terrestrial carbon balance, and vegetation dynamics. Global Biogeochemical Cycles 10

Folland, CK, Colman, AW, Rowell, DP, Davey, MK (2001): Predictability of Northeast Brazil rainfall and real{time forecast skill 1987-1998. Journal of Climate(14): 1937-1958.

Fu, R, Dickinson, RE, Chen, MX, Wang, H (2001): How do tropical sea surface temperatures influence the seasonal distribution of precipitation in the equatorial Amazon? Journal of Climate(14): 4003-4026.

Gash, J.H.C., C. Nobre, J.M. Roberts, and R.L. Victoria (1996): Amazonian deforestation and climate. Chicester, UK: John Wiley, p. 549-576.

Gash, J. H. C. and C.A. Nobre, (1997): Climatic effects of Amazonian deforestation: some results from ABRACOS. Bulletin of the American Meteorological Society, v.78, n.5, p.823-830, 1997.

Gerten D, Schaphoff S, Haberland U, Lucht W and Sitch S (2004): Terrestrial vegetation and water balance - hydrological evaluation of a dynamic global vegetation model. Journal of Hydrology 286: 249-270

Gerten D, Lucht W, Schaphoff S, Cramer W, Hickler T and Wagner W (2005): Hydrologic resilience of the terrestrial biosphere. Geophysical Research Letters 32: L21408

Hickler T, Eklundh L, Seaquist JW, Smith B, Ardö J, Olsson L, Sykes M and Sjöström M (2005). Precipitation controls Sahel greening trend. Geophysical Research Letters 32: L21415

Hickler T, Smith B, Prentice IC, Mjöfors K, Miller P, Arneth A and Sykes M (2008): CO_2 fertilization in temperate FACE experiments not representative of boreal and tropical forests. Global Change Biology 14: 1531-1542

Houghton RA, Lawrence KT, Hackler JL and Brown S (2001): The spatial distribution of forest biomass in the Brazilian Amazon: a comparison of estimates. Global Change Biology 7: 731-746

Huffman G.J., R.F. Adler, M.M. Morrissey, D.T. Bolvin, S. Curtis, R. Joyce, B. McGavock and J. Susskind, (2001): Global precipitation at one-degree daily resolution from multi-satellite observations. J. Hydrometeorol., 2, 36-50.

Hughes JK, Valdes PJ and Betts R (2006): Dynamics of a globalscale vegetation model. Ecological Modelling 198: 452-462

IBGE (1988). Mapa de vegetacao do Brasil

Intergovernmental Panel on Climate Change, 2000

IPCC (2007): Climate Change (2007): The Physical Science Basis. Contribution of Working Group I to the Fourth Assessment Report of the Intergovernmental Panel on Climate Change Cambridge, United Kingdom and New York, NY, USA, Cambridge University Press.996 pp.

Kauffman JB and Uhl C (1990): Interactions of anthropogenic activities, fire, and rain forests in the Amazon basin. Fire in the Tropical Biota: Ecosystem Processes and Global Challenges. Goldammer JG. Berlin, Springer Verlag: 117-134.

Kamiguchi, K., A. Kitoh, T. Uchiyama, R. Mizuta and A. Noda, (2006): Changes in precipitation-based extremes indices due to global warming projected by a global 20-km-mesh atmospheric model. SOLA, 2, 64-67

Kleidon A and Heimann M (2000): Assessing the role of deep rooted vegetation in the climate system with model simulations: mechanism, comparison to observations and implications for Amazonian deforestation. Climate Dynamics 16: 183-199

Korner, Ch. (2004): Through enhanced tree dynamics carbon dioxide enrichment may cause tropical forests to lose carbon. Philos Trans R Soc Lond Ser B-Biol Sci 359:493-498

Korner, Ch., R. Asshoff, O. Bignucolo, S. Hattenschwiler, S.G. Keel, S. Pelaez-Riedl, S. Pepin, R.T.W. Siegwolf and G. Zotz. (2005): Carbon flux and growth in mature deciduous forest trees exposed to elevated CO2. Science, 309, 1360-1362.

Korner, Ch. (2006): Plant CO_2 responses: an issue of definition, time and resource supply. New Phytol 172:393-411

Korner Ch, Morgan J, Norby R (2007): CO_2 Fertilisation: When, where, how much? In: Canadell JG, Pataki DE, Pitelka LF (eds) Terrestrial ecosystems in a changing world series: Global change - The IGBP series. Springer, Berlin p. 9-21

Krinner G, Viovy N, de Noblet-Ducoudre N, Ogee J, Polcher J, Friedlingstein P, Ciais P, Sitch S and Prentice IC (2005): A dynamic global vegetation model for studies of the coupled atmosphere biosphere system. Global Biogeochemical Cycles 19: GB1015

Kutzbach et al., 1998

Lapola, D. M., M. D. Oyama, C. A. Nobre, and G. Sampaio (2008): A new world natural vegetation map for global changes studies, An. Acad. Bras. Cienc., 80 (2), 397-408, doi: 10.1590/S0001- 37652008000200017.

Lapola, D.M., M.D. Oyama, C.A. Nobre (2009): Exploring the range of climate-biome projections for tropical South America: the role of CO_2 fertilization and seasonality. Global Biogeochemical Cycles, Submitted

Li, W, Fu, R, Dickinson, RE (2006): Rainfall and its seasonality over the Amazon in the 21st century as assessed by the coupled models for the IPCC AR4. Journal of Geophysical Research (111): D02111.

Lucht W, Prentice IC, Myneni RB, Sitch S, Friedlingstein P, Cramer W, Bousquet P, Buermann W and Smith B (2002): Climatic control of the high-latitude vegetation greening trend and Pinatubo effect. Science 296: 1687-1689.

Liebmann, B, Marengo, J (2001): Interannual variability of the rainy season and rainfall in the Brazilian Amazon basin. Journal of Climate (14): 4308-318.

Malhi Y and Grace J (2000): Tropical forests and atmospheric carbon dioxide. Trends in Ecology & Evolution 15: 332-337.

Malhi Y, Wood D, Baker TR, Wright J, Phillips OL, Cochrane T, Meir P, Chave J, Almeida S, Arroyo L, Higuchi N, Killeen TJ, Laurance SG, Laurance WF, Lewis SL, Monteagudo A, Neill DA, Nunez Vargas P, Pitman NCA, Quesada CA, Salamao R, Silva JNM, Torres-Lezama A, Terborgh J, Vasquez Martinez R and Vinceti B (2006) : The regional variation of aboveground live biomass in old-growth Amazonian forests. Global Change Biology 12: 1107-1138.

Malhi Y, Roberts JT, Betts RA, Killeen TJ, Li W and Nobre CA (2008): Climate change, Deforestation, and the Fate of the Amazon. Science 319: 169-172

Meehl, GA,Washington, WM (1996): El Nino-like climate change in a model with increased atmospheric CO_2 concentrations. Nature (382): 56-60.

Monserud, R. A. and R. Leemans, (1992): Comparing global vegetation maps with the Kappa statistic. Ecological Modelling, v.62, p.275-293.

Mizuta, R., K. Oouchi, H. Yoshimura, A. Noda, K. Katayama, S. Yukimoto, M. Hosaka, S. Kusunoki, H. Kawai and M. Nakagawa (2006): 20-km-mesh global climate simulations using JMA-GSM model –Mean climate states–. J. Meteor. Soc. Japan, 84, 165-185.

Nakicenovic N, Alcamo J, Davis G, De Vries B, Fenhann J, Gaffin S, Gregory K, Grübler A, Jung TY, Kram T, La Rovere EL, Michaelis L, Mori S, Morita T, Pepper W, Pitcher H, Price L, Riahi K, Roehrl A, Rogner H-H, Sankovski A, Schlesinger M, Shukla P, Smith S, Swart RV, Van Rooijen S, Victor N and Dadi Z (2000) : IPCC Special report on emission scenarios. Cambridge, Cambridge University Press. 612 pp.

Nepstad D, De Carvalhos CR, Davidson EA, Jipp PH, Lefebvre PA, Negreiros GH, Da Silva ED, Stone TA, Trumbore SE and Vieira S (1994): The role of deep roots in the hydrological and carbon cycles of Amazonian forests and pastures. Nature 372: 666-669

Nepstad et al., 2001

Nepstad DC, Tohver IM, Ray D, Moutinho P and Cardinot G (2007): Mortality of large trees and lianas following experimental drought in an Amazon forest. Ecology 88: 2259-2269

New M, Hulme M and Jones P (2000): Representing twentiethcentury space-time climate variability. Part II: Development of 1901–1996 monthly grids of terrestrial surface climate. Journal of Climate 13: 2217-2238

Nobre, C.A., P.J. Sellers, P.J. and J. Shukla (1991): Amazonian deforestation and regional climate change. Journal of Climate, v.4, p.957-988.

Nobre (2003)

Nobre, P, Shukla, J (1996): Variations of sea surface temperature, wind stress and rainfall over the tropical Atlantic and South America. Journal of Climate (9): 2464-2479.

Nohara, D., A. Kitoh, M. Hosaka and T. Oki, 2006: Impact of climate change on river discharge projected by multi-model ensemble. J. Hydrometeorol., 7, 1076-1089

Norby RJ, Wullschleger SD, Gunderson CA, Johnson DW and Ceulemans R (1999): Tree response to rising CO_2 in field experiments: implications for the future forest. Plant, Cell and Enviroment 22: 683-714.

Norby RJ, DeLucia EH, Gielen B, Calfapietra C, Giardina CP, King JS, Ledford J, McCarthy HR, Moore DJP, Ceulemans R, De Angelis P, Finzi AC, Karnosky DF, Kubiske ME, Lukac M, Pregitzer KS, Scarascia-Mugnozza GE, Schlesinger WH and Oren R (2005): Forest response to elevated CO_2 is conserved across a broad range of productivity. Proceedings of the National Academy of Sciences of the United States of America 102: 18052-18056

Oyama, M.D. and C.A. Nobre (2004): A simple potencial vegetation model for coupling with the Simple Biosphere Model (SIB). Revista Brasileira de Meteorologia, v. 19, n. 2, p. 203-216, 2004.

Phillips OL, Lewis SL, Baker TR, Chao K-J and Higuchi N (2008): The changing Amazon forest. Philosophical Transactions of the Royal Society Ser. B 363: 1819-1827.

Phillips OL, Aragao LE, Lewis SL, Fisher JB, Lloyd J, Lopez-Gonzalez G, Malhi Y, Monteagudo A, Peacock J, Quesada CA, van der Heijden G, Almeida S, Amaral I, Arroyo L, Aymard G, Baker TR, Banki O, Blanc L, Bonal D, Brando P, Chave J, de Oliveira AC, Cardozo ND, Czimczik CI, Feldpausch TR, Freitas MA, Gloor E, Higuchi N, Jimenez E, Lloyd G, Meir P, Mendoza C, Morel A, Neill DA, Nepstad D, Patino S, Penuela MC, Prieto A, Ramirez F, Schwarz M, Silva J, Silveira M, Thomas AS, Steege HT, Stropp J, Vasquez R, Zelazowski P, Alvarez Davila E, Andelman S, Andrade A, Chao KJ, Erwin T, Di Fiore A, Honorio CE, Keeling H, Killeen TJ, Laurance WF, Pena Cruz A, Pitman NC, Nunez Vargas P, Ramirez-Angulo H, Rudas A, Salamao R, Silva N, Terborgh J and Torres-Lezama A (2009): Drought sensitivity of the Amazon rainforest. Science 323: 1344-7.

Prentice IC, Bondeau A, Cramer W, Harrison SP, Hickler T, Lucht W, Sitch S, Smith B and Sykes M (2007): Dynamic global vegetation modeling: Quantifying terrestrial ecosystem responses to large-scale environmental change. Terrestrial Ecosystems in a changing world. Canadell JG, Pataki DE and Pitelka LF. Berlin, Heidelberg, New York, Springer: 175-192

Raschke, E., S. Bakan, and S. Kinne (2006): An assessment of radiation budget data provided by the ISCCP and GEWEX-SRB, Geophys. Res. Lett., 33, L07812, doi:10.1029/2005GL025503.

Saatchi SS, Houghton RA, Dos Santos Alvala RC, Soares JV and Yu Y (2007): Distribution of aboveground live biomass in the Amazon basin. Global Change Biology 13: 816-837.

Sahagian, D. L., and K. Hibbard (1998): GAIM 1993-1997, The first five years: setting the stage for synthesis, IGBP/GAIM Report Series, Report #6, 78p.

Salazar LF, Nobre C and Oyama MD (2007): Climate change consequences on the biome distribution in tropical South America. Geophysical Research Letters 34: L09708

Sampaio G, Nobre C, Costa MH, Satyamurty P, Soares-Filho BS and Cardoso M (2007): Regional climate change over eastern Amazonia caused by pasture and soybean cropland expansion. Geophysical Research Letters 34: L17709

Sellers et al., 1996

Sitch S, Smith B, Prentice IC, Arneth A, Bondeau A, Cramer W, Kaplans JO, Levis S, Lucht W, Sykes MT, Thonicke K and Venevsky S (2003): Evaluation of ecosystem dynamics, plant geography and terrestrial carbon cycling in the LPJ dynamic global vegetation model. Global Change Biology 9: 161-185

Sitch S, Huntingford C, Gedney N, Levy PE, Lomass M, Piao S, Betts RA, Ciais P, Cox PM, Friedlingstein P, Jones CD, Prentice IC and Woodward FI (2008): Evaluation of the terrestrial carbon cycle, future plant geography and climate-carbon cycle feedbacks usin five Dynamic Global Vegetation Models (DGVMs). Global Change Biology 14: 1-25

Soares-Filho BS, Nepstad DC, Curran LM, Cerqueira GC, Garcia RA, Ramos CA, Voll E, McDonald A, Lefebvre P and Schlesinger P (2006): Modelling conservation in the Amazon basin. Nature 440: 520-523

Thonicke K, Spessa A, Prentice IC, Harrison SP and Carmona-Morena C (in review): The influence of vegetation, fire spread and fire behaviour on global biomass burning and trace gas emissions. Global Change Biology

Turner, D. P., W. D. Ritts, W. B. Cohen, S. T. Gower, S. W. Running, M. Zhao, M. H. Costa, A. A. Kirschbaum, J. M. Ham, S. R. Saleska, and D. E. Ahl (2006): Evaluation of MODIS NPP and GPP products across multiple biomes, Remote Sens. Environ., 102 (3-4), 282-292, doi: 10.1016/j.rse.2006.02.017.

Van Nieuwstadt MGL and Sheil D (2005): Drought, fire and tree survival in a Borneo rain forest, East Kalimatan, Indonesia. Journal of Ecology 93: 191-201

Vergara, W (ed.) (2009). Assessing the Consequences of Climate Destabilization in Latin America. Sustainable Development Working Paper 32. The World Bank.

Williamson GB, Laurance SG, Oliveira PJC, Gascon C, Lovejoy TE and Pohl L (2000): Amazonia tree mortality during the 1997 El Nino drought. Conservation Biology 14: 1538-1542.

Willmott, C. J., C. M. Rowe, and Y. Mintz (1985), Climatology of the terrestrial seasonal water cycle, Int. J. Climatology, 5(6), 589-606, doi: 10.1002/joc.3370050602

Willmott, C. J. and K. Matsuura (1998): Terrestrial air temperature and precipitation: monthly and annual climatologies, <http://climate.geog.udel.edu/_climate/html pages/archive.html>, University of Delaware, Newark.

Xie, P. and P.A. Arkin, 1997: Global precipitation: A 17-year monthly analysis based on gauge observations, satellite estimates, and numerical model outputs. Bull. Am. Meteorol. Soc., 78, 2539-2558.

Xue, Y., P.J. Sellers, J.L. Kinter, and J.A. Shukla (1991): Simplified biosphere model for global climate studies. Journal of Climate, v.4, p.345-364.

Xue, Y. H.G. Bastable, P.A. Dirmeyer, and P.J. Sellers (1996): Sensitivity of simulated surface fluxes to changes in land surface parameterizations – a study using ABRACOS data. Journal of Applied Meteorology, v. 35, p. 386-400.